TESI DI DOTTORATO

Enrico Manfredi

Knots and links in lens spaces

Dottorato in Matematica, Bologna (2014).

<http://www.bdim.eu/item?id=tesi_2014_ManfrediEnrico_1>

Knots and links
in lens spaces

Tesi di Dottorato presentata da: Enrico Manfredi

Coordinatore Dottorato:
Prof.ssa
Giovanna Citti

Relatore:
Prof.
Michele Mulazzani

Contents

Introduction

Importance of knots and links in lens spaces

History of knots Knot theory is a widespread branch of geometric topology, with many applications to theoretical physics, chemistry and biology.

The starting point has been the study of knots in the $\mathbb{R}^3$, introduced by Gauss in the beginning of 19th century and then improved by Kelvin and Tait at the end of the same century, in order to study the atoms conformation. During the first half of the 20th century knots became important in order to describe 3-manifolds using Dehn surgery, and they obtained a central role in geometric topology. In the second half of the 20th century physicists turned again their attention to knots, by involving them in the description of topological quantum field theories. A recent progress of this work is topological quantum computation, a difficult road that may lead to the development of quantum computers, by exploiting knot theory. In the last decade also biologists directed their attention to knot theory, because it can explain how the entanglement of DNA helps or prevents the genes expression.

Topology of knots A knot in the 3-sphere $\mathbf{S}^3$ is an embedding of the circle $\mathbf{S}^1$ into $\mathbf{S}^3$. A link is an embedding of ν copies of $\mathbf{S}^1$. Two links are equivalent if there exists an ambient isotopy between them. The easiest way to represent a link is through a regular projection on a plane, and we can understand if two knots are equivalent because their diagrams can be connected by a finite sequence of Reidemeister moves. It is hard to distinguish non-equivalent

links, because we don't know when to stop the test with Reidemeister moves. For this reason, invariants of links were introduced: when they are distinct, the two links are inequivalent.

We may consider polynomial invariants, such as Alexander, Jones or HOMFLY-PT polynomials; these invariants cannot distinguish some pairs of knots or links. We may also consider more geometric and powerful invariant, like the fundamental group (it is a complete invariant for prime knots [72]) or like the fundamental quandle (a complete invariant for all knots in $\mathbf{S}^3$ [71, 86]), alas if you compute one of these invariants on two knots, it is usually very difficult to understand if the two results are different.

Surgery on knots   Other interesting topological problems about knots are the ones that arises from the following construction: when you consider a knot K, take a tubular neighborhood of it, cut it and re-paste sending a meridian of the torus to the (p, q)-torus knot, then you are performing a rational p/q surgery on K and you get another 3-manifold $M(K)_{p,q}$. For example, the p/q surgery over the unknot U (a knot that bounds a disk) gives us the lens space $L(p, q) := \mathbf{S}^3(U)_{p,q}$.

It is really useful to understand which surgeries on which knots give certain 3-manifolds. For instance, which knots in $\mathbf{S}^3$ give us a lens space? There is a conjecture of Berge [9] on this problem. An interesting program, established by Baker, Grigsby and Hedden in [6] and independently by Rasmussen in [96], attempts to solve this conjecture. The key step we are interested in is that the solution requires the study of some knots in lens spaces. A further step in this conjecture has been done by Greene [60]. A recent generalization of Berge conjecture is exposed in [11], while other conjectures [87, 4] investigate what happens when the surgery is performed on knots in lens spaces.

Motivations to study knots in lens spaces   These just cited conjectures are the most valuable reason that leads us to study knots and links in lens spaces, which is the argument of this dissertation. Furthermore there are

interesting articles explaining applications of knots in lens spaces to other fields of science: [102] exploits them to describe topological string theories and [15] uses them to describe the resolution of a biological DNA recombination problem.

Review of existing literature

Several works on links in lens spaces have been published and different representations for links in lens spaces are available in literature. We try to collect the most important results for the representations we are interested in.

Mixed link diagram   The most common representation of links in general 3-manifolds are mixed link diagrams, that is to say, links in $\mathbf{S}^3$ where some components are decorated by a surgery coefficient, since every 3-manifold can be constructed as a rational surgery on a link. Usually the papers on this representation deal with surgery problems, such as [3, 4, 15, 87]. Other works, involving a rigorous definition of these diagrams, Reidemeister-type moves and a Markov theorem for generic 3-manifolds are [76, 77, 78]. Another very important result is the algebraic Markov theorem of [38] with rational surgery description. The statement of this theorem simplify in the case of lens spaces and the authors announced the computation of the HOMFLY-PT skein module of $L(p,q)$ using this theorem.

Grid diagram   Grid diagrams are an interesting representation of links in $\mathbf{S}^3$, very useful to represent also legendrian links, since they use a piecewise linear orthogonal projection of the link. For this reason, Baker and Grigsby introduced in [5] the notion of grid diagram for links in lens spaces. It immediately became clear that grid diagrams were useful also for topological links in lens space. Manolescu, Ozsváth and Sarkar, in [83], showed a combinatorial method to compute knot Floer homology for $\mathbf{S}^3$, and in [6] there

is an improvement of this combinatorial technique for knots in lens spaces (generalized to links in [20]).

In a similar way, Cornwell in his Ph.D. thesis [30] used grid diagrams to produce Bennequin-type inequalities for legendrian links in lens spaces (also published in [32]), and for this reason he developed an HOMFLY-PT invariant for topological links in lens spaces [31].

Band diagram   Hoste and Przytycki [67] introduced band diagrams to compute the $(2, \infty)$-skein module of $L(p, q)$, that is to say, the Kauffman bracket skein module (KBSM for sake of brevity). The idea came from analogous computations for the KBSM of the solid torus made by Turaev [107].

Gabrovšek and Mroczkowski improved this idea, using a slightly different version of band diagrams, that is to say, punctured disk diagrams. They first set up a tabulation of knots in the solid torus, telling apart different links with the KBSM [51]. Then, in his Ph.D. thesis [50], Gabrovšek extends that work to knots in lens spaces. The key for a tabulation in so many different spaces is that a punctured diagram describe a knot in every lens space. For this reason, it is enough to identify different knots in the solid torus that are equivalent in the lens space considered to get a tabulation. Besides this work on KBSM, they have also found a basis for the HOMFLY-PT skein module of $L(p, 1)$ [52].

On a similar diagram Stitz obtained a combinatorial description of the linking number [105], of the Alexander polynomial (using the Alexander matrix of linking numbers) and of the Jones polynomial for links in lens spaces [104]. Finally, another diagram, which belongs to this family of representations in the solid torus, is the arrow diagram of Mroczkowski that is displayed in [50].

Other representations/results   Other possible representations of links in lens spaces are $(1, b)$-decompositions [39] and thin presentations [49, 35]. Several works investigates the particular case of $(1, 1)$-decompositions [88, 115, 47, 63, 29, 21, 22, 23, 24, 18], while few others regard thin presentations

[36, 37, 2]. Studies on links in lens spaces are also performed without fixing a representation. It is interesting to investigate fibered links in lens spaces [7, 55] and legendrian links in lens spaces [54, 79, 80]. Other invariants of (framed) links in lens spaces may be found by specializing the existing invariants of links in 3-manifolds [44, 114, 98, 10, 89, 90, 84].

Structure of the dissertation

The aim of this thesis is to improve the knowledge of knots and links in lens spaces. The first chapter is an introduction to lens spaces, considering four different representations that will be useful to our purpose. The second chapter shows the known representations of links in lens spaces that we will use in this thesis (mixed link diagrams, band diagrams and grid diagrams), along with Reidemeister-type moves for these representations. From the third chapter on, it starts the original part of this dissertation.

A new diagram   In 1991, Drobotukhina [42] introduced a disk diagram for knots and links in the projective space, which is a special case of lens spaces. Several invariants have been computed on this diagram [42, 69, 91, 92, 58, 59] and a tabulation of knots up to 6 crossing has been made [43]. This disk diagram can be generalized to links in lens spaces as suggested in [56] and in [81], so we decided to study it in order to find further invariants of links in lens spaces.

In the third chapter we explain the rigorous construction of the disk diagram, then we prove a Reidemeister-type theorem stating that two disk diagrams represent equivalent links if and only if they can be connected by a finite sequence of Reidemeister-type moves. These moves are of seven different types and all these results are published in [19]. Moreover we show the connection between the grid diagrams of [5] and the band diagrams of [52], because in the subsequent chapters of the thesis we want to investigate the invariants defined on these other two representations of links in lens

spaces.

Presentation of the group of the link and twisted Alexander polynomials   In this part of the thesis, published in [19], we focus on the generalization of the paper of Huynh and Le about links in the projective space [69]: in the fourth chapter a Wirtinger-type presentation for the group of the link is developed, improving our previous results exposed in [81]. In this contest the homology groups are not abelian free groups (as in $\mathbf{S}^3$), since a torsion part appears, and we present a method to compute the torsion directly from the diagram. The provided examples show that some well known results for the group of links in $\mathbf{S}^3$ (that is to say, [93] and [72, Theorem 6.1.12]) cannot generalize to lens spaces.

In the fifth chapter we deal with a certain class of twisted Alexander polynomials of links in lens spaces. The twisted Alexander polynomials are constructed as in [110], using the previous presentation of the group of the link and the Fox calculus [33]. The considered polynomials are the ones associated to the one dimensional representation of the group of the link over some particular domains. We find different properties of these polynomials and the most interesting one is that a subclass of these polynomials becomes trivial if the link is local, that is to say, if it is contained in a 3-ball. Finally we show the connection between the twisted Alexander polynomials and the Reidemeister torsion.

The lift in $\mathbf{S}^3$ of links in lens spaces   Consider the ciclic covering $P\colon \mathbf{S}^3 \to L(p,q)$, the lift of a link $L \subset L(p,q)$ is the link $\widetilde{L} := P^{-1}(L) \subset \mathbf{S}^3$. This geometric invariant is really important: when an invariant for links in lens spaces is defined, one should check that is not just an invariant of their lifts in $\mathbf{S}^3$ (in this case the invariant is said *essential*). Sometimes the lift is used to help the definition of invariants of links in lens spaces [6, 79].

In the sixth chapter of this dissertation we construct a planar diagram of the lift in $\mathbf{S}^3$ starting from a disk diagram of the original link in $L(p,q)$. A similar construction can be done with band diagrams and it is exactly

a (p,q)-lens link of Chbili [28], and hence a freely periodic link in the 3-sphere [61]. In addition, we construct some examples of diagrams of the lift, showing its behavior under connected sum, for split links and when the link is described by a braid.

In the seventh chapter we discuss if the lift is a complete invariant, that is to say, if we can recognize the isotopy class of a link in $L(p,q)$ just by knowing the isotopy class of its lift. Using the preceding braid form of the lift, we can perform a small tabulation of the possible lifts of a certain class of braid links and get some examples of different unoriented links in lens spaces with equivalent lift, that is to say, a counterexample to the previous question. Finally we investigate the case of oriented links and the case where the knots are equivalent up to homeomorphism of pairs. The results of these two chapters are collected in [82].

Behavior of invariants with respect to the lift   In the eighth chapter we investigate if several invariants are essential or not. From [44], the fundamental quandle of a link in a lens space is isomorphic to the fundamental quandle of its lift, therefore it is inessential and incomplete. Otherwise, an essential invariant can be detected by the following method: compute it on two different links with equivalent lift, if the two values of the invariant are different, then it is essential. We apply this strategy to several geometric invariants of links in lens spaces, like fundamental group and twisted Alexander polynomials. Moreover we investigate the relationship between the invariants of a link in lens spaces and the corresponding invariants of the lift, by adapting some known results [65, 27].

In the ninth chapter, after remembering the construction of the KBSM of $L(p,q)$ [67], we show that it is an essential invariant of links in lens spaces. In a similar way we show that the HOMFLY-PT invariant of [31] defined on grid diagrams, is an essential invariant: in order to do this we state a proposition relating the invariant of an oriented link with the invariant of the link with opposite orientation and then we prove that the invariant is essential also for

the unoriented case. This result on the HOMFLY-PT polynomial, together
with a similar result about Heegaard Link Homology for lens spaces, are
collected in [20].

Chapter 1

Representation of lens spaces

The lens spaces are the simplest family of oriented closed 3-dimensional manifolds. During the first half of the 20th century, several different constructions were elaborated for them. See [109] for an interesting historical introduction. In this chapter, four different equivalent definitions of lens spaces are described, after giving some basic notations. Moreover we explain when two different lens spaces are "equivalent".

The first definition of lens spaces we give is the most intuitive one, and lens spaces are described as a 3-dimensional ball with points identified on its boundary. The second definition of lens spaces is obtained by the action of a finite group on $\mathbf{S}^3$. The equivalence between these two definitions is given in [111]. Since we will use this equivalence, we show a sketch of it. A definition of lens spaces via Heegaard splittings is also possible, and the equivalence with the first definition is shown in [99, §9.B] and [103, §8.3] . The second and the third definitions are equivalent according to [95, §11]. The fourth definition of lens spaces is obtained by using rational Dehn surgery. It is easy to find its equivalence with the Heegaard splitting definition.

1.1   Basic definitions

Let *Top* denote the category of topological manifolds and continuos maps, let *Diff* be the category of differential manifolds and differentiable functions and let *PL* (piecewise linear) be the category of *PL* manifolds and of *PL* maps. For details see [73].

Theorem 1.1. [73] *In dimension three, the categories Top, Diff and PL are equivalent.*

In particular, we can provide every topological 3-manifold with a piecewise linear or a differential structure. For this reason, when necessary, we will consider *PL* or differential structures on the object of our study. Moreover, for all this thesis, we consider only closed compact oriented 3-manifolds.

Let X and Y be two topological spaces. An *embedding* is a continuos function $f : X \to Y$ such that $f : X \to f(X)$ is a homeomorphism. A *curve* α in Y is an embedding $\alpha \colon [0,1] \to Y$.

Let $f_0, f_1 \colon X \to Y$ be two homeomorphisms. We say that f_0 and f_1 are *isotopic* if there exists a map $F \colon X \times [0,1] \to Y \times [0,1]$ with $F(x,t) = (f_t(x), t)$, $x \in X$, $t \in [0,1]$ such that $\forall t \in [0,1]$, f_t is an homeomorphism. The map F is called *isotopy* between f_0 and f_1.

The set $B^{n+1} := \{(x_1, \ldots, x_{n+1}) \in \mathbb{R}^{n+1} \mid x_1^2 + \ldots + x_{n+1}^2 \leq 1\}$, is the $(n+1)$-dimensional ball, that has as boundary the n-dimensional sphere $\mathbf{S}^n := \{(x_1, \ldots, x_{n+1}) \in \mathbb{R}^{n+1} \mid x_1^2 + \ldots + x_{n+1}^2 = 1\}$.

The torus $T = \mathbf{S}^1 \times \mathbf{S}^1$ has the following description as a subset of $\mathbb{R}^3$:

$$T = \{(x_1, x_2, x_3) \in \mathbb{R}^3 \mid x_1 = (2 + \cos b) \cos a, \quad x_2 = (2 + \cos b) \sin a,$$
$$x_3 = \sin b, \ \text{with } a, b \in [0, 2\pi]\}.$$

A *parallel* of the torus T is a curve of the following type:

$$\alpha := \{(x_1, x_2, x_3) \in \mathbb{R}^3 \mid x_1 = (2 + \cos k_1) \cos a, \quad x_2 = (2 + \cos k_1) \sin a,$$
$$x_3 = \sin k_1, \ \text{with } a \in [0, 2\pi]\},$$

where k_1 is a constant chosen in $[0, 2\pi]$.

A *meridian* of T is a curve of the following type:

$$\beta := \{(x_1, x_2, x_3) \in \mathbb{R}^3 \mid x_1 = (2 + \cos b) \cos k_2, \quad x_2 = (2 + \cos b) \sin k_2,$$
$$x_3 = \sin b, \text{ with } b \in [0, 2\pi]\},$$

where k_2 is a constant chosen in $[0, 2\pi]$.

The solid torus $V = \mathbf{S}^1 \times B^2$ is the compact subset of $\mathbb{R}^3$ bounded by T.

On the torus T let $p\beta + q\alpha$ be the closed curve that winds p times around a meridian and q times around a parallel.

Proposition 1.2 ([95], §14.1). *Let $p\beta + q\alpha$ be a closed curve on T.*

(a) *The numbers p and q are coprime.*

(b) *If two closed curves on the torus are homotopic, then they are isotopic.*

Remark 1.3. On the torus T, all meridians are isotopic to each other, and the same fact holds for parallels. Moreover, Proposition 1.2 shows that any closed curve J on T is isotopic to $p\beta + q\alpha$ for suitable integer coprime numbers p and q.

1.2   A lens model for lens spaces

All the following definitions are given fixing two integer numbers, p and q, such that $\gcd(p, q) = 1$ and $0 \leqslant q < p$.

Lens spaces may be defined by a lens model: considering the 3-dimensional ball, let E_+ and E_- be respectively the upper and the lower closed hemisphere of ∂B^3. The equatorial disk B_0^2 is defined by the intersection of the plane $x_3 = 0$ with B^3. Label with N and S respectively the "north pole" $(0, 0, 1)$ and the "south pole" $(0, 0, -1)$ of B^3. Let $g_{p,q} \colon E_+ \to E_+$ be the counter-clockwise rotation of $2\pi q/p$ radians around the x_3-axis, as in Figure 1.1, and let $f_3 \colon E_+ \to E_-$ be the reflection with respect to the plane $x_3 = 0$.
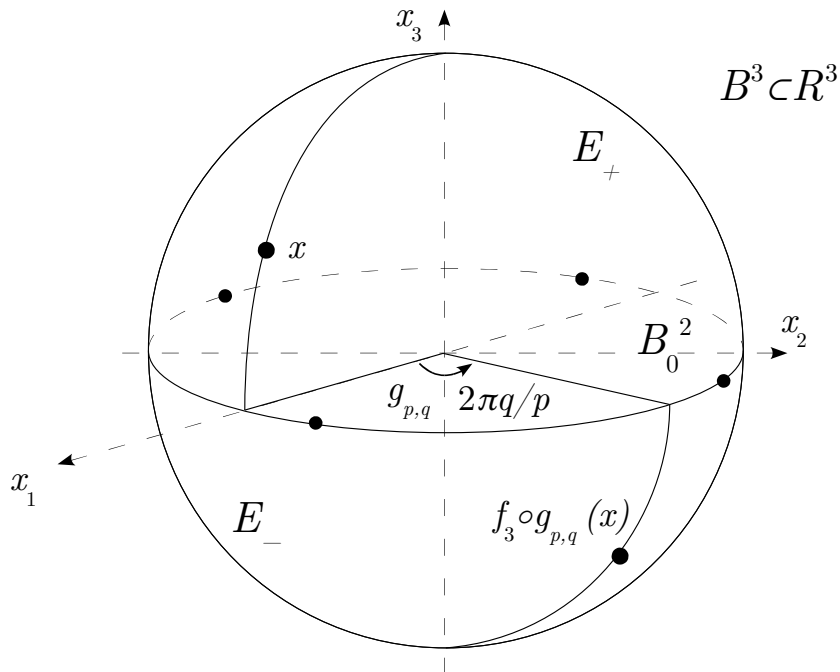
Figure 1.1: Representation of $L(p,q)$.

The *lens space* $L(p,q)$ is the quotient of B^3 by the equivalence relation on ∂B^3 which identifies $x \in E_+$ with $f_3 \circ g_{p,q}(x) \in E_-$. The quotient map is denoted by $F\colon B^3 \to L(p,q) = B^3/\sim$. Note that on the equator $\partial B_0^2 = E_+ \cap E_-$ each equivalence class contains p points, instead of the two points contained in the equivalence classes of points outside the equator. The first example is $L(1,0) \cong \mathbf{S}^3$ and the second example is $L(2,1) \cong \mathbb{RP}^3$, where the construction gives the usual model of the projective space: opposite points on ∂B^3 are identified.

1.3   Quotient of $\mathbf{S}^3$ model

Another classical model for the lens space is the following: consider $\mathbf{S}^3$ as the join of two copies of $\mathbf{S}^1$ (in a Hopf link configuration), denote with $G_{p,q}$ the cyclic group generated by the action corresponding to the rotation

of $2\pi/p$ radians of the first circle and of $2\pi q/p$ radians of the second one, according to Figure 1.2. Clearly $G_{p,q}$ is isomorphic to $\mathbb{Z}_p$ and it acts freely, in a properly discontinuous way on $\mathbf{S}^3$. Therefore the quotient space is a 3-manifold that indeed results to be the lens space $L(p,q)$. Denote with $P\colon \mathbf{S}^3 \to L(p,q)$ the quotient map.
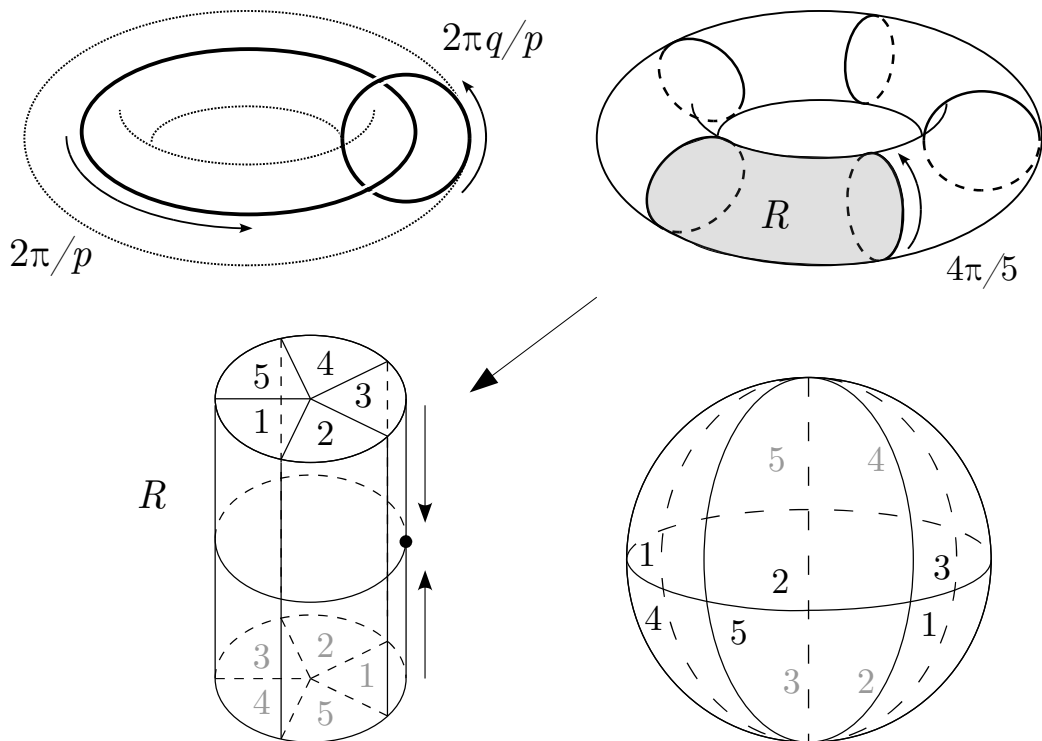
Figure 1.2: Lens space $L(5,2)$ from the solid torus model of $\mathbf{S}^3$.

Remark 1.4 (Equivalence with lens model). The proof of the equivalence of these two constructions can be found in [111], and since it is relevant for our purpose, we shall remember it briefly here. The construction of $\mathbf{S}^3$ as the join of two circles is the following: $\mathbf{S}^3 = \mathbf{S}^1 \times \mathbf{S}^1 \times [0,1]/\sim_J$, where $\sim_J$ is the equivalence relation defined by $(a_1, b, 0) \sim_J (a_2, b, 0)$ for all $a_1, a_2 \in \mathbf{S}^1, b \in \mathbf{S}^1$ and $(a, b_1, 1) \sim_J (a, b_2, 1)$ for all $a \in \mathbf{S}^1, b_1, b_2 \in \mathbf{S}^1$. It is essential to visualize the two circles in a Hopf configuration. This model of $\mathbf{S}^3$ is equivalent to the following one: considering the solid torus $\mathbf{S}^1 \times B^2$, for each $Q \in \mathbf{S}^1 = \partial B^2$,

each parallel $\mathbf{S}^1 \times \{Q\}$ of the torus $\mathbf{S}^1 \times \partial B^2$ collapses to the point Q. Under this equivalence, the first circle of the join can be thought of as $\mathbf{S}^1 \times \{(0,0)\}$ while the second circle can be thought of as $\{P\} \times \partial B^2 / \sim_J$, with $P \in \mathbf{S}^1$.

The effect of the action of $G_{p,q}$ on this model of $\mathbf{S}^3$ is the following: the circle $\mathfrak{l} = \mathbf{S}^1 \times \{(0,0)\}$ of the solid torus is rotated by $2\pi/p$ radians, thus we identify p equidistant copies of a meridian disk. The second $\mathbf{S}^1$, visualized as a meridian $\mathfrak{m} = \{P\} \times \partial B^2$ of the torus, is rotated by $2\pi q/p$ radians, thus each of the p copies of the meridian disk is identified with a rotation of $2\pi q/p$ radians.

As Figure 1.2 shows, a fundamental domain under this action is a solid truncated cylinder $R = [0,1] \times B^2$ with identification on the boundary, precisely each segment $[0,1] \times \{Q\}$ (with $Q \in \partial B^2$) of the lateral surface collapses to the point $\{1/2\}$, and the top and the bottom disks are identified with each other after a rotation of $2\pi q/p$ radians; in this way we can recognize the first model of the lens space.

1.4   Genus one Heegaard splitting model

Heegaard splittings are one of the most powerful methods to represent 3-manifolds. They consist of two handlebodies of genus g connected by an homeomorphism of their boundaries. The lens spaces are the class of 3-manifolds that can be described by genus one Heegaard splittings: consider two copies V_1 and V_2 of a solid torus $V = \mathbf{S}^1 \times B^2$, a genus one Heegaard splitting $V_1 \cup_{\varphi_{p,q}} V_2$ of the lens space $L(p,q)$ is the gluing of the two solid tori V_1 and V_2 via the homeomorphism of their boundaries $\varphi_{p,q} \colon \partial V_2 \to \partial V_1$ that sends the curve β to the curve $q\beta + p\alpha$. In Figure 1.3 it is illustrated the case $L(5,2)$.

Remark 1.5 (Equivalence with lens model). Figure 1.4 explains how to get the presentation of $L(5,2)$ via Heegaard splitting starting from the lens model, and vice versa. The visualization of the general case $L(p,q)$ is left to the reader.
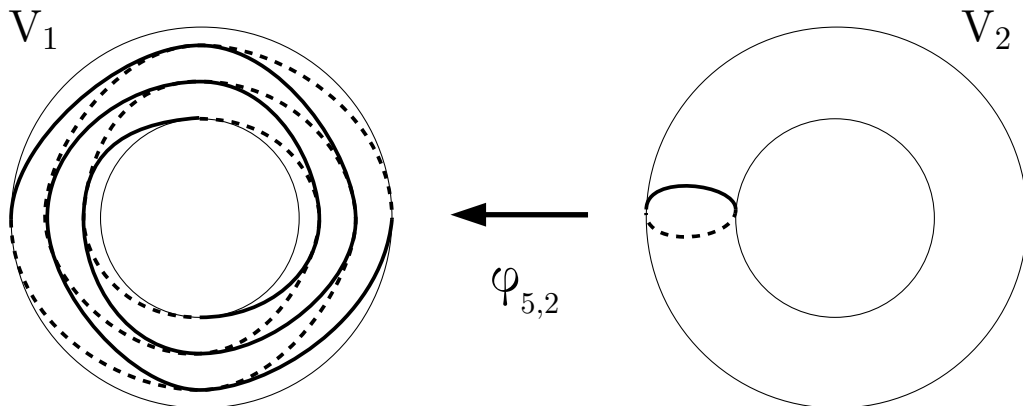
Figure 1.3: Heegaard splitting of $L(5,2)$.

1.5   Dehn surgery model

Dehn surgery is a remarkable method that describes 3-manifolds using knots and links. Since we are interested only in the rational surgery over the unknot U, we describe here only this case.

An embedding of a circle in $\mathbf{S}^3$ is said to be the *unknot U* if it bounds a disk. Considering the ϵ-neighborhood of U, that is a solid torus H_1, we can remove it from $\mathbf{S}^3$ and then paste it back by an homeomorphism between the boundaries that identify the original meridian β of T to the curve $p\beta + q\alpha$. We denote this surgery operation by labeling U with the framing p/q (see Figure 1.5), and from this construction arise the 3-manifold $L(p,q)$.

Remark 1.6 (Equivalence with Heegaard splitting model). Since the standard genus one Heegaard splitting of $\mathbf{S}^3$ is the one where the homeomorphism sends a meridian β to a parallel α of the boundary torus, then it is enough to exchange the role of α and β of the description of the genus one Heegaard splitting of the lens space to get the rational Dehn surgery over the unknot.
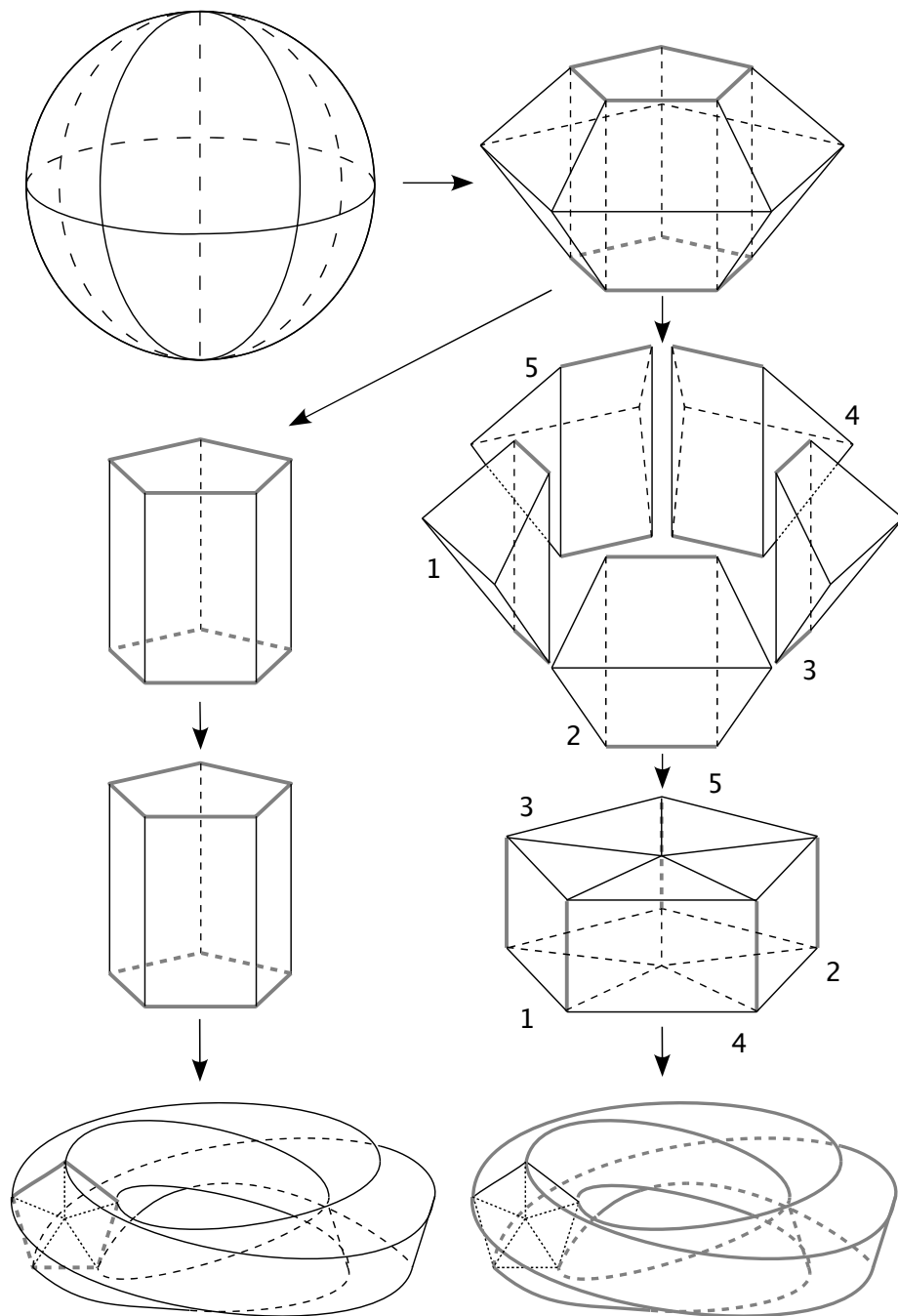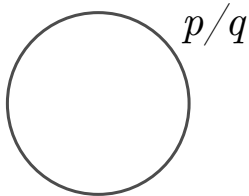
Figure 1.4: From the lens model to Heegaard splitting.

Figure 1.5: Rational surgery over the unknot for $L(p,q)$.

1.6 Results about lens spaces

In this paragraph we will present classical theorems about lens spaces.

Proposition 1.7. [62] *The fundamental group $\pi_1(L(p,q),*)$ is isomorphic to $\mathbb{Z}_p$, where $*$ is any point of $L(p,q)$. The homology groups of the lens spaces are:*

- $H_0(L(p,q)) \cong \mathbb{Z}$;
- $H_1(L(p,q)) \cong \mathbb{Z}_p$;
- $H_2(L(p,q)) \cong 0$;
- $H_3(L(p,q)) \cong \mathbb{Z} \implies L(p,q)$ is orientable.

Therefore two lens spaces $L(p,q)$ and $L(p',q')$, if $p \neq p'$, are neither homeomorphic nor of the same homotopy type. The classification has been obtained using Reidemeister torsion.

Proposition 1.8. [14] *The lens space $L(p,q)$ is homeomorphic to another lens space $L(p',q')$ if and only if*

$$p = p' \ and \ \begin{cases} q \equiv \pm q' \bmod p \\ qq' \equiv \pm 1 \bmod p. \end{cases}$$

Proposition 1.9. [112] *The lens space $L(p,q)$ has the same homotopy type of $L(p',q')$ if and only if $p = p'$ and $\pm qq'$ is a quadratic residue* mod p.

For example, $L(5,1)$ and $L(5,2)$ are neither homeomorphic nor with the same homotopy type, while $L(7,1)$ and $L(7,2)$ are still not homeomorphic, but they are homotopy equivalent, since $1 \cdot 2 \equiv 3^2 \bmod 7$.

Chapter 2

Links in lens spaces

In this chapter we overview the definition of links in lens spaces, and we show several presentations for them that can be found in literature: mixed link diagrams, band diagrams and grid diagrams.

2.1 General definitions

A link L in a 3-manifold M is a pair (M, L), where L is a submanifold of M diffeomorphic to the disjoint union of ν copies of $\mathbf{S}^1$, with $\nu > 0$. We call *component* of L each connected component of the topological space L. When $\nu = 1$ the link is called a *knot*. We usually refer to $L \subset M$ meaning the pair (M, L). A link $L \subset M$ is *trivial* if its components bound embedded pairwise disjoint 2-disks $B_1^2, \ldots, B_\nu^2$ in M.

There are at least two possible definitions of link equivalence. The one we are going to use throughout the thesis is the equivalence by ambient isotopy: two links $L, L' \subset M$ are called *equivalent* if there exists a smooth map $H \colon M \times [0, 1] \to M$ where, if we define $h_t(x) := H(x, t)$, then $h_0 = id_M$, $h_1(L) = L'$ and h_t is a diffeomorphism of M for each $t \in [0, 1]$.

Anyway in some cases it will also be useful to consider the equivalence by diffeomorphism of pairs. Two links L and L' in M are *diffeo-equivalent* if there exists a diffeomorphism of pairs $h : (M, L) \to (M, L')$, that is to say a

diffeomorphism $h : M \to M$ such that $h(L) = L'$. It is not necessary that the diffeomorphism is orientation preserving.

Remark 2.1. Two equivalent links L and L' in M are necessarily diffeo-equivalent, since from the ambient isotopy $H \colon M \times [0,1] \to M$, the map $h_1 \colon (M, L) \to (M, L')$ is a diffeomorphism of pairs.

The two definitions are equal for links in $\mathbf{S}^3$ up to an orientation reversing diffeomorphism. For the lens spaces, this is no more true, as we can see from the construction of the diffeotopies group of lens spaces made by [13] and [66].

The setting of this thesis is the *Diff* category (of smooth manifolds and smooth maps). Every result also holds in the *PL* category, and in the *Top* category if we consider only tame links, that is to say, we exclude situations like the one of Figure 2.1 (wild knots).
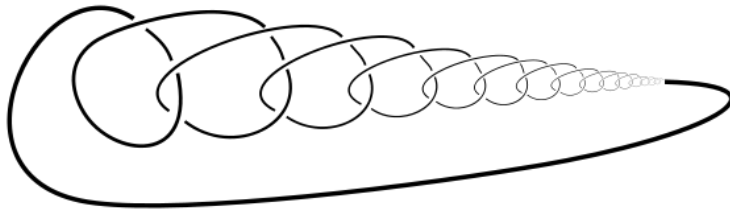
Figure 2.1: Example of wild knot.

Links in 3-manifolds can also be oriented, therefore throughout the thesis we will state each time whether it will be necessary a specification of the orientation or not.

The case $M = \mathbf{S}^3$ is the classical knot theory and it has been intensively studied. The best way to represent a knot in the 3-sphere is the planar diagram obtained by a "regular" projection of the knot onto a plane. On this diagram, the equivalence problem reduces to Reidemeister theorem.

Theorem 2.2. [1, 97] *Two links L and L' in $\mathbf{S}^3$ are equivalent if and only if their diagrams can be connected by a finite sequence of the three Reidemeister moves described in Figure 2.2.*
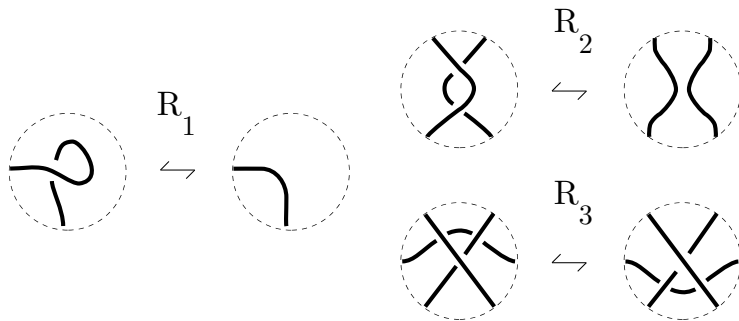
Figure 2.2: Reidemeister moves.

These and other results on knots in the 3-sphere can be found with many details in [16].

Now let us turn our attention to links in lens spaces. Before seeing some diagrams for them, we adapt the definitions of certain link constructions to the case of lens spaces.

Local and split links   A link $L \subset L(p,q)$ is *local* if it is contained inside a 3-ball. The definition of split links in $\mathbf{S}^3$ can be generalized to lens spaces: a link $L \subset L(p,q)$ is *split* if there exists a 2-sphere in the complement $L(p,q) \smallsetminus L$ that separates one or more components of L from the other ones. The 2-sphere separates $L(p,q)$ into a ball $\hat{B}^3$ and $\overline{L(p,q) \smallsetminus \hat{B}^3}$; as a consequence, a split link is the disjoint union of a local link and of another link in lens space.

Satellite and cable links   We can easily generalize the definition of satellite knot to lens space, following Section C, Chapter 2 of [16]. Take K_p a knot in the solid torus T that is neither contained inside a 3-ball nor it is the core of the solid torus, and call it *pattern*. Let $e\colon T \to L(p,q)$ be an embedding such that $e(T)$ is the tubular neighborhood of a non-trivial knot $K_c \subset L(p,q)$. The knot $K := e(K_p) \subset L(p,q)$ is the *satellite* of the knot K_c, called *companion* of K. The satellite of a link can be constructed by specifying the pattern of each component. In addition the pattern of a satellite

knot can be a link too. A *cable* link is a satellite knot with a torus link as
pattern.

Composite and prime links   Consider two knots $K_1 \subset L(p,q)$ and $K_2 \subset$
$\mathbf{S}^3$, let P_i be a point on K_i, and (B_i^3, B_i^1) a regular neighborhood of P_i for
$i = 1, 2$ respectively in $(L(p,q), K_1)$ and in $(\mathbf{S}^3, K_2)$. The *connected sum* of
two knots K_1 and K_2 in $L(p,q)$, denoted by $K_1 \sharp K_2$, is still a knot, obtained
from the disjoint union of the manifold pairs $(L(p,q) \smallsetminus \operatorname{int}(B_1^3), K_1 \smallsetminus \operatorname{int}(B_1^1))$
and $(\mathbf{S}^3 \smallsetminus \operatorname{int}(B_2^3), K_2 \smallsetminus \operatorname{int}(B_2^1))$, pasting their boundaries along an orientation
reversing homeomorphism $\varphi : (\partial B_2^3, \partial B_2^1) \to (\partial B_1^3, \partial B_1^1)$. In order to define
the connected sum for links we have to specify the component of each link
on which we choose the attaching points. A *prime* link is a link $L \subset L(p,q)$
such that, if $L = L_1 \sharp L_2$ then necessarily either L_1 or L_2 is the trivial knot.

2.2   Mixed link diagrams

Rational Dehn surgery on a knot K in $\mathbf{S}^3$, with coefficient p/q, is the
following topological operation: take a tubular neighborhood of K, cut it out
of $\mathbf{S}^3$ and re-paste it back, sending a meridian of this torus to the (p,q)-torus
knot around it. The result is a 3-manifold $M(K)_{p,q}$. This operation can be
generalized to links and a theorem of Lickorish and Wallace states that every
3-manifold can be obtained by surgery on some link. Another interesting
result states that two links with surgery coefficients representing the same
manifold can be transformed one into the other by two moves, the Kirby
moves. These results are clearly exposed for example in [95, §19].

The notion of mixed link diagram for links in 3-manifolds is common and
can be found for example in [77]. A *mixed link diagram* of a link $L \cup J$ is a
classical diagram of $L \cup J$ in $\mathbf{S}^3$, where every component of J is marked, that
is to say, if we call $J_1, \ldots, J_\mu$ the connected components of J, then every
connected component J_i is decorated with a framing index of surgery m_i.
The link J is called the *surgery link*.

The surgery description of lens spaces can be done by a rational p/q surgery over the unknot U, so a link L in $L(p, q)$ can be described by a mixed link diagram of the link $L \cup U$. An example can be seen in Figure 2.3. Any other surgery description of lens spaces can be reduced to this one by Kirby moves.
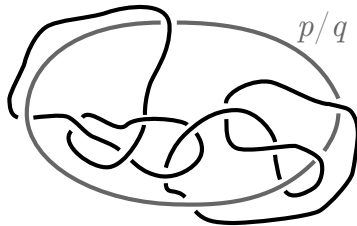
Figure 2.3: Example of a mixed link diagram of a link in $L(p, q)$.

For mixed link diagrams of this kind, the Reidemeister-type moves can be reduced to the classical Reidemeister moves R_1, R_2 and R_3 over the projection of $L \cup U$ and one additional move, usually called SL (slide move) that tells us what happens when an overpass of L crosses U: instead of one underpass, a (p, q)-torus knot along U arises. This is a simplification of Theorem 5.8 of [77].

2.3   Band diagrams

Band diagrams were introduced in [67], while the equivalent representation of punctured disk diagrams can be found in [50].

Consider the link L in the lens space $L(p, q)$ described with rational surgery over the unknot U, that is to say, consider the mixed link $L \cup U \subset \mathbf{S}^3$. Let x be a point of U and send it to ∞ in order to describe $\mathbf{S}^3$ with the one-point compactification of $\mathbb{R}^3$. Let (x_1, x_2, x_3) be the coordinates of $\mathbb{R}^3$. Assume that U is now described by the x_3 axis. Consider the orthogonal projection $\mathbf{p}$ of L on the $x_1 x_2$ plane. Up to small isotopies on L, we can assume that this projection is *regular*, that is to say:

1) the projection of L contains no cusps;

2) all auto-intersections of $\mathbf{p}(L)$ are transversal;

3) the set of multiple points is finite, and all of them are actually double points.

The *punctured disk diagram* of $L \subset L(p,q)$ is a regular projection of L, with the addition of a dot representing the projection of U (see an example in Figure 2.4).
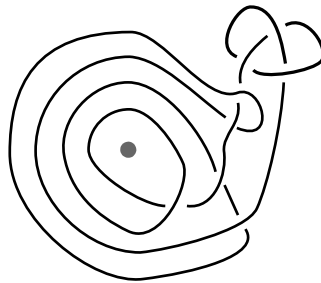
Figure 2.4: An example of punctured disk diagram for a link in lens space.

If we just consider a dotted diagram without surgery, we are describing links in the solid torus [51].

A *band diagram* for a link $L \subset L(p,q)$ is obtained from a punctured disk diagram of L through the following construction: suppose that all the arc projections are contained inside a disk in the plane $x_1 x_2$ and remove a small disk around the fixed dot, in order to get an annulus containing the diagram of L. Then cut this annulus along a line orthogonal to the boundary and avoiding the crossings of L. Finally, deform the annulus into a rectangle: this is a band diagram of L (see an example in Figure 2.5). By reversing this operation we can obtain a punctured disk diagram from a band diagram of a link in a lens space.

Reidemeister-type moves for this diagrams are described in [67], but is better to represent them on punctured disk diagrams as in [50]. They are really similar to the moves on mixed link diagrams described in Section 2.2
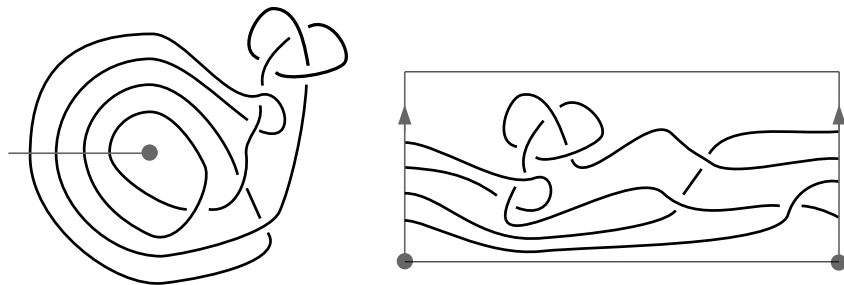
Figure 2.5: Deforming a punctured disk diagram to get a band diagram.

and they work in the following way: besides the classical three Reidemeister moves, there is a fourth SL move (slide move). This move acts in the following way: when a strand crosses the dot, a (p, q)-torus knot that contains all the diagram is added to that strand (see an example in Figure 2.6).
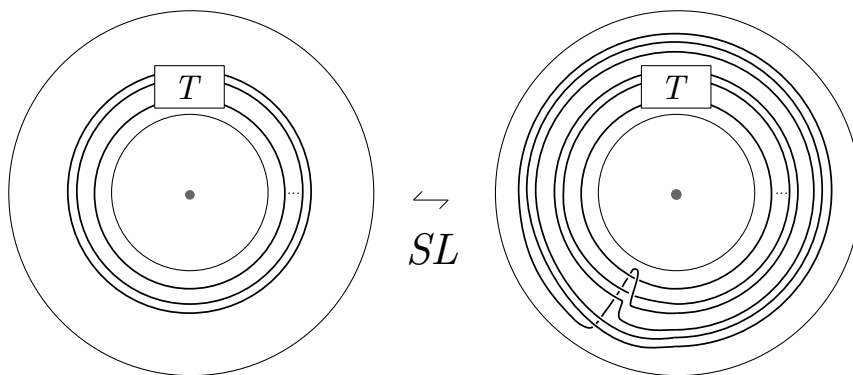
Figure 2.6: SL move on punctured disk diagram for the case $L(3, 1)$.

2.4 Grid diagrams

Grid diagrams for links in the 3-sphere have a long history and are known also as asterisk presentations, fences and arc presentations. They were used to describe links in lens spaces for the first time in [6]. The key idea is a

projection of the link on the separating torus of the genus one Heegaard splitting of $L(p,q)$, where the arcs of the projection consist of an orthogonal piecewise linear approximation.

Grid diagram of links in lens space   A *(toroidal) grid diagram G* in $L(p,q)$ with grid number n is a quintuple $(T, \boldsymbol{\alpha}, \boldsymbol{\beta}, \mathbb{O}, \mathbb{X})$ that satisfies the following conditions (see an example with grid number 3 in $L(4,1)$ in Figure 2.7)
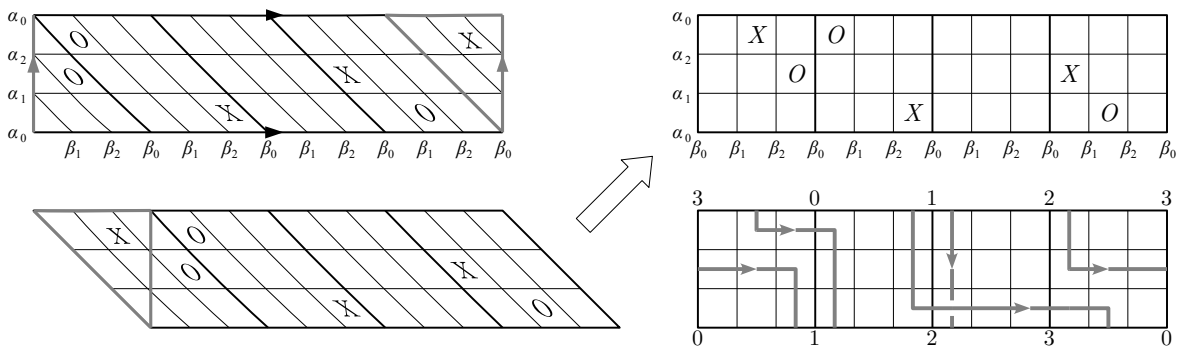
Figure 2.7: From a grid diagram with grid number 3 to its corresponding link in $L(4,1)$.

- T is the standard oriented torus $\mathbb{R}^2/\mathbb{Z}^2$, where $\mathbb{Z}^2$ is the lattice generated by the vectors $(1,0)$ and $(0,1)$;

- $\boldsymbol{\alpha} = \{\alpha_0, \dots, \alpha_{n-1}\}$ are the images in T of the n lines in $\mathbb{R}^2$ described by the equations $y = i/n$, for $i = 0, \dots, n-1$; the complement $T \smallsetminus (\alpha_0 \cup \dots \cup \alpha_{n-1})$ has n connected annular components, called the *rows* of the grid diagram;

- $\boldsymbol{\beta} = \{\beta_0, \dots, \beta_{n-1}\}$ are the images in T of the n lines in $\mathbb{R}^2$ described by the equations $y = -\frac{p}{q}(x - \frac{i}{pn})$, for $i = 0, \dots, n-1$; the complement $T \smallsetminus (\beta_0 \cup \dots \cup \beta_{n-1})$ has n connected annular components, called the *columns* of the grid diagram;

- $\mathbb{O} = \{O_0, \dots, O_{n-1}\}$ (resp. $\mathbb{X} = \{X_0, \dots, X_{n-1}\}$) are n points in $T \smallsetminus (\boldsymbol{\alpha} \cup \boldsymbol{\beta})$ called *markings*, such that any two points in $\mathbb{O}$ (resp.

$\mathbb{X}$) lie in different rows and in different columns.

In order to make the identifications of the diagram boundary easier to understand, it is possible to perform the "shift" illustrated in Figure 2.7. Notice that, if we omit the $L(p, q)$ identifications, the curve β_0 divides the rectangle of a grid diagram into p adjacent squares, that we will call *boxes* of the diagram.

The following construction explains why a grid diagram G represents an oriented link $L \subset L(p, q)$. In the case of non-oriented links, you can exchange the X with the O markings. Denote with V_1 and V_2 the two solid tori having, respectively, $\boldsymbol{\alpha}$ and $\boldsymbol{\beta}$ as meridians. Clearly $V_1 \cup_{\varphi_{p,q}} V_2$ is a genus one Heegaard splitting representing $L(p, q)$. Then connect

(1) each X_i to the unique O_j lying in the same row with an arc embedded in the row and disjoint from the curves of $\boldsymbol{\alpha}$, and

(2) each O_j to the unique X_l lying in the same column by an arc embedded in the column and disjoint from the curves of $\boldsymbol{\beta}$,

obtaining a multicurve immersed in T. Finally remove the self-intersections, pushing the lines of (1) into V_1 and the lines of (2) into V_2. The orientation on L is obtained by orienting the horizontal arcs connecting the markings from the X to the O. An example in $L(4, 1)$ can be seen in Figure 2.7.

Notice that, the presence in the grid diagram of a pair of marking X and O in the same position corresponds to a trivial component of the represented link (see the bottom row of the first box of Figure 9.6).

By Theorem 4.3 of [6], each link $L \subset L(p, q)$ can be represented by a grid diagram. The idea of the proof is a PL-approximation with orthogonal lines of the link projection on the torus.

Equivalence moves for grid diagrams A *grid (de)stabilization* is a move that (decreases) increases by one the grid number. Figure 2.8 shows an example in $L(5, 2)$ of a $X : NW$ grid (de)stabilization, where X is the grid marking chosen for the stabilization and NW refers to the arrangement of

the new markings. Of course, we can have also (de)stabilization with respect to O markings and with NE, SW and SE arrangements.

	X			O

		X					O
		X	O				

Figure 2.8: An example of $X : NW$ (de)stabilization in $L(5,2)$.

A grid diagram *commutation* interchanges either two adjacent columns or two adjacent rows as follows. Let A be the annulus containing the two considered columns (or rows) c_1 and c_2. The annulus is divided into pn parts by the rows (columns). Let s_1 and s_2 be the two bands of the annulus containing the markings of c_1. Then the commutation is *interleaving* if the markings of c_2 are in different components of $A - s_1 - s_2$, and *non-interleaving* otherwise (see Figure 2.9).
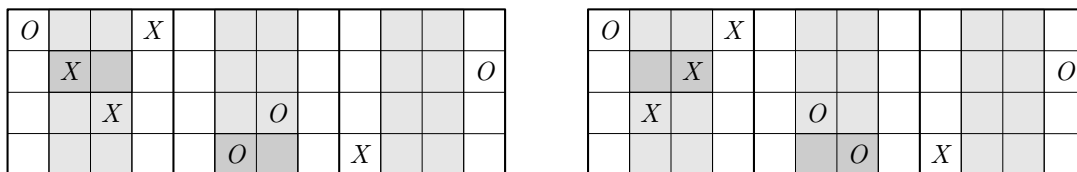
Figure 2.9: An example of non-interleaving commutation in $L(3,1)$.

Proposition 2.3. [5] *Two grid diagrams of links in $L(p,q)$ represent the same link if and only if there exists a finite sequence of (de)stabilizations and non-interleaving commutations connecting the two grid diagrams.*

There are also two other hidden moves on a grid diagram, depending directly on the projection of the link on the Heegaard torus: we can make a *cyclic permutation* of the rows or of the columns – following the pasting of the torus – and we can do a *reverse connection* by connecting the grid markings also in the opposite direction.

Chapter 3

Disk diagram and Reidemeister-type moves

In 1991, Drobotukhina introduced a disk diagram for knots and links in the projective space $\mathbb{RP}^3 \cong L(2,1)$. Using this diagram, she found a Jones polynomial [42] and a tabulation of prime non-local knots in $\mathbb{RP}^3$ [43]. Other authors showed interesting results working on this diagram [69, 91, 92, 58, 59]. Since this disk diagram can be generalized to links in lens spaces, we decided to study it in order to find further invariants of links in lens spaces.

In this chapter this new disk diagram for links in lens spaces is introduced and a generalization of the Reidemeister moves to lens spaces is obtained, with a proof similar to the one of Roseman [100]. One of these moves allows the reduction of the disk diagram to a standard form. Moreover we show the connection of this disk diagram with other representations of links in lens spaces, such as band and grid diagrams.

The connection between disk diagram and mixed link diagram is omitted. It is quite simple to transform a punctured disk diagram into a mixed link diagram and vice versa; as a consequence, it is enough to study the equivalence between disk and band diagrams.

In this chapter all links in $L(p,q)$ are considered up to ambient isotopy and up to link orientation, unless the ending section on grid diagrams.

3.1   Disk diagram

In this section, we improve the definition of diagram for links in lens spaces given by Gonzato [56]. This exposition is reported in [19]. Let us assume $p > 1$, since the case of $\mathbf{S}^3$ is not of our interest. Let L be a link in the lens space $L(p, q)$ described by the lens model of Section 1.2. Remember that $F\colon B^3 \to L(p, q)$ is the quotient map and consider $L' = F^{-1}(L)$. By moving L via a small isotopy in $L(p, q)$, we can suppose that:

i) L' does not meet the poles N and S of B^3;

ii) $L' \cap \partial B^3$ consists of a finite set of points;

iii) L' is not tangent to ∂B^3;

iv) $L' \cap \partial B_0^2 = \emptyset$.

The small isotopy that allows L' to avoid the equator ∂B_0^2 is illustrated in Figure 3.1.
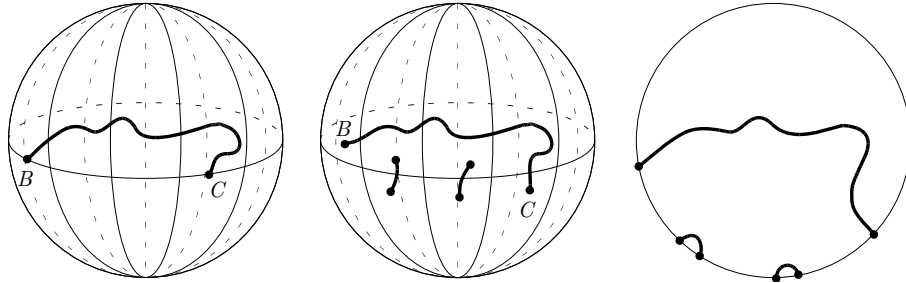
Figure 3.1: Avoiding ∂B_0^2 in $L(9, 1)$.

As a consequence, L' is the disjoint union of closed curves in $\mathrm{int}\, B^3$ and arcs properly embedded in B^3. Let $\mathbf{p}\colon B^3 \smallsetminus \{N, S\} \to B_0^2$ be the projection defined by $\mathbf{p}(x) = c(x) \cap B_0^2$, where $c(x)$ is the circle (possibly a line) through N, x and S. Take L' and project it using $\mathbf{p}_{|L'}\colon L' \to B_0^2$. As in the classical link projection, taken a point $P \in \mathbf{p}(L')$, its counterimage $\mathbf{p}^{-1}(P)$ in L' may contain more than one element, in this case we say that P is a *multiple* point; moreover when $\mathbf{p}^{-1}(P)$ contains exactly two points, P is a *double* point.

We can assume, by moving L via a small isotopy, that the projection $\mathbf{p}_{|L'} \colon L' \to B_0^2$ of L is *regular*, namely:

1) the projection of L' contains no cusps;
2) all auto-intersections of $\mathbf{p}(L')$ are transversal;
3) the set of multiple points is finite, and all of them are actually double points;
4) no double point is on ∂B_0^2.

Finally, double points are represented by underpasses and overpasses as in the diagram for links in $\mathbf{S}^3$. A *disk diagram* of a link L in $L(p,q)$ is a regular projection of $L' = F^{-1}(L)$ on the equatorial disk B_0^2, with specified overpasses and underpasses. Note that for the case $L(2,1) \cong \mathbb{RP}^3$ we get exactly the diagram described in [42].
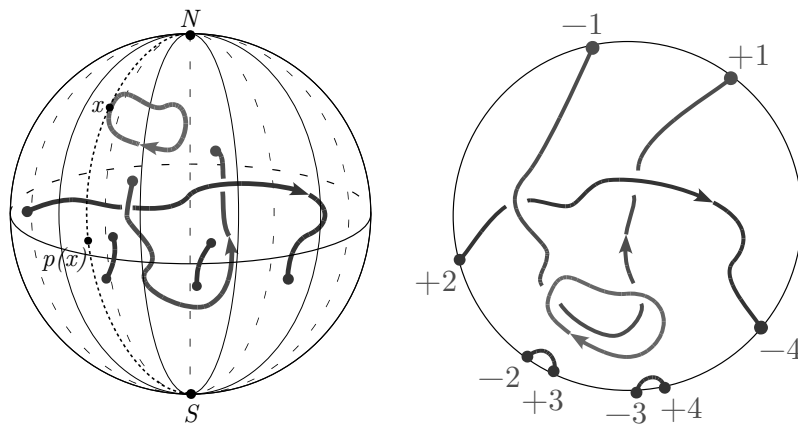
Figure 3.2: A link in $L(9,1)$ and its corresponding disk diagram.

In order to have a more comprehensible diagram (even if this is not a necessary operation), we index the boundary points of the projection as follows: at first, we assume that the equator ∂B_0^2 is oriented counterclockwise if we look at it from N, then, according to this orientation, we label with $+1, \dots, +t$ the endpoints of the projection of the link coming from the upper hemisphere, and with $-1, \dots, -t$ the endpoints coming from the lower hemisphere, respecting the rule $+i \sim -i$. An example is shown in Figure 3.2.

3.2   Generalized Reidemeister moves

In this section, published in [19], a Reidemeister-type theorem is shown for links in lens spaces. The *generalized Reidemeister moves* on a diagram of a link $L \subset L(p,q)$, are the moves $R_1, R_2, R_3, R_4, R_5, R_6$ and R_7 of Figure 3.3. Observe that, when $p = 2$ the moves R_5 and R_6 are equal, and R_7 is a trivial move.

Theorem 3.1. *Two links L_0 and L_1 in $L(p,q)$ are equivalent if and only if their diagrams can be joined by a finite sequence of generalized Reidemeister moves $R_1, \ldots, R_7$ and diagram isotopies, when $p > 2$. If $p = 2$, moves $R_1, \ldots, R_5$ are sufficient.*

Proof. On one hand, it is easy to see that each Reidemeister move connects equivalent links, hence a finite sequence of Reidemeister moves and diagram isotopies does not change the equivalence class of the link.

On the other hand, if we have two equivalent links L_0 and L_1, then there exists an isotopy of the ambient space $H \colon L(p,q) \times [0,1] \to L(p,q)$ such that $h_1(L_0) = L_1$. For each $t \in [0,1]$ we have a link $L_t = h_t(L_0)$.

The link L_t may violate conditions i), ii), iii), iv) and its projection can violate the regularity conditions 1), 2), 3) and 4), producing some singularities.

It is easy to see that the isotopy H can be chosen in such a way that conditions i) and ii) are satisfied at any time. Moreover, using general position theory (see [100] for details) we can assume that there is a finite number of singularities and that for each $t \in [0,1]$, only one of them may occur. The remaining conditions might be violated during the isotopy as illustrated in the left part of Figure 3.3. More precisely,

- conditions 1), 2) and 3) are necessary to avoid the singularities V_1, V_2 and V_3;
- condition iii) prevents the singularity V_4;
- condition 4) avoids the singularities represented in V_5 and V_6; the difference between the two configurations is that V_5 involves two arcs of
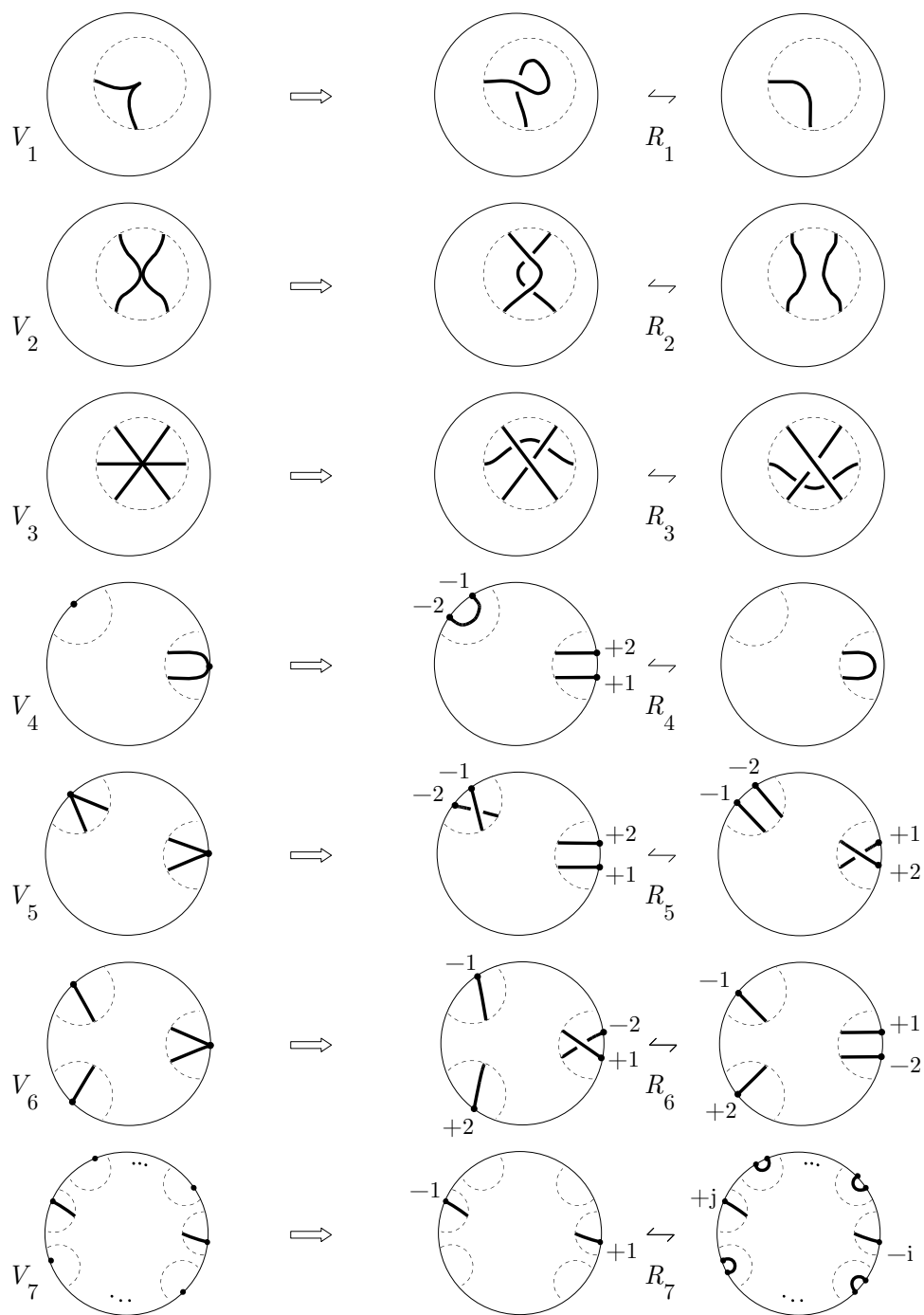
Figure 3.3: Singularities and corresponding generalized Reidemeister moves.

L' ending in the same hemisphere of ∂B^3, while V_6 involves arcs ending in different hemispheres;

– from condition iv) arises a family of singularities $V_{7,1}, \ldots, V_{7,p-1}$ (see Figure 3.4); the difference between them is that $V_{7,1}$ has the endpoints of the projection identified directly by the map $g_{p,q}$ of Section 1.2, while $V_{7,k}$ has the endpoints identified by $g_{p,q}^k$, for $k = 2, \ldots, p-1$.
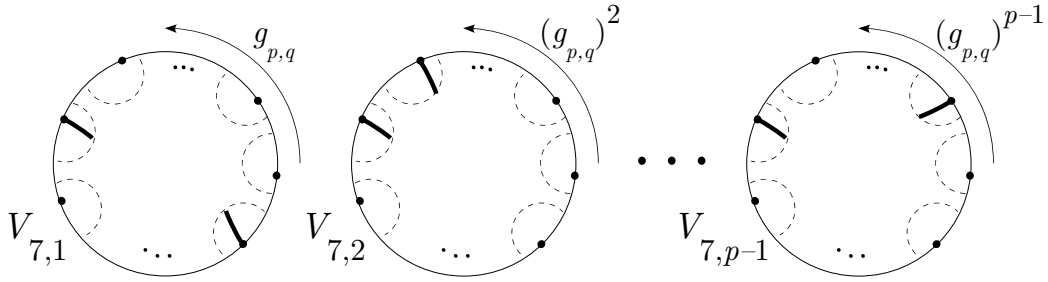
Figure 3.4: Singularities $V_{7,1}, V_{7,2}, \ldots, V_{7,p-1}$.

From each type of singularity, a generalized Reidemeister move appears as follows (see Figure 3.3):

– from V_1, V_2 and V_3 we obtain the usual Reidemeister moves R_1, R_2 and R_3;

– from V_4 we obtain move R_4;

– from V_5, we obtain two different moves: R_5 if the overpasses endpoints belong to the same hemisphere, and R_6 otherwise;

– from $V_{7,1}, \ldots, V_{7,p-1}$ we obtain the moves $R_{7,1}, \ldots, R_{7,p-1}$.

Nevertheless the moves $R_{7,2}, \ldots, R_{7,p-1}$ can be seen as the composition of $R_7 = R_{7,1}$, R_6, R_4 and R_1 moves. More precisely, the move $R_{7,k}$, with $k = 2, \ldots, p-1$, is obtained by the following sequence of moves: first we perform an R_7 move on the two overpasses corresponding to the points $+i$ and $-i$, then we repeat $k-1$ times the three moves R_6-R_4-R_1 necessary to retract the small arc having the endpoints with the same sign (see an example in Figure 3.5).
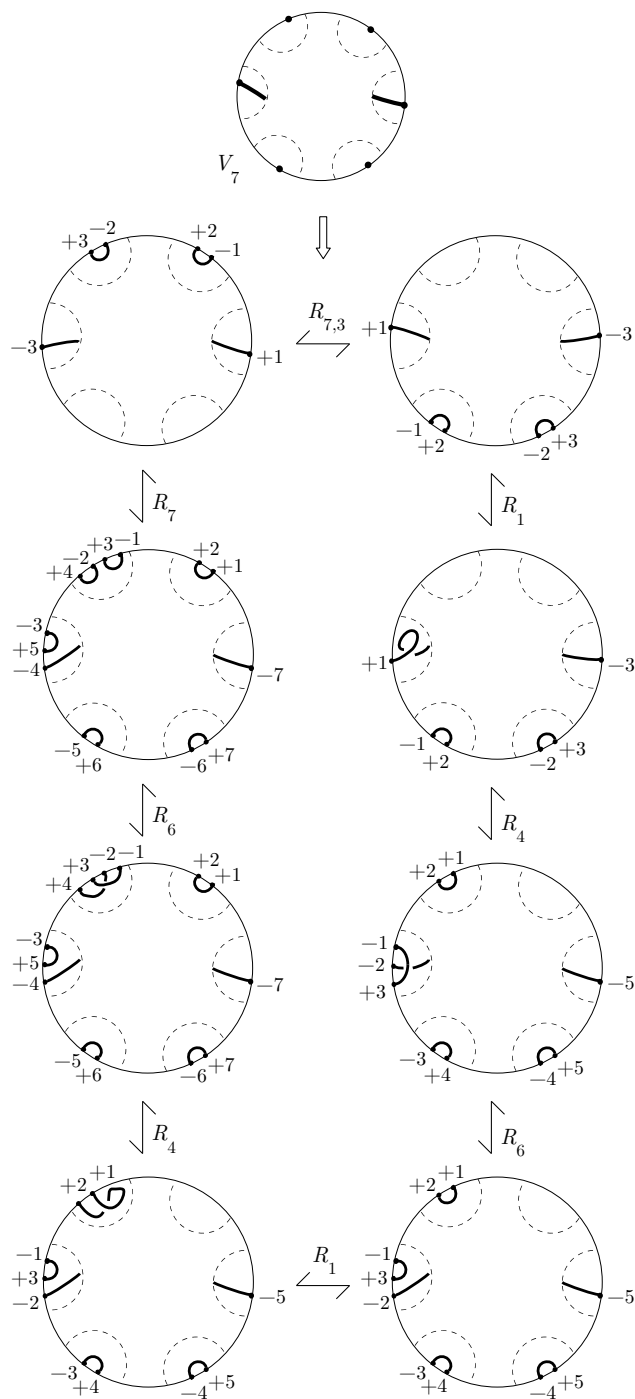
Figure 3.5: How to decompose a move $R_{7,3}$.

Therefore we can drop out $R_{7,2}, \ldots, R_{7,p-1}$ from the set of moves and keep only $R_{7,1} = R_7$. As a consequence, any pair of diagrams of two equivalent links can be joined by a finite sequence of generalized Reidemeister moves $R_1, \ldots, R_7$ and diagram isotopies. When $p = 2$, it is easy to see that R_6 coincides with R_5, and R_7 is a trivial move; so in this case moves $R_1, \ldots, R_5$ are sufficient (see also [42]). $\square$

Remark 3.2. Diagram isotopies have to respect the identifications of boundary points of the link projection. Therefore, move R_6 is possible only if there are no other arcs inside the small circles of the move R_6, as illustrated in Figure 3.3. For example, Figure 3.6 shows the case of a link in $L(3, 1)$ where the R_6 move removing the crossing cannot be performed.
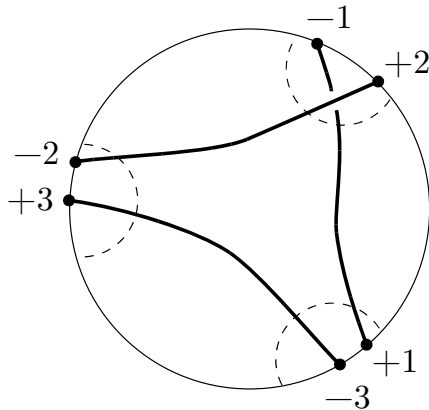
Figure 3.6: A diagram in $L(3, 1)$ where an R_6 move cannot be applied.

3.3 Standard form of the disk diagram

A disk diagram is defined *standard* if the labels on its boundary points, read according to the orientation on ∂B_0^2, are $(+1, \ldots, +t, -1, \ldots, -t)$.

Proposition 3.3. *Every disk diagram can be reduced to a standard disk diagram using some isotopy on the link: if $p = 2$, the signs of its boundary*

points can be exchanged; if $p > 2$, a finite sequence of R_6 moves can be applied in order to bring all the plus-type boundary points aside.

Proof. For $p = 2$, the exchange of the signs of a boundary point corresponds to a small isotopy on the link, that crosses the equator of B^3.

For $p > 2$, we have the following situation. By definition, the endpoints $+1, \ldots, +t$ on the boundary are always in this order if we forget the minus-type points. The endpoints $+i$ and $-i$ can be moved together along the boundary, with their respective arcs. Moreover we can assume that this small isotopy is performed close enough to the boundary that the arcs avoid the crossings. Our aim is to bring all the plus-type boundary points one aside the other, respecting their labeling order. The isotopy performed can exchange $+i$ and $-j$ producing an R_6 move.

The algorithm is the following: up to a finite sequence of R_6 moves on the points near $+1$ and $-t$, we can assume that the boundary sequence is of the type $(+1, \ldots, -t)$. In order to get the final desired sequence of boundary points $(+1, \ldots, +t, -1, \ldots, -t)$, it is enough to apply another finite sequence of R_6 moves, this time with one more attention: when we exchange $-j$ and $+i$ (with $i < j$) we move with an isotopy also the other arcs/boundary points, because we do not want to create other exchanges in the boundary sequence. An example in shown in Figure 3.7. $\qquad\square$
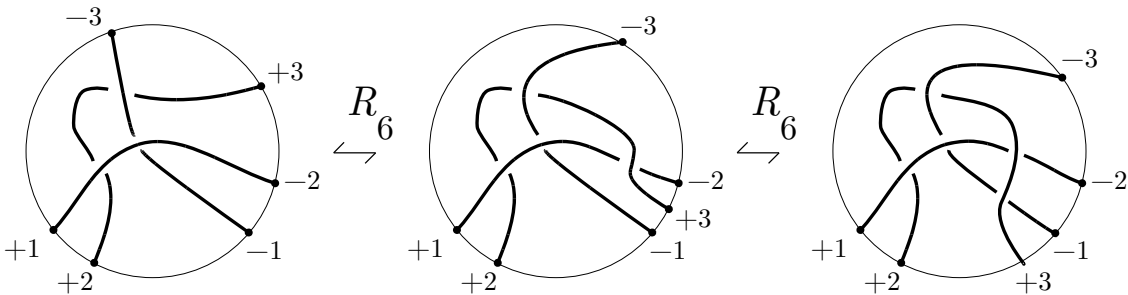
Figure 3.7: Example of R_6-reduction to standard disk diagram.

3.4   Connection with band diagram

In this section is described a geometric transformation between disk and punctured disk diagrams. This is the result of a collaboration with Bostjan Gabrovšek. The motivation of this effort is the possibility to connect our findings about links in lens spaces. The results of Section 9.2 are an outcome of this work. Since punctured disk and band diagrams are similar, it is more convenient to show the connection between disk and band diagrams.

Let B_t be the braid group on t letters and let $\sigma_1, \ldots, \sigma_{t-1}$ be the Artin generators of B_t. Consider the Garside braid Δ_t on t strands defined by $(\sigma_{t-1}\sigma_{t-2}\cdots\sigma_1)(\sigma_{t-1}\sigma_{t-2}\cdots\sigma_2)\cdots(\sigma_{t-1})$, and illustrated in Figure 3.8. It is a positive half-twist of all the braid strands. The braid Δ_t^2 belongs to the center of the braid group, that is to say, it commutes with every braid. Moreover Δ_t^{-1} can be written, after some braid operations, as

$$(\sigma_{t-1}^{-1}\sigma_{t-2}^{-1}\cdots\sigma_1^{-1})(\sigma_{t-1}^{-1}\sigma_{t-2}^{-1}\cdots\sigma_2^{-1})\cdots(\sigma_{t-1}^{-1}).$$
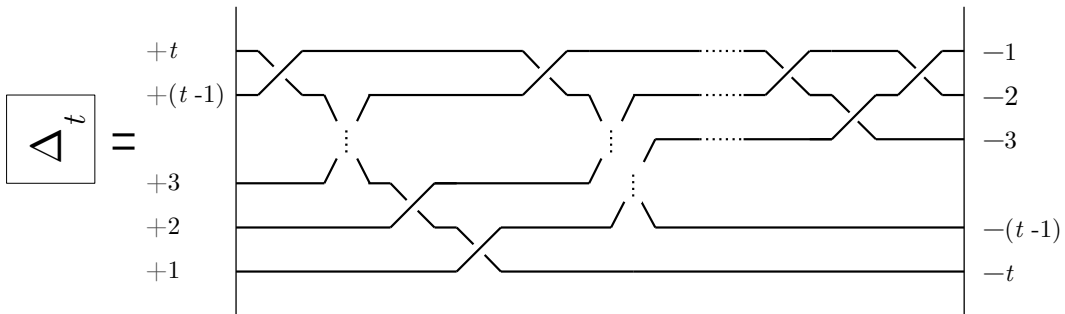
Figure 3.8: The braid Δ_t.

The following proposition explains how to transform a band diagram into a standard disk diagram.

Proposition 3.4. *Let L be a link in $L(p,q)$ assigned via a band diagram B_L. A standard disk diagram D_L representing L can be obtained with the following construction, described in Figure 3.9. Consider the band diagram*
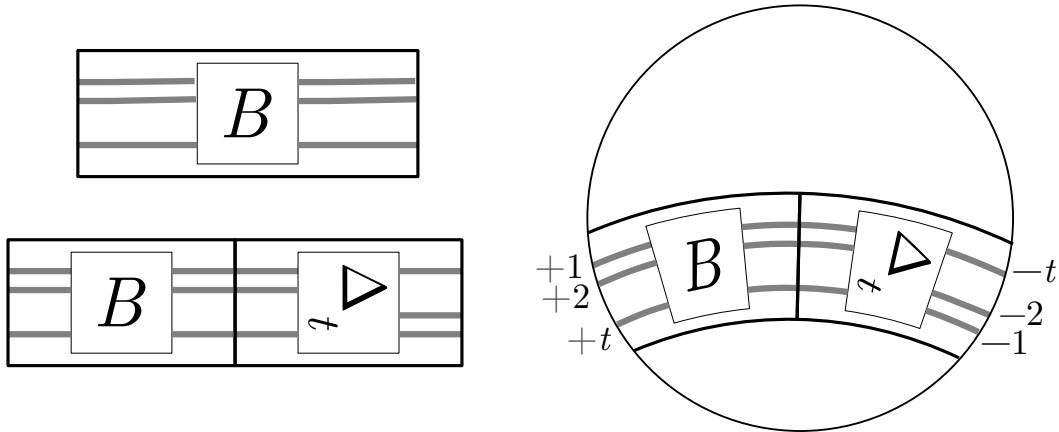
Figure 3.9: From band diagram B_L to disk diagram D_L in $L(p,q)$.

B_L, the rectangle has two opposite identified sides, with t points on each of them; add to the right side of the band diagram the braid Δ_t, then put the resulting band inside a disk, with the opposite sides of the new rectangle on the boundary of the disk. Add the indexation $+1, +2, \dots, +t$ on the points of the left side of the rectangle and $-1, -2, \dots, -t$ on the other boundary points: the result is the desired disk diagram D_L.

Proof. The band diagram may also be seen as the result of a genus one Heegaard splitting of the lens space $L(p,q)$, where the link is wholly contained inside one of the two solid tori, and it is regularly projected on an annulus which has as boundary two longitudes of the solid torus. Equivalently, as described in Figure 3.10, the band diagram may be seen as an annulus immersed in a solid torus, which has as boundary a longitude and the core. Following the geometric description of the equivalence between the Heegaard splitting model and the lens model of the lens spaces, described in Figure 1.4, we can put the band diagram in one solid torus as described by Figure 3.10, then put the solid torus inside the lens model of the lens space, and project

the band diagram onto the equatorial disk. During this operation, we have a twist, described by the braid Δ_t. Finally, adding the labels to the boundary points, we get the desired standard disk diagram D_L. $\square$
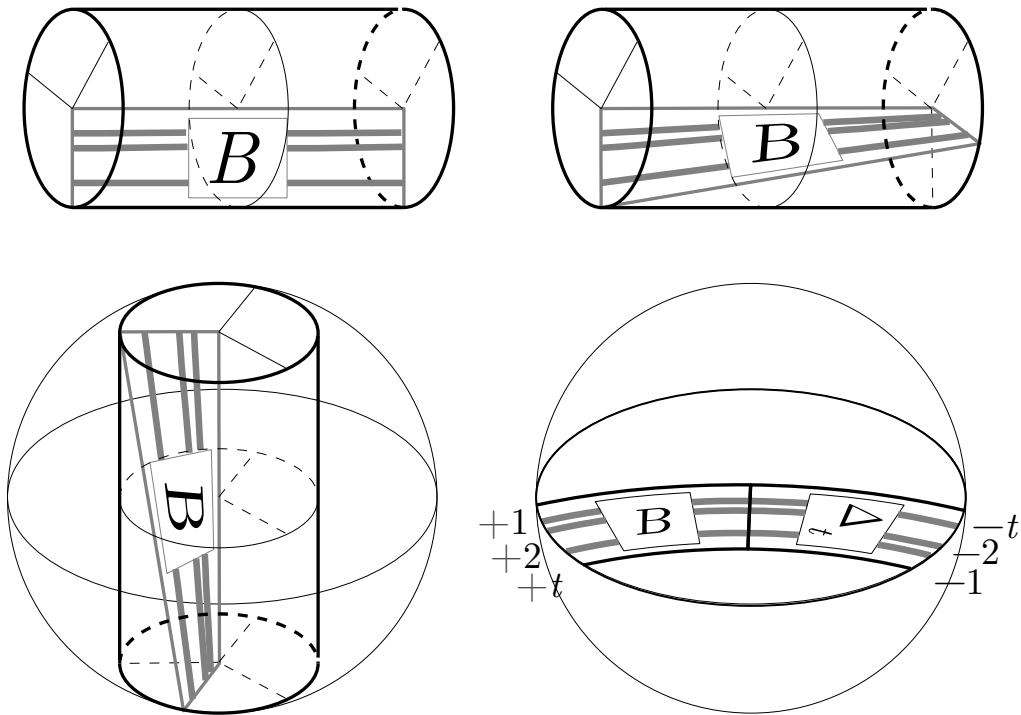
Figure 3.10: From the Heegaard splitting to the lens model of $L(p,q)$.

On the other way, when we have the disk diagram of a link $L \subset L(p,q)$, how can we recover the band diagram B_L?

Proposition 3.5. *Let L be a link in $L(p,q)$, defined by a disk diagram; let D_L be the standard disk diagram obtained from it as Proposition 3.3 suggests. A band diagram B_L for L can be constructed using the following geometric algorithm, described in Figure 3.11. Consider the disk diagram D_L and open the disk on the right of the $+1$ point, as Figure 3.11 shows; this way a rectangle is obtained, with identified points only on the left and right sides, at last add the braid Δ_t^{-1} on the right side and this is the desired band diagram for L.*
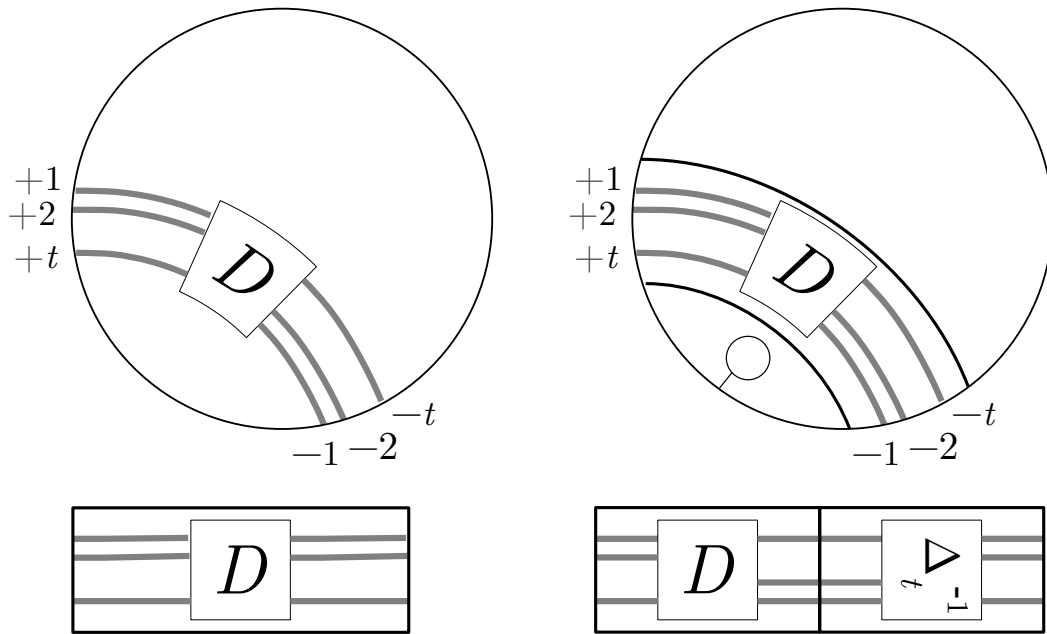
Figure 3.11: From disk diagram D_L to band diagram B_L in $L(p,q)$.

Proof. It is exactly the converse geometric construction of the proof of Proposition 3.4. □

A naif interpretation of the Reidemeister-type moves on this two kind of diagrams brings to Table 3.4.

Disk diagram	Band diagram
R_1	R_1
R_2	R_2
R_3	R_3
R_4	isotopy of an arc and R_1
R_5	isotopy of a crossing
R_6	not allowed on standard diagram
R_7	SL

3.5   Connection with grid diagram

The following two propositions describe how to transform a disk diagram into a grid diagram representing the same link and vice versa. These results are reported in [20], and they are carried out in order to investigate the HOMFLY-PT invariant of links in lens spaces as explained in Chapter 9. Oriented links are considered in order to have the correct information for the X and the O markings.

Proposition 3.6. *Let L be a link in $L(p,q)$ assigned via a grid diagram G_L. Then we can obtain the disk diagram D_L representing L in the following way (see Figure 3.12):*
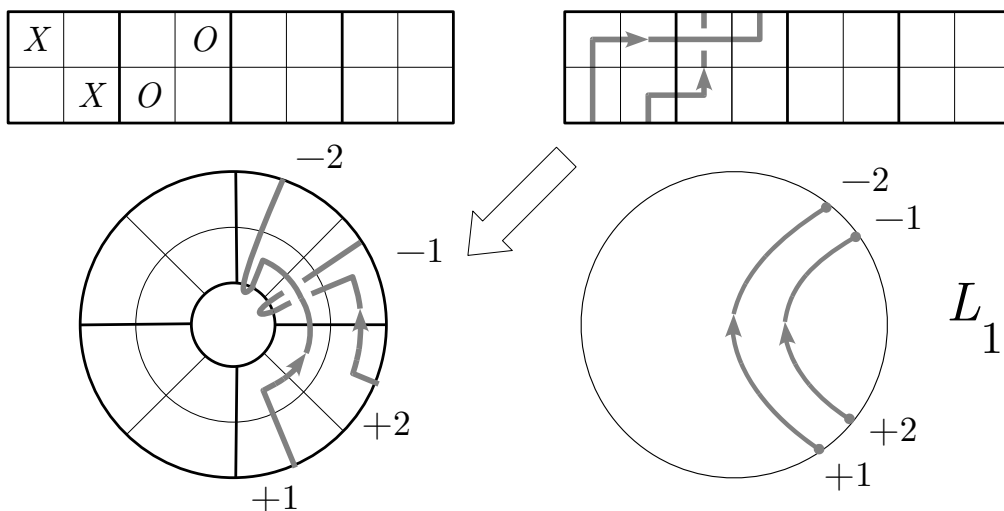
Figure 3.12: From grid diagram G_L to disk diagram D_L in $L(4,1)$.

- *consider the grid diagram G_L and draw the link according to the previous convention;*
- *round the rectangle into a circular annulus, joining the first and the last columns, that is to say, the horizontal lines become circles and the vertical lines become radial lines on the disk diagram;*

- *the lower boundary points on the rectangle become plus-type boundary points on the disk; the upper boundary points, instead, are inside the disk, that is to say, by moving them under all the circle lines we can bring them on the boundary of the disk, so that they become minus-type boundary points.*

Proof. The grid diagram of a link in a lens space comes from the representation of lens spaces as Heegaard splitting, namely our grid diagram is the toric Heegaard surface. If we want to transform the grid diagram into the disk diagram D_L we have to put our Heegaard surface inside the ball B^3 of the lens model of $L(p,q)$. This can be done as Figure 3.13 shows. Now we want
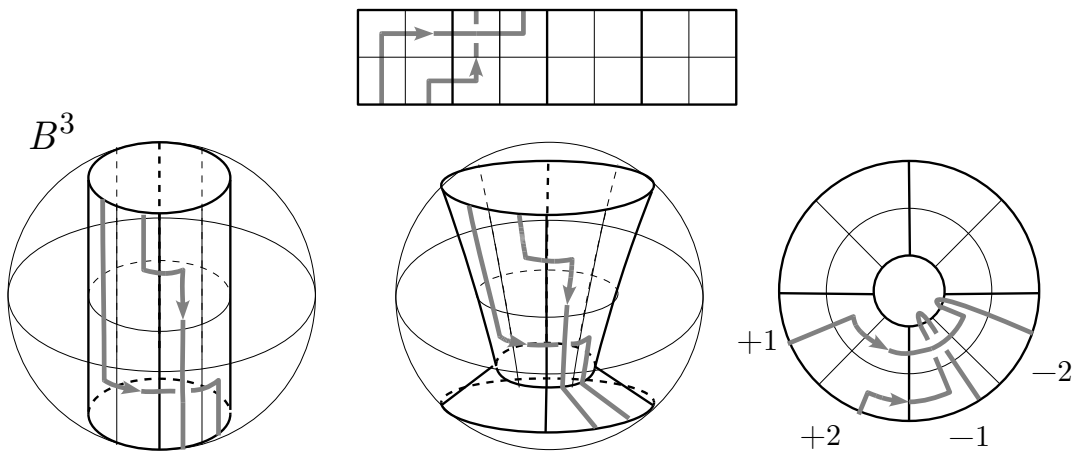
Figure 3.13: How to insert the grid diagram of L into the lens model of $L(4,1)$.

to project this surface on the equatorial disk B_0^2, and, in order to have a regular projection of the link, we deform the Heegaard torus as in Figure 3.13. The projection of the deformed grid diagram on B_0^2 gives D_L. □

Remark 3.7. If the grid diagram G_L has grid number n, then the disk diagram D_L, obtained from G_L, has at most $n(p-1)$ boundary points. Indeed, the number of boundary points of D_L is exactly the number of the points onto the lower and upper sides of the rectangle of G_L, that is, at most, $n(p-1)$.

In the opposite direction, when we know the disk diagram D_L of a link $L \subset L(p,q)$, how can we recover the grid diagram G_L?

Proposition 3.8. *Let L be a link in $L(p,q)$, defined by a disk diagram D_L, we can then get a grid diagram G_L of L as follows (see Figure 3.14):*
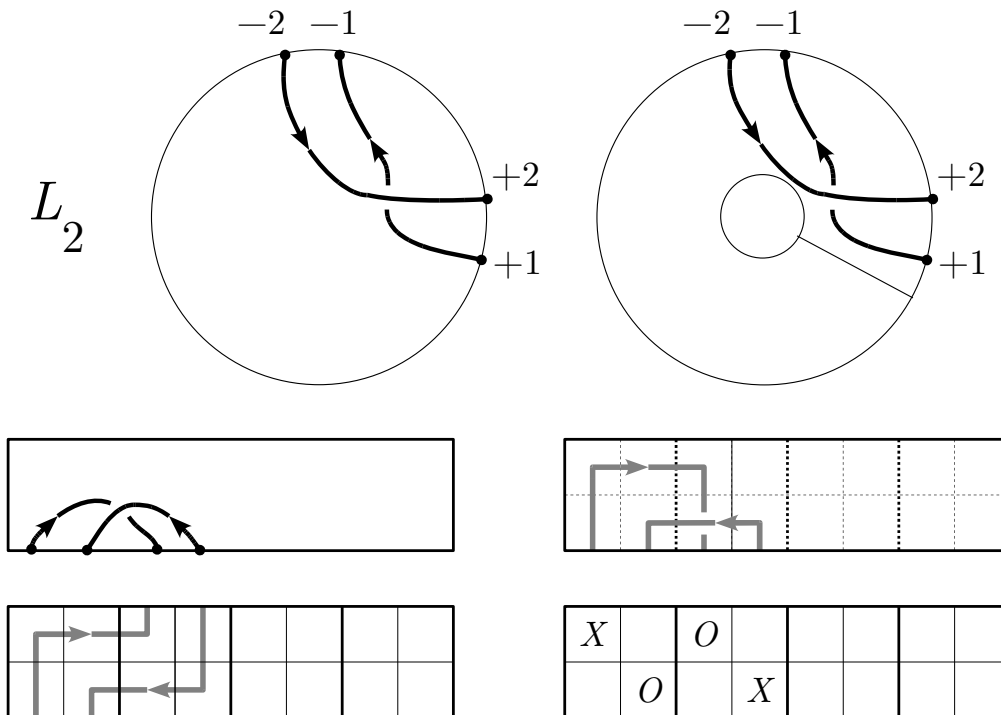
Figure 3.14: From disk diagram D_L to grid diagram G_L in $L(4,1)$.

- *consider the disk diagram D_L and cut the disk along a ray between the $+1$ point and the previous boundary point (according to the orientation of the disk), obtaining a rectangle;*

- *make an orthogonal PL-approximation of the link arcs, putting all the crossings with horizontal overpass and vertical underpass;*

- *shift the boundary endpoint of $-1, \dots, -t$ from the lower to the upper side of the rectangle, passing under all the lines;*

- *put X and O markings on the square corners of the link projection.*

Proof. It is exactly the converse of the proof of Proposition 3.6. The only difference is that here we have to use the orthogonal PL-approximation suggested by Theorem 4.3 of [6]. □

Using Propositions 3.6 and 3.8, it is also possible to find a correspondence between the Reidemeister moves on the disk diagrams (illustrated in Figure 3.3) and the grid diagram equivalence moves described in the previous paragraph. This correspondence is summed up in Table 3.5.

Disk diagram	Grid diagram
R_1	(de)stab.
R_2	non-inter. comm.
R_3	non-inter. comm.
R_4	cyclic perm. of rows
R_5	cyclic perm. of rows
R_6	non-inter. comm.
R_7	column reverse connection

Chapter 4

Group of links in lens spaces via Wirtinger presentation

The main topological problem of knot theory is to distinguish non-equivalent links, for this reason we look for invariants of links in lens spaces. If two links are equivalent (or just diffeo-equivalent), then their complement are homeomorphic. Hence when the fundamental groups of these two spaces are different, the links are not equivalent. Can this invariant (named the group of the link) classify links in lens spaces? For the 3-sphere case we have the following result: two prime knots are equivalent if and only if their fundamental groups are isomorphic (see Theorem 6.1.12 of [72], that is a corollary of two results, one obtained by [57] and the other one by [113]). Therefore a method for the computation of the link group in lens spaces is an important starting point for the classification of links in these manifolds. In order to investigate this question, in this chapter we generalize the Wirtinger presentation for the group of links in the 3-sphere to lens spaces, taking hints from the article [69] that shows the case of the projective space $L(2, 1)$. Furthermore we prove that the first homology group of the complement may have a non-trivial torsion part. These results are published in [19]. Finally we present several examples of the group of the knot. These show that the group of the knot cannot classify prime knots in lens space and that if the

knot group has two generators, this does not imply that the knot is prime
(this is a theorem of Norwood for knots in the 3-sphere [93]).

4.1   Group of the link

Let L be a link in $L(p,q)$, where the lens space is described by the lens
model of Section 1.2 and the link is described by a disk diagram as in Section
3.1. Assume $p > 1$. Fix an orientation for L, which induces an orientation
on the projection of the link. Perform an R_1 move on each overpass of the
diagram having both endpoints on the boundary of the disk; in this way
every overpass has at most one boundary point. Then label the overpasses
as follows: $A_1, \ldots, A_t$ are the ones ending in the upper hemisphere, namely
in $+1, \ldots, +t$, while $A_{t+1}, \ldots, A_{2t}$ are the overpasses ending in $-1, \ldots, -t$.
The remaining overpasses are labelled by $A_{2t+1}, \ldots, A_r$. For each $i = 1 \ldots, t$,
let $\epsilon_i = +1$ if, according to the link orientation, the overpass A_i starts from
the point $+i$; otherwise, if A_i ends in the point $+i$, let $\epsilon_i = -1$.
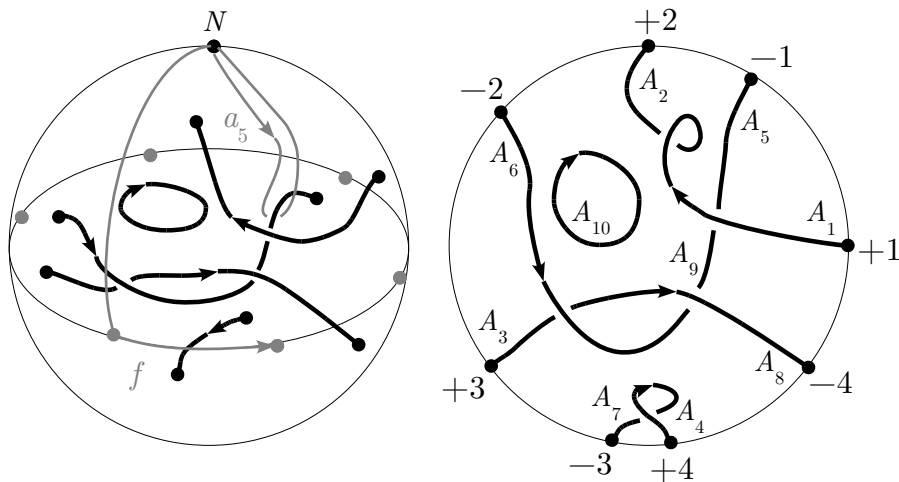
Figure 4.1: Example of overpasses labeling for a link in $L(6,1)$.

Associate to each overpass A_i a generator a_i, which is a loop around the
overpass as in the classical Wirtinger theorem, oriented following the left

hand rule. Moreover let f be the generator of the fundamental group of the lens space illustrated in Figure 4.1. The relations are the following:

W: $w_1, \ldots, w_s$ are the classical Wirtinger relations for each crossing, that is to say $a_i a_j a_i^{-1} a_k^{-1} = 1$ or $a_i a_j^{-1} a_i^{-1} a_k = 1$, according to Figure 4.2;

$$a_i a_j a_i^{-1} a_k^{-1} = 1 \qquad\qquad a_i a_j^{-1} a_i^{-1} a_k = 1$$
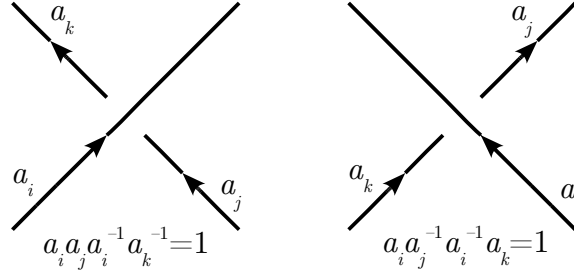
Figure 4.2: Wirtinger relations.

L: l is the lens relation $a_1^{\epsilon_1} \cdots a_t^{\epsilon_t} = f^p$;

M: $m_1, \ldots, m_t$ are relations (of conjugation) between loops corresponding to overpasses with identified endpoints on the boundary. If $t = 1$ the relation is $a_2^{\epsilon_1} = a_1^{-\epsilon_1} f^q a_1^{\epsilon_1} f^{-q} a_1^{\epsilon_1}$. Otherwise, consider the point $-i$ and, according to equator orientation, let $+j$ and $+j + 1$ (mod t) be the type $+$ points aside of it. We distinguish two cases:

- if $-i$ lies on the diagram between -1 and $+1$, then the relation m_i is

$$a_{t+i}^{\epsilon_i} = \Big(\prod_{k=1}^{j} a_k^{\epsilon_k} \Big)^{-1} f^q \Big(\prod_{k=1}^{i-1} a_k^{\epsilon_k} \Big) \; a_i^{\epsilon_i} \; \Big(\prod_{k=1}^{i-1} a_k^{\epsilon_k} \Big)^{-1} f^{-q} \Big(\prod_{k=1}^{j} a_k^{\epsilon_k} \Big);$$

- otherwise, the relation m_i is

$$a_{t+i}^{\epsilon_i} = \Big(\prod_{k=1}^{j} a_k^{\epsilon_k} \Big)^{-1} f^{q-p} \Big(\prod_{k=1}^{i-1} a_k^{\epsilon_k} \Big) \; a_i^{\epsilon_i} \; \Big(\prod_{k=1}^{i-1} a_k^{\epsilon_k} \Big)^{-1} f^{p-q} \Big(\prod_{k=1}^{j} a_k^{\epsilon_k} \Big).$$

Theorem 4.1. *Let $* = F(N)$, then the group of the link $L \subset L(p,q)$ is:*

$$\pi_1(L(p,q) \smallsetminus L, *) = \langle a_1, \ldots, a_r, f \mid w_1, \ldots, w_s, l, m_1, \ldots, m_t \rangle.$$

Proof. Remember that the map $F\colon B^3 \to L(p,q)$ is the quotient map of the lens model of $L(p,q)$ described in Section 1.2. Suppose that $L' = F^{-1}(L)$ is such that $\mathbf{p}_{|L'}\colon L' \to B_0^2$ is a regular projection. Consider a sphere $\mathbf{S}_\varepsilon^2$ of radius $1 - \varepsilon$, with $0 < \varepsilon < 1$; this sphere splits the 3-ball B^3 into two parts: call B_ε^3 the internal one and E_ε the external one. Choose ε small enough such that all the underpasses belong into $\mathrm{int}(B_\varepsilon^3)$. If N_ε is the north pole of B_ε^3, let $\tilde{\mathbf{S}}_\varepsilon^2 = \mathbf{S}_\varepsilon^2 \cup \overline{NN_\varepsilon}$ and $\tilde{B}_\varepsilon^3 = B_\varepsilon^3 \cup \overline{NN_\varepsilon}$.

In order to compute $\pi_1(L(p,q) \smallsetminus L, *)$, we apply Seifert-Van Kampen theorem with decomposition $(L(p,q) \smallsetminus L) = (F(\tilde{B}_\varepsilon^3) \smallsetminus L) \cup (F(E_\varepsilon) \smallsetminus L)$.

The fundamental group of $F(\tilde{B}_\varepsilon^3) \smallsetminus L$ can be obtained as in the classical Wirtinger Theorem:

$$\pi_1(F(\tilde{B}_\varepsilon^3) \smallsetminus L, *) = \langle a_1, \ldots, a_r \mid w_1, \ldots, w_s \rangle.$$

For $F(E_\varepsilon) \smallsetminus L$, we proceed in the following way: first of all observe that is possible to retract $F(E_\varepsilon) \smallsetminus L$ to $E \smallsetminus L$, where E is $\partial B^3/\sim$. According to the orientation, fix a point T_1 in ∂B_0^2 just before $+1$, such that its equivalent points $T_2, \ldots, T_p$ (via $\sim$) do not belong to $\mathbf{p}(L')$. Following the example of Figure 4.3, the 2-complex E is a CW-complex composed by: two 0-cells $N = S$ and $T_1 = T_2 = \ldots = T_p$, two 1-cells $\widehat{NT_1}$ (chosen as a maximal tree in the 1-skeleton) and $\widehat{T_1 T_2}$ (corresponding to f), and one 2-cell, that is the upper hemisphere. In order to obtain $\pi_1(E \smallsetminus L, *)$, we need to add the loops $d_1, \ldots, d_t$ around the points of L. The relation given by the 2-simplex is $d_1 \cdots d_t = f^p$. Hence the fundamental group of $E \smallsetminus L$ is:

$$\pi_1(E \smallsetminus L, *) = \langle d_1, \ldots, d_t, f \mid d_1 \cdots d_t = f^p \rangle. \qquad (4.1)$$

Finally, the fundamental group of $F(\tilde{\mathbf{S}}_\varepsilon^2) \smallsetminus L = (F(\tilde{B}_\varepsilon^3) \smallsetminus L) \cap (F(E_\varepsilon) \smallsetminus L)$ is generated by $a_1, \ldots, a_{2t}$. By Seifert-Van Kampen theorem, we identify each $a_1, \ldots, a_t$ with the corresponding generator $d_1, \ldots, d_t$, according to orientation: $a_i^{\epsilon_i} = d_i$. Furthermore we need to identify $a_{t+1}, \ldots a_{2t}$ with suitable loops in the CW-complex, by distinguishing two cases:

- if $-i$ lies on the diagram between -1 and $+1$, then we obtain the
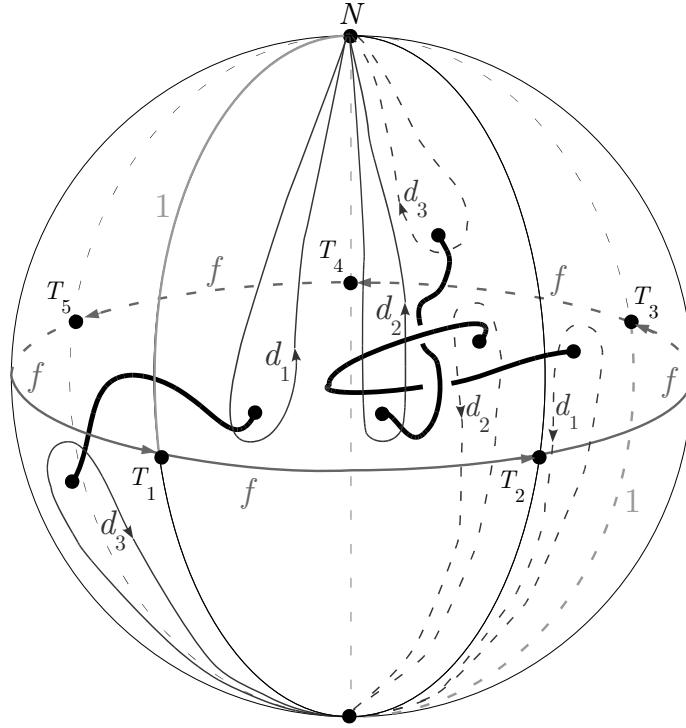
Figure 4.3: Boundary complex for a knot in $L(5,2)$.

following relation (see an example in Figure 4.4)

$$a_{t+i}^{\epsilon_i} = \Big(\prod_{k=1}^{j} d_k \Big)^{-1} f^q \Big(\prod_{k=1}^{i-1} d_k \Big) \, d_i \, \Big(\prod_{k=1}^{i-1} d_k \Big)^{-1} f^{-q} \Big(\prod_{k=1}^{j} d_k \Big);$$

- otherwise, the relation is

$$a_{t+i}^{\epsilon_i} = \Big(\prod_{k=1}^{j} d_k \Big)^{-1} f^{q-p} \Big(\prod_{k=1}^{i-1} d_k \Big) \, d_i \, \Big(\prod_{k=1}^{i-1} d_k \Big)^{-1} f^{p-q} \Big(\prod_{k=1}^{j} d_k \Big).$$

At last we remove $d_1, \dots, d_t$ from the group presentation, obtaining:

$$\pi_1(L(p,q) \smallsetminus L, *) = \langle a_1, \dots, a_r, f \mid w_1, \dots, w_s, l, m_1, \dots, m_t \rangle. \qquad \square$$

In the special case of $L(2,1) = \mathbb{RP}^3$, the presentation is equivalent (via Tietze transformations) to the one given in [69].
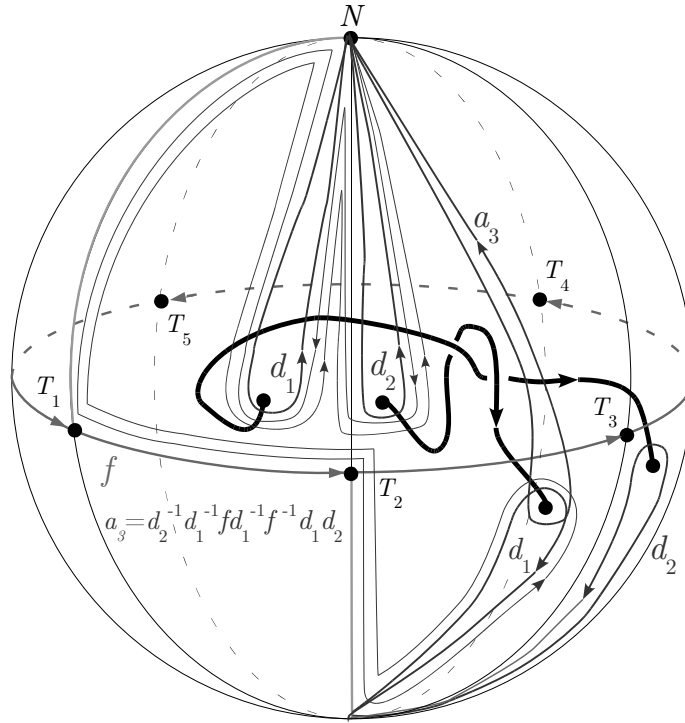
Figure 4.4: Example of relation for a link in $L(5,1)$.

Remark 4.2. If the link diagram does not contain overpasses which are circles (we can avoid this case by using suitable R_1 moves), then the presentation of Theorem 4.1 is balanced (i.e., the number of generators equals the number of relations). Indeed, it is enough to think at each intersection between the diagram and the boundary disk as a fake crossing. Moreover, the product of the Wirtinger relators represents a loop that is trivial in $\pi_1(E \smallsetminus L, *)$, so any of the Wirtinger relations can be deduced from the other ones, obtaining a presentation of deficiency one (see [68] for the $L(2,1)$ case).

4.2   First homology group

In this section we show how to determine, directly from the diagram, the first homology group of links in $L(p,q)$, which is useful for the computation

of twisted Alexander polynomials.

Consider a diagram of an oriented knot $K \subset L(p,q)$ and let ϵ_i be as defined in the previous section. If $n_1 = |\{\epsilon_i \mid \epsilon_i = +1, \ i = 1, \ldots, t\}|$ and $n_2 = |\{\epsilon_i \mid \epsilon_i = -1, \ i = 1, \ldots, t\}|$, define $\delta_K = q(n_2 - n_1) \bmod p$.

Lemma 4.3. *If $K \subset L(p,q)$ is an oriented knot and $[K]$ is the homology class of K in $H_1(L(p,q))$, then $[K] = \delta_K$.*

Proof. Let f be the generator of $H_1(L(p,q)) = \mathbb{Z}_p$, as illustrated in Figure 4.5. Let $K \cap (\partial B^3 / \sim) = \{P_1, \ldots, P_t\}$. For $i = 1, \ldots, t$, consider the identification class $[P_i]_\sim = \{P_i', P_i''\}$, with $P_i' \in E_+$ and $P_i'' \in E_-$. Denote with γ_i the path (actually a loop in $L(p,q)$) connecting P_i' with P_i'' as in Figure 4.5, oriented as depicted if $\epsilon_i = +1$ and in the opposite direction if $\epsilon_i = -1$. Of course its homology class is $[\gamma_i] = \epsilon_i q$. The loop $K' = K \cup \gamma_1 \cup \cdots \cup \gamma_t$ is homologically trivial, so we have: $0 = [K'] = [K] + \sum_{i=1}^t [\gamma_i] = [K] + (n_1 - n_2)q$, and therefore $[K] = \delta_K$.
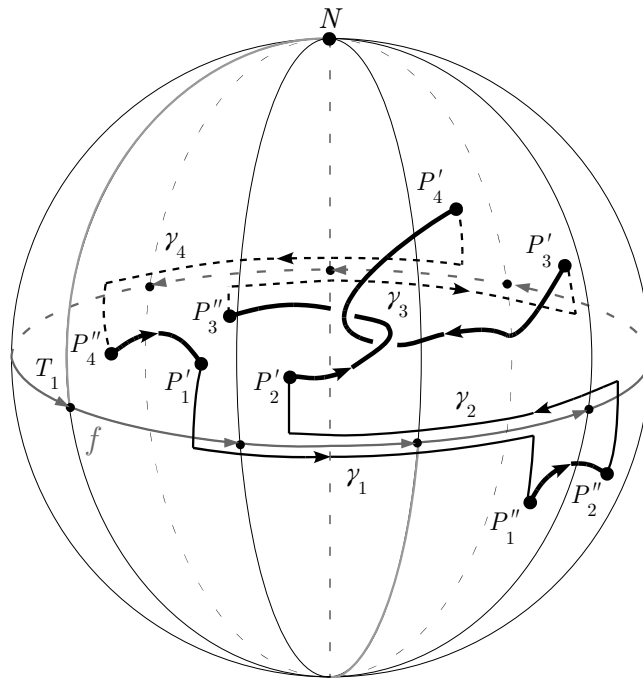
Figure 4.5: Equatorial arcs for a knot in $L(7,2)$.

$\square$

Corollary 4.4. *Let L be a link in $L(p, q)$, with components $L_1, \ldots L_\nu$. For each $j = 1, \ldots, \nu$, let $\delta_j = [L_j] \in \mathbb{Z}_p = H_1(L(p, q))$. Then*

$$H_1(L(p, q) \smallsetminus L) \cong \mathbb{Z}^\nu \oplus \mathbb{Z}_d,$$

where $d = \gcd(\delta_1, \ldots, \delta_\nu, p)$.

Proof. We abelianize the fundamental group presentation of Theorem 4.1. Relations of type W and M imply that generators corresponding to the same link component are homologous. Therefore $H_1(L(p, q) \smallsetminus L)$ is generated by $g_1, \ldots, g_\nu$, which are generators corresponding to the link components, and f. Relation L becomes: $pf - (\tilde{\delta}_1 g_1 + \ldots + \tilde{\delta}_\nu g_\nu) = 0$, with $\tilde{\delta}_j = \sum_{A_h \subset L_j} \epsilon_h$, where L_j is the j-th component of L. Therefore $H_1(L(p, q) \smallsetminus L) \cong \mathbb{Z}^\nu \oplus \mathbb{Z}_d$, where $d = \gcd(\tilde{\delta}_1, \ldots, \tilde{\delta}_\nu, p)$. Since $\gcd(p, q) = 1$ and, by Lemma 4.3, $\delta_j = -q\tilde{\delta}_j$, we obtain $d = \gcd(\tilde{\delta}_1, \ldots, \tilde{\delta}_\nu, p) = \gcd(\delta_1, \ldots, \delta_\nu, p)$. $\square$

4.3   Relevant examples

Example 4.5. The knots K_1 and K_2 in $L(p, q)$ described in Figure 4.6 have the following groups.

$$\pi_1(L(p, q) \smallsetminus K_1, *) = \langle a_1, a_2, f \mid a_1 = a_2, \ a_1 = f^p, \ a_2 = a_1^{-1} f^q a_1 f^{-q} a_1 \rangle =$$

$$= \langle a_1, f \mid a_1 = f^p, \ a_1 = a_1^{-1} f^q a_1 f^{-q} a_1 \rangle = \langle f \rangle \cong \mathbb{Z}$$
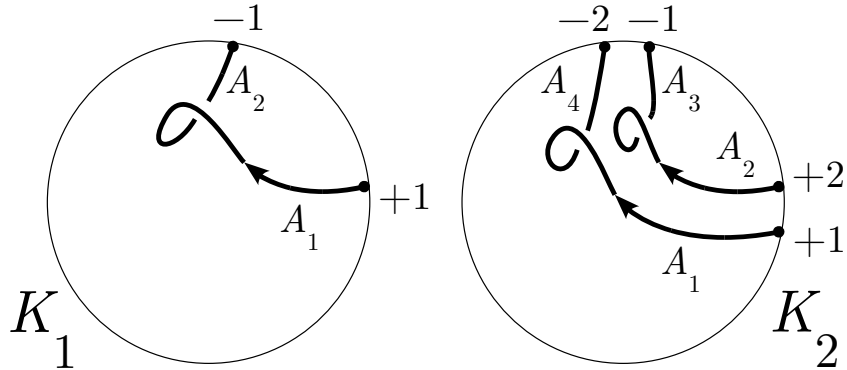
Figure 4.6: The knots K_1 and K_2 in $L(p, q)$.

$$\pi_1(L(p,q) \smallsetminus K_2, *) = \langle a_1, a_2, a_3, a_4, f \mid a_1 = a_4, \ a_2 = a_3, \ a_1 a_2 = f^p,$$
$$a_3 = a_2^{-1} a_1^{-1} f^q a_1 f^{-q} a_1 a_2, \ a_4 = a_2^{-1} a_1^{-1} f^q a_1 a_2 a_1^{-1} f^{-q} a_1 a_2 \rangle =$$
$$= \langle a_1, a_2, f \mid a_2 = a_1^{-1} f^p, (a_1 a_2 = f^p),$$
$$a_2 = a_2^{-1} a_1^{-1} f^q a_1 f^{-q} a_1 a_2, \ a_1 = a_2^{-1} a_1^{-1} f^q a_1 a_2 a_1^{-1} f^{-q} a_1 a_2 \rangle =$$
$$= \langle a_1, f \mid a_1^{-1} f^p = f^{-p} f^q a_1 f^{-q} f^p, \ a_1 = f^{-p} f^q f^p a_1^{-1} f^{-q} f^p \rangle =$$
$$= \langle a_1, f, z \mid f^q a_1^{-1} f^{p-q} a_1^{-1} = 1, \ z = f^q a_1^{-1} \rangle =$$
$$= \langle f, z \mid z f^{p-2q} z = 1 \rangle = \langle f, z \mid z^2 = f^{2q-p} \rangle$$

When $2q - p = \pm 1$, the group of K_2 is isomorphic to $\mathbb{Z}$. As a consequence, for every odd p, we have found two prime knots, K_1 and K_2 in $L\left(p, \frac{p \pm 1}{2}\right)$ that have isomorphic group. Are K_1 and K_2 distinct?

The homology class $[K] = \delta$ of a knot in $L(p, q)$ can be $0, 1, \ldots p - 1$, but since we do not consider the orientation of the knots, we have to identify $\pm \delta$, so that the knots are partitioned into $\lfloor p/2 \rfloor + 1$ classes: $\delta = 0, 1, \ldots, \lfloor p/2 \rfloor$, where $\lfloor x \rfloor$ denotes the integer part of x. If two knots stay in different homology classes, they are necessarily different. The same reasoning holds also for links, with a more subtle partition.

Since $[K_1] = 1$ and $[K_2] = 2$, the knots are different when $p > 3$ and this shows that is not possible to extend the result of [72, Theorem 6.1.12]

to prime knots in lens spaces.

Example 4.6. Let T be the trefoil knot in $\mathbf{S}^3$. Let K_1 be the knot of the previous example and consider the connected sum $K_1 \sharp T$ in $L(p,q)$, as Figure 4.7 shows.
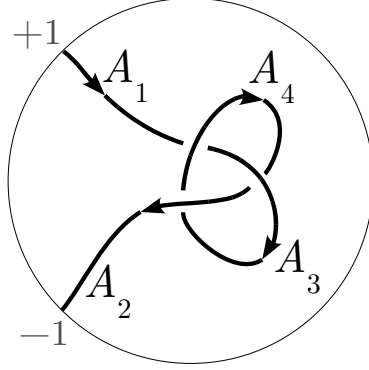
Figure 4.7: The knot $K_1 \sharp T$ in $L(p,q)$.

$$\pi_1(L(p,q) \smallsetminus (K_1 \sharp T), *) = \langle a_1, a_2, a_3, a_4, f \mid a_1 a_4 a_3^{-1} a_4^{-1} = 1, \ a_4 a_3 a_2^{-1} a_3^{-1} = 1,$$
$$a_3 a_2 a_4^{-1} a_2^{-1} = 1, \ a_1 = f^p, \ a_2 = a_1^{-1} f^q a_1 f^{-q} a_1 \rangle =$$
$$\langle a_1, a_2, a_3, a_4, f \mid a_1 a_4 a_3^{-1} a_4^{-1} = 1, \ a_4 a_3 a_2^{-1} a_3^{-1} = 1, \ a_3 a_2 a_4^{-1} a_2^{-1} = 1,$$
$$a_1 = f^p, \ a_2 = f^p \rangle =$$
$$= \langle a_3, a_4, f \mid f^p a_4 a_3^{-1} a_4^{-1} = 1, \ a_4 a_3 f^{-p} a_3^{-1} = 1, \ a_3 f^p a_4^{-1} f^{-p} = 1 \rangle$$
$$= \langle a_3, a_4, f \mid f^p a_4 a_3^{-1} a_4^{-1} = 1, \ a_4 a_3 f^{-p} a_3^{-1} = 1, \ a_4 = f^{-p} a_3 f^p \rangle$$
$$= \langle a_3, f \mid f^p f^{-p} a_3 f^p a_3^{-1} f^{-p} a_3^{-1} f^p = 1, \ f^{-p} a_3 f^p a_3 f^{-p} a_3^{-1} = 1 \rangle$$
$$= \langle a_3, f \mid f^{-p} a_3 f^p a_3 f^{-p} a_3^{-1} = 1 \rangle$$

A theorem of Norwood [93] states that every knots in the 3-sphere that has a minimal presentation for its group with only two generator is prime. For every lens space $L(p,q)$ with $p > 1$, we have just found a knot that has a minimal presentation of the group with two generator, but it is not prime; as a consequence, this theorem cannot generalize to lens spaces.

Chapter 5

Twisted Alexander polynomials for links in lens spaces

In this chapter we analyze the twisted Alexander polynomials of links in lens spaces that are described by 1-dimensional representation over particular domains that take into account the torsion part of the group of the link. Then we investigate their relationship with Reidemeister torsion. These results are published in [19].

5.1 The computation of the twisted Alexander polynomials

The twisted Alexander polynomials are defined in the following way (for further references see [110], [108], [46]). Given a finitely generated group π, denote with $H = \pi/\pi'$ its abelianization and let $G = H/\mathrm{Tors}(H)$. Take a presentation $\pi = \langle x_1, \ldots, x_m \mid r_1 \ldots, r_n \rangle$ and consider the Alexander-Fox matrix A associated to the presentation, that is $A_{ij} = \mathcal{P}(\frac{\partial r_i}{\partial x_j})$, where $\mathcal{P}$ is the natural projection $\mathbb{Z}[F(x_1, \ldots, x_m)] \to \mathbb{Z}[\pi] \to \mathbb{Z}[H]$ and $\frac{\partial r_i}{\partial x_j}$ is the Fox derivative of r_i. Moreover let $E(\pi)$ be the first elementary ideal of π, which is the ideal of $\mathbb{Z}[H]$ generated by the $(m-1)$-minors of A. For each homomorphism $\sigma : \mathrm{Tors}(H) \to \mathbb{C}^* = \mathbb{C} \smallsetminus \{0\}$ we can define a twisted Alexander polynomial

$\Delta^\sigma(\pi)$ of π as follows: fix a splitting $H = \text{Tors}(H) \times G$ and consider the ring homomorphism that we still denote with $\sigma : \mathbb{Z}[H] \to \mathbb{C}[G]$ sending (f, g), with $f \in \text{Tors}(H)$ and $g \in G$, to $\sigma(f)g$, where $\sigma(f) \in \mathbb{C}^*$. The ring $\mathbb{C}[G]$ is a unique factorization domain and we set $\Delta^\sigma(\pi) = \gcd(\sigma(E(\pi)))$. This is an element of $\mathbb{C}[G]$ defined up to multiplication by elements of G and non-zero complex numbers. If $\Delta(\pi)$ denote the classical Alexander polynomial we have $\Delta^1(\pi) = \alpha\Delta(\pi)$, with $\alpha \in \mathbb{C}^*$.

Application to links in lens spaces   If $L \subset L(p, q)$ is a link in a lens space then the σ-*twisted Alexander polynomial* of L is $\Delta_L^\sigma = \Delta^\sigma(\pi_1(L(p, q) \smallsetminus L))$. Since in this case $\text{Tors}(H) = \mathbb{Z}_d$ then $\sigma(\text{Tors}(H))$ is contained in the cyclic group generated by ζ, where ζ is a d-th primitive root of the unity. When $\mathbb{Z}[\zeta]$ is a principal ideal domain, in order to define Δ_L^σ we can consider the restriction $\sigma \colon \mathbb{Z}[H] \to \mathbb{Z}[\zeta][G]$. Note that $\Delta_L^\sigma \in \mathbb{Z}[\zeta][G]$ is defined up to multiplication by $\zeta^h g$, with $g \in G$. In this setting we recall the following theorem.

Proposition 5.1. [85] *If ζ is a d-th primitive root of unity, then the ring $\mathbb{Z}[\zeta]$ is a principal ideal domain if and only if $d \equiv 2 \mod 4$ or d is one of the following 30 integers: 1, 3, 4, 5, 7, 8, 9, 11, 12, 13, 15, 16, 17, 19, 20, 21, 24, 25, 27, 28, 32, 33, 35, 36, 40, 44, 45, 48, 60, 84.*

If L has at least two components we can consider the projection $\varphi \colon \mathbb{Z}[\zeta][G] = \mathbb{Z}[\zeta][t_1, \ldots, t_m, t_1^{-1}, \ldots, t_m^{-1}] \to \mathbb{Z}[\zeta][t, t^{-1}]$, sending each variable t_i to t. The *one-variable* twisted Alexander polynomial of L is $\bar{\Delta}_L^\sigma = \varphi(\Delta_L^\sigma)$. Since this is the polynomial on which we focused our attentions, the computation of $\bar{\Delta}_L^\sigma$ for knots in arbitrary lens spaces has been implemented in a program using Mathematica code: the input is a knot diagram in $L(p, q)$ given via a generalization of the Dowker-Thistlewaithe code (see [41, 40, 106]).

The following proposition remember us some properties of the twisted Alexander polynomials. It is useful to check if errors have been committed during computations.

Proposition 5.2. [108] *Let L be a knot in a lens space, then:*

1) $\Delta_L^\sigma(t) = \Delta_L^\sigma(t^{-1})$ *(i.e., the twisted Alexander polynomial is symmetric);*

2) $\Delta(1) \equiv |\mathrm{Tors}(H_1(L(p,q) \smallsetminus L))| \bmod p.$

5.2 Properties of the twisted Alexander polynomials

Remember that a link is called *local* if it is contained in a ball embedded in $L(p,q)$. For local links the following properties hold.

Proposition 5.3. *Let L be a local link in $L(p,q)$. Then $\Delta_L^\sigma = 0$ if $\sigma \neq 1$, and $\Delta_L = p \cdot \Delta_{\bar{L}}$, where $\bar{L}$ is the link L considered as a link in $\mathbf{S}^3$.*

Proof. The fundamental group of L can be presented with the relations of Wirtinger-type and the lens relation $f^p = 1$ only. Therefore the column in the Alexander-Fox matrix A corresponding to the Fox derivative of the lens relation is everywhere zero except for the entry corresponding to the f-derivative, which is $1 + f + f^2 + \cdots + f^{p-1}$. Moreover, the cofactor of this non-zero entry is equal to the Alexander-Fox matrix of $\bar{L}$. The statement follows by observing that in the case of Δ_L, the generator f is sent to 1, while if $\sigma \neq 1$, the generator f is sent in a k-th root of the unity, where k divides p, and so $\sigma(1 + f + f^2 + \cdots + f^{p-1}) = 0$. $\square$

As a consequence, a knot with a non trivial twisted Alexander polynomial cannot be local. Let T be the trefoil knot in $\mathbf{S}^3$. Figure 5.1 shows the twisted Alexander polynomials of a local trefoil knot $\overline{T} \subset L(4,1)$ and proves that twisted Alexander polynomial may distinguish knots with the same Alexander polynomial.

Let $L = L_1 \sharp L_2$, where $\sharp$ denote the connected sum and L_2 is a local link. The decomposition $(L(p,q), L) = (L(p,q), L_1) \sharp (\mathbf{S}^3, L_2)$ induces monomorphisms $j_1 \colon H_1(L(p,q) \smallsetminus L_1) \to H_1(L(p,q) \smallsetminus L)$ and $j_2 \colon H_1(\mathbf{S}^3 \smallsetminus L_2) \to H_1(L(p,q) \smallsetminus L)$. Given $\sigma \colon \mathbb{Z}[H_1(L(p,q) \smallsetminus L)] \to \mathbb{C}[G]$ induced by $\sigma \in \hom(\mathrm{Tors}(H_1(L(p,q) \smallsetminus L)), \mathbb{C}^*)$, denote with σ_1 and σ_2 its restrictions

$\Delta_T^1 = 4(t^2 - t + 1)$ $\Delta_K^1 = 4(t^2 - t + 1)$

$\Delta_T^{-1} = 0$ $\Delta_K^{-1} = 0$

$\Delta_T^i = 0$ $\Delta_K^i = 2(t - 1)$

$\Delta_T^{-i} = 0$ $\Delta_K^{-i} = 2(t - 1)$
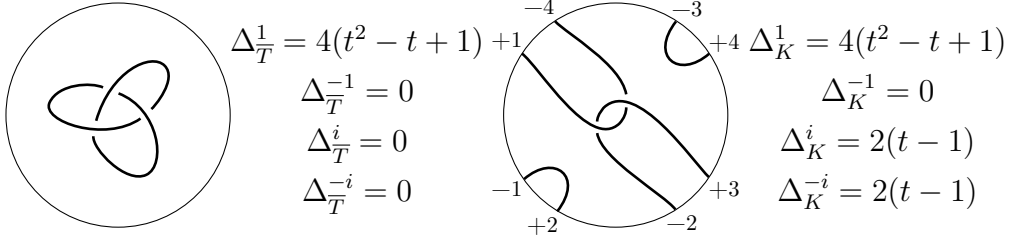
Figure 5.1: Twisted Alexander polynomials for two knots in $L(4, 1)$.

to $\mathbb{Z}[j_1(H_1(L(p, q) \smallsetminus L_1))]$ and $\mathbb{Z}[j_2(H_1(\mathbf{S}^3 \smallsetminus L_2))]$ respectively. We have the following result.

Proposition 5.4. *Let* $L = L_1 \sharp L_2 \subset L(p, q)$, *where* L_2 *is local link. With the above notations we have* $\Delta_L^\sigma = \Delta_{L_1}^{\sigma_1} \cdot \Delta_{L_2}^{\sigma_2}$.

Proof. Since $(L(p, q), L) = (L(p, q), L_1) \sharp (\mathbf{S}^3, L_2)$, by Van Kampen theorem we get $\pi_1(L(p, q) \smallsetminus L) = \langle a_1, \ldots, a_n, b_1, \ldots, b_m \mid r_1, \ldots, r_{n-1}, s_1, \ldots, s_{m-1}, a_1 = b_1 \rangle$, where $\pi_1(L(p, q) \setminus L_1, *) = \langle a_1, \ldots, a_n \mid r_1, \ldots, r_{n-1} \rangle$ and $\pi_1(\mathbf{S}^3 \setminus L_2, *) = \langle b_1, \ldots, b_m \mid s_1, \ldots, s_{m-1} \rangle$. As a consequence, the Alexander-Fox matrix of L is

$$A_L = \begin{pmatrix} A_{L_1} & & & 0 & \\ & 0 & & & A_{L_2} \\ -1\ 0 & \cdots & 0 & 1\ 0 & \cdots & 0 \end{pmatrix},$$

where A_{L_i} is the Alexander-Fox matrix of L_i, for $i = 1, 2$. If $d_k(A)$ denotes the greatest common division of all k-minors of a matrix A, then a simple computation shows that $d_{m+n-1}(A_L) = d_{n-1}(A_{L_1}) \cdot d_{m-1}(A_{L_2})$. Therefore it is easy to see that $\Delta_L^\sigma = \Delta_{L_1}^{\sigma_1} \cdot \Delta_{L_2}^{\sigma_2}$. $\square$

In Figure 5.2 we compute the twisted Alexander polynomials of the connected sum of a local trefoil knot T with the three knots $K_0, K_1, K_2 \subset L(4, 1)$ depicted in the left part of the figure, respectively. Note that for the case of $K_2 \sharp T$, the map σ_2, that is the restriction of σ to $\mathbb{Z}[j_2(H_1(\mathbf{S}^3 \smallsetminus T))]$, sends the generator $g \in \mathbb{Z}[H_1(\mathbf{S}^3 \smallsetminus T)]$ in $t^2 \in \mathbb{Z}[H_1(L(p, q) \smallsetminus K_2 \sharp T)]$ (resp. in $-t^2$) if $\sigma = 1$ (resp. if $\sigma = -1$), instead of t as it does for the classical Alexander polynomial.

$$\Delta^1_{K_0} = 4$$
$$\Delta^{-1}_{K_0} = 0$$
$$\Delta^i_{K_0} = 0$$
$$\Delta^{-i}_{K_0} = 0$$

$$\Delta^1_{K_0 \sharp T} = 4(t^2 - t + 1)$$
$$\Delta^{-1}_{K_0 \sharp T} = 0$$
$$\Delta^i_{K_0 \sharp T} = 0$$
$$\Delta^{-i}_{K_0 \sharp T} = 0$$

$$\Delta^1_{K_1} = 1$$

$$\Delta^1_{K_1 \sharp T} = t^2 - t + 1$$

$$\Delta^1_{K_2} = t + 1$$
$$\Delta^{-1}_{K_2} = 1$$

$$\Delta^1_{K_2 \sharp T} = (t + 1)(t^4 - t^2 + 1)$$
$$\Delta^{-1}_{K_2 \sharp T} = t^4 + t^2 + 1$$
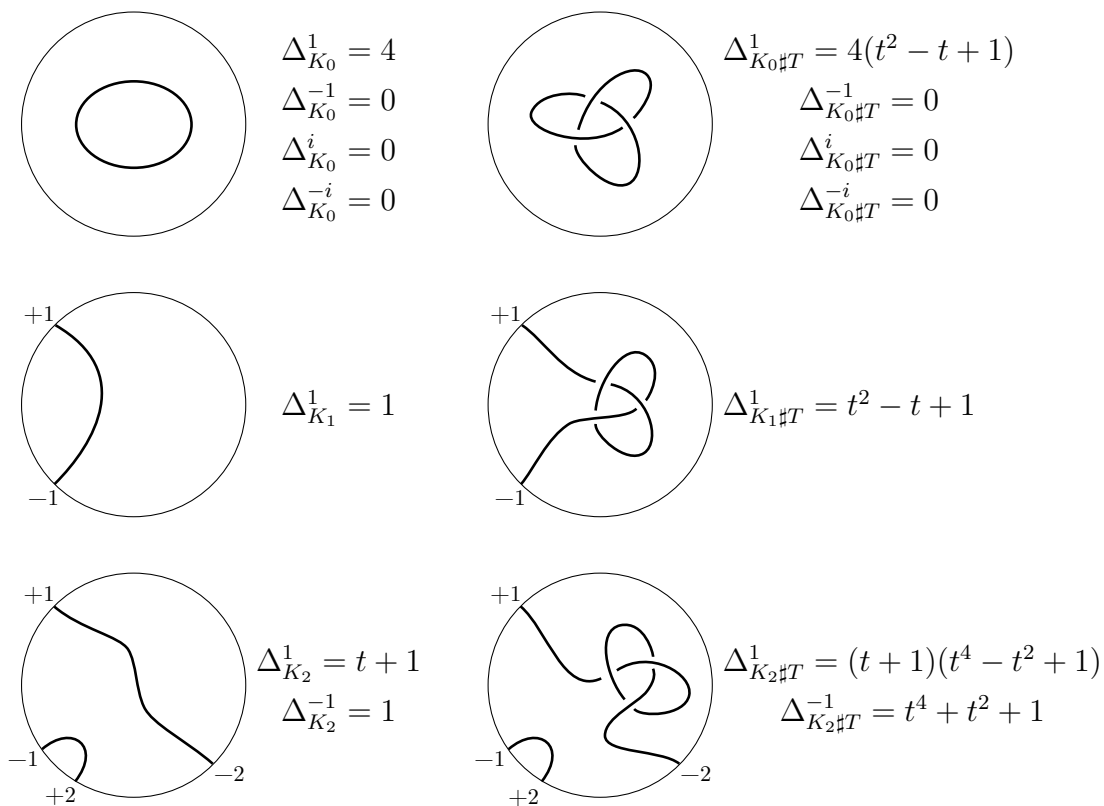
Figure 5.2: Twisted Alexander polynomials for six knots in $L(4, 1)$.

5.3 Connection with Reidemeister torsion

Before establishing the relationship between the twisted Alexander polynomials and the Reidemeister torsion we briefly remember the definition of Reidemeister torsion (for further references see [108]).

If c and c' are two basis of a finite-dimensional vector space over a field $\mathbb{F}$, denote with $[c/c']$ the determinant of the matrix whose columns are the coordinates of the elements of c respect to c'. Let C be a finite chain complex of vector spaces

$$0 \to C_m \overset{\delta_m}{\to} C_{m-1} \overset{\delta_{m-1}}{\to} \cdots \overset{\delta_1}{\to} C_0 \to 0$$

which is acyclic (i.e., the sequence is exact) and based (i.e., a distinguished base is fixed for each vector space). For each $i \leq m$, let b_i be a sequence of

vectors in C_i such that $\delta_i(b_i)$ is a base of $\mathrm{Im}\delta_i$, and let c_i be the fixed base of C_i. The juxtaposition of $\delta_{i+1}(b_{i+1})$ and b_i gives a base of C_i denoted by $\delta_{i+1}(b_{i+1})b_i$. The torsion of C is defined as

$$\tau(C) = \Pi_{i=0}^{m}[\delta_{i+1}(b_{i+1})b_i/c_i]^{(-1)^{i+1}} \in \mathbb{F}.$$

If C is not acyclic the torsion is defined to be zero.

For a finite connected CW-complex X, let $\pi = \pi_1(X)$ and $H = H_1(X) = \pi/\pi'$. Consider a ring homomorphism $\varphi \colon \mathbb{Z}[H] \to \mathbb{F}$ and let $\hat{X}$ be the maximal abelian covering of X (corresponding to π'). Let $C_*(\hat{X})$ be the cellular chain complex associated to $\hat{X}$. Since H acts on $\hat{X}$ via deck transformations, $C_*(\hat{X})$ is a complex of left $\mathbb{Z}[H]$-modules. Moreover the homomorphism φ endows F with the structure of a $\mathbb{Z}[H]$-module via $fz = f\varphi(z)$, with $f \in F$ and $z \in \mathbb{Z}[H]$. Then $\mathbb{F} \otimes_\varphi C_*(\hat{X})$ is a chain complex of finite dimensional vector spaces. The φ-torsion of X is defined to be $\tau(\mathbb{F} \otimes_\varphi C_*(\hat{X}))$. It depends on the choice of a base for $\mathbb{F} \otimes_\varphi C_*(\hat{X})$, hence the φ-torsion is defined up to multiplication by $\pm\varphi(h)$, with $h \in H$.

Let L be a link in $L(p,q)$ and let $X = L(p,q) \smallsetminus L$, then X is homotopic to a 2-dimensional cell complex Y. The φ-torsion τ_L^φ of a link L is the φ-torsion of Y. In order to investigate the relationship between the torsion and the twisted Alexander polynomial, let $H = \mathrm{Tors}(H) \times G$ and consider a map $\sigma \colon \mathbb{Z}[H] \to \mathbb{C}[G]$ associated to a certain $\sigma \in \mathrm{hom}(\mathrm{Tors}(H), \mathbb{C}^*)$, as described in the beginning of this section. If $\mathbb{C}(G)$ denotes the field of quotients of $\mathbb{C}[G]$, then by composing with the projection into the quotient, σ determines a homomorphism $\mathbb{Z}[H] \to \mathbb{C}(G)$ that we still denote with σ. In this way each $\sigma \in \mathrm{hom}(\mathrm{Tors}(H), \mathbb{C}^*)$ determines both a twisted Alexander polynomial Δ_L^σ and a torsion τ_L^σ.

We say that a link $L \subset L(p,q)$ is *nontorsion* if $\mathrm{Tors}(H_1(L(p,q) \smallsetminus L)) = 0$, otherwise we say that L is *torsion*. Note that a local link L in a lens space different from $\mathbf{S}^3$ is clearly torsion.

Theorem 5.5. *Let L be a link in $L(p,q)$. If L is a nontorsion knot and t is a generator of its first homology group, then $\tau_L^\sigma(t-1) = \Delta_L^\sigma$. Otherwise $\tau_L^\sigma(t) = \Delta_L^\sigma$.*

Proof. According to Theorem 4.1 and Remark 4.2, the group $\pi_1(L(p,q) \smallsetminus L)$ admits a presentation with m generators and $m-1$ relations. The Alexander-Fox matrix A associated to such presentation is a $(m-1) \times m$ matrix. This means that $\Delta^\sigma(L) = \gcd(\sigma(A_1), \ldots, \sigma(A_m))$, where A_i is the $(m-1)$-minor of A obtained removing the i-th column. Let a_i be a generator of $\pi_1(L(p,q) \smallsetminus L)$. The formula $(\sigma(a_i) - 1)\tau_L^\sigma = \det A_i$ that holds for links in the projective space (see [69]) generalizes to lens spaces. Therefore, in order to obtain the statement it is enough to prove that $\gcd(\sigma(a_1) - 1, \ldots, \sigma(a_m) - 1)$ is equal to $t - 1$, where t is a generator of the free part of $H_1(L(p,q) \smallsetminus L)$, if L is a torsion knot, and equal to 1 otherwise.

Let L be a torsion knot and denote with t and u a generator of the free part and the torsion part of $H_1(L(p,q) \smallsetminus L)$ respectively. Moreover let d be the order of the torsion part of $H_1(L(p,q) \smallsetminus L)$. If $\mathcal{P}(a_i) = t^{h_i} u^{n_i}$ then $\sigma(a_i) = t^{h_i} \zeta^{n_i}$ where ζ is a d-th root of the identity. A simple computation shows that g divides $t^{\sum_{i=1}^m h_i} \zeta^{\sum_{i=1}^m n_i} - 1$, for any $\alpha_i \in \mathbb{Z}$, where $g = \gcd(\sigma(a_1) - 1, \ldots, \sigma(a_m) - 1)$. Since $t \in \mathcal{P}(\pi_1(L(p,q) \smallsetminus L))$, there exist α_i such that $t = \Pi_{i=1}^m \mathcal{P}(a_i^{\alpha_i}) = t^{\sum_{i=1}^m \alpha_i h_i} u^{\sum_{i=1}^m \alpha_i n_i}$; so $\sum_{i=1}^m \alpha_i h_i = 1$ and d divides $\sum_{i=1}^m \alpha_i n_i$. Then g divides $t-1$ and therefore either $g = 1$ or $g = t-1$. Analogously, since $u \in \mathcal{P}(\pi_1(L(p,q) \smallsetminus L))$, there exists i_0 such that g divides $\sigma(a_{i_0}) - 1 = t^{h_{i_0}} \zeta^{n_{i_0}} - 1$ and n_{i_0} is not divided by d. The statement follows by observing that, in this case, $\gcd(t - 1, t^{h_{i_0}} \zeta^{n_{i_0}} - 1) = 1$.

If L is torsion and has at least two components then $\sigma(a_i) = t_1^{h_{11}} \cdots t_\nu^{h_{1\nu}} \zeta^{n_i}$, where ν is the number of components. The statement is obtained by setting $t_2 = \cdots = t_\nu = 1$ and applying the previous argument to t_1.

If L is a nontorsion knot, then $H_1(L(p,q) \smallsetminus L) = \langle t \rangle$ and $\sigma(a_i) = t^{h_i}$. In this case it is easy to prove that $\gcd(t^{h_1} - 1, \ldots, t^{h_m} - 1) = t - 1$.

Finally, if L is nontorsion and has at least two components, then $\sigma(a_i) = t_1^{h_{11}} \cdots t_\nu^{h_{1\nu}}$. By letting $t_j = 1$ for $j \neq i$ and applying the previous reasoning to t_i, for each $i = 1, \ldots, \nu$, we obtain $\gcd(\sigma(a_1) - 1, \ldots, \sigma(a_m) - 1) = \gcd(t_1 - 1, \ldots, t_\nu - 1) = 1$. $\qquad\square$

These results generalize those ones obtained in [75] for knots in $\mathbf{S}^3$ and [69]

for link in $L(2,1) \cong \mathbb{RP}^3$. Moreover, in [74] an analogous result is obtained for CW-complexes but considering only a one-variable Alexander polynomial associated to an infinite cyclic covering of the complex.

The same argument used in the previous proof leads to the following statement, regarding the one-variable twisted polynomial.

Theorem 5.6. *Let L be a link in $L(p,q)$ with at least two components. If L is a nontorsion link and t is a generator of its first homology group then $\tau_L^\sigma(t-1) = \bar{\Delta}_L^\sigma$. Otherwise $\tau_L^\sigma(t) = \bar{\Delta}_L^\sigma$.*

Chapter 6

Lifting links from lens spaces to the 3-sphere

In this chapter we deal with the following powerful invariant of links in lens spaces: let L be a link in $L(p,q)$, the *lift* $\widetilde{L}$ is the counterimage $P^{-1}(L)$ in $\mathbf{S}^3$ under the quotient map $P\colon \mathbf{S}^3 \to L(p,q)$ of Section 1.3. To be more precise, a diagram for the lift $\widetilde{L}$ is constructed from a disk diagram of L. Then analogous constructions for band and grid diagrams are illustrated. The behavior of the lift on split links and composite knots is investigated. Finally we show a formula for the lift of a family of links in lens spaces that can be easily described by a braid. All these results are reported in [82].

How many components has the lift?   Let L be a link in $L(p,q)$, denote with ν its number of components, and with $\delta_1, \ldots, \delta_\nu$ the homology class in $H_1(L(p,q)) \cong \mathbb{Z}_p$ of the i-th component L_i of L. In Section 4.4 it is described a method that allows the computation of the homology classes from the disk diagram.

Proposition 6.1. *Given a link $L \subset L(p,q)$, the number of components of $\widetilde{L}$ is*

$$\sum_{i=1}^{\nu} \gcd(\delta_i, p).$$

Proof. The covering $P \colon \mathbf{S}^3 \to L(p,q)$ is cyclic of order p, so that each component L_i of L has lift $\widetilde{L}_i$ with $\gcd(\delta_i, p)$ components. As a consequence, if we sum over all the components of L, the lift $\widetilde{L}$ has $\sum_{i=1}^{\nu} \gcd(\delta_i, p)$ components. $\square$

6.1   Diagram for the lift via disk diagrams

The construction of a diagram for $\widetilde{L} \subset \mathbf{S}^3$ starting from a disk diagram of $L \subset L(p,q)$ is explained by the following two theorems. The case of $L(2,1) \cong \mathbb{RP}^3$ is outlined in [42]. Remember that the Garside braid Δ_t on t strands is defined by $(\sigma_{t-1}\sigma_{t-2}\cdots\sigma_1)(\sigma_{t-1}\sigma_{t-2}\cdots\sigma_2)\cdots(\sigma_{t-1})$ and it is illustrated in Figure 3.8.

Theorem 6.2. *Let L be a link in the lens space $L(p,q)$ and let D be a standard disk diagram for L; then a diagram for the lift $\widetilde{L} \subset \mathbf{S}^3$ can be found as follows (refer to Figure 6.1):*

- *consider p copies $D_1, \ldots, D_p$ of the standard disk diagram D;*
- *for each $i = 1, \ldots, p-1$, using the braid Δ_t^{-1}, connect the diagram D_{i+1} with the diagram D_i, joining the boundary point $-j$ of D_{i+1} with the boundary point $+j$ of D_i;*
- *connect D_1 with D_p via the braid Δ_t^{2q-1}, where the boundary points are connected as in the previous case.*

Proof. Let L be a link in $L(p,q)$ and let D be a standard disk diagram for it. The lift in $\mathbf{S}^3$ can be obtained from the model of $\mathbf{S}^3$ where the solid torus has each parallel collapsing to a point. In this model of the 3-sphere, the lens space $L(p,q)$ is described as in Remark 1.4, so we can embed into the solid torus the p copies $D_1, \ldots, D_p$ of the standard disk diagram D in $L(p,q)$. The p copies of the diagram are embedded as disks bounded by a meridian. Each of them is rotated by $2\pi q/p$ radians around $\mathfrak{l} = \mathbf{S}^1 \times \{0\}$, with respect to the previous copy of the diagram. By this rotation, if you consider the parallel
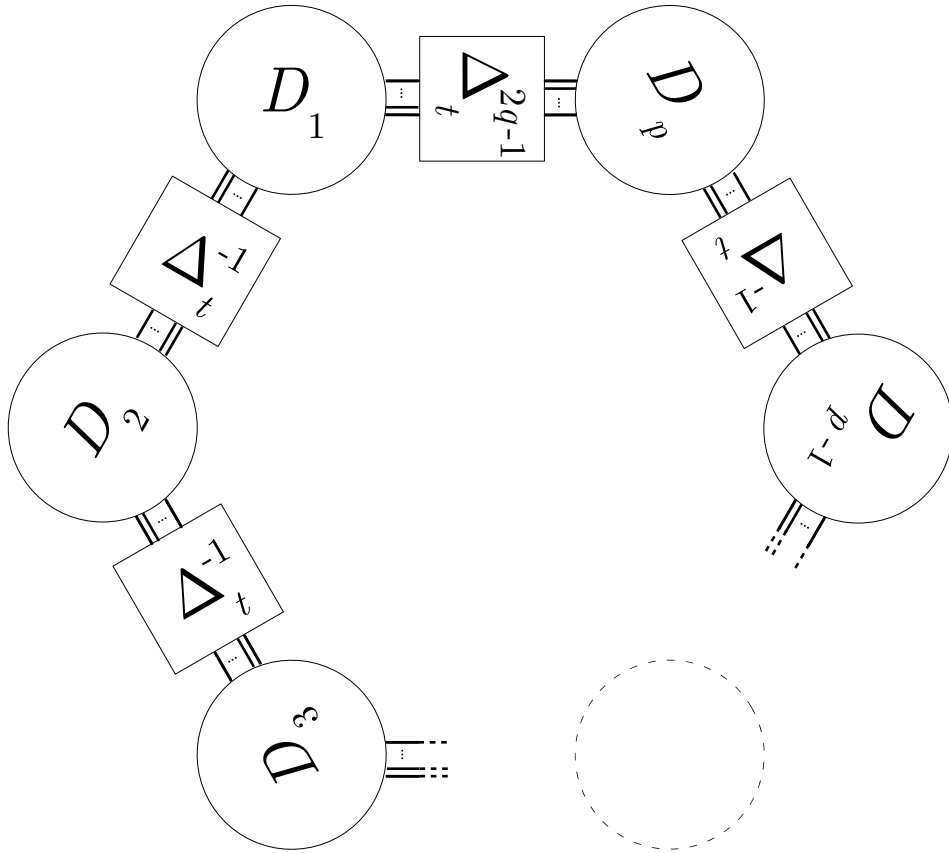
Figure 6.1: Diagram of the lift in $\mathbf{S}^3$ of a link in $L(p,q)$.

$\mathbf{S}^1 \times \{Q\}$ on the boundary of the torus that passes through the endpoint $+j$ of D_i, then it passes also through $-j$ of D_{i+1}. In the solid torus model, each of these parallels collapses to a point, so that all the pairs previously described are identified. If we want to show this identification, we can draw on our torus each arc of the parallel from $+j \in D_i$ to $-j \in D_{i+1}$, as Figure 6.2 shows, obtaining a representation for the lift $\widetilde{L}$ in the solid torus model of $\mathbf{S}^3$. In order to get a planar diagram for $\widetilde{L}$ that comes from this representation, we can do as follows. Embed the solid torus $\mathbf{S}^1 \times B^2$ into $\mathbb{R}^3$ as described in Section 1.1 and fix cartesian axis (x_1, x_2, x_3), where x_3 is orthogonal to the plane containing $\mathbf{S}^1$. For each copy D_i of D, consider its intersection with
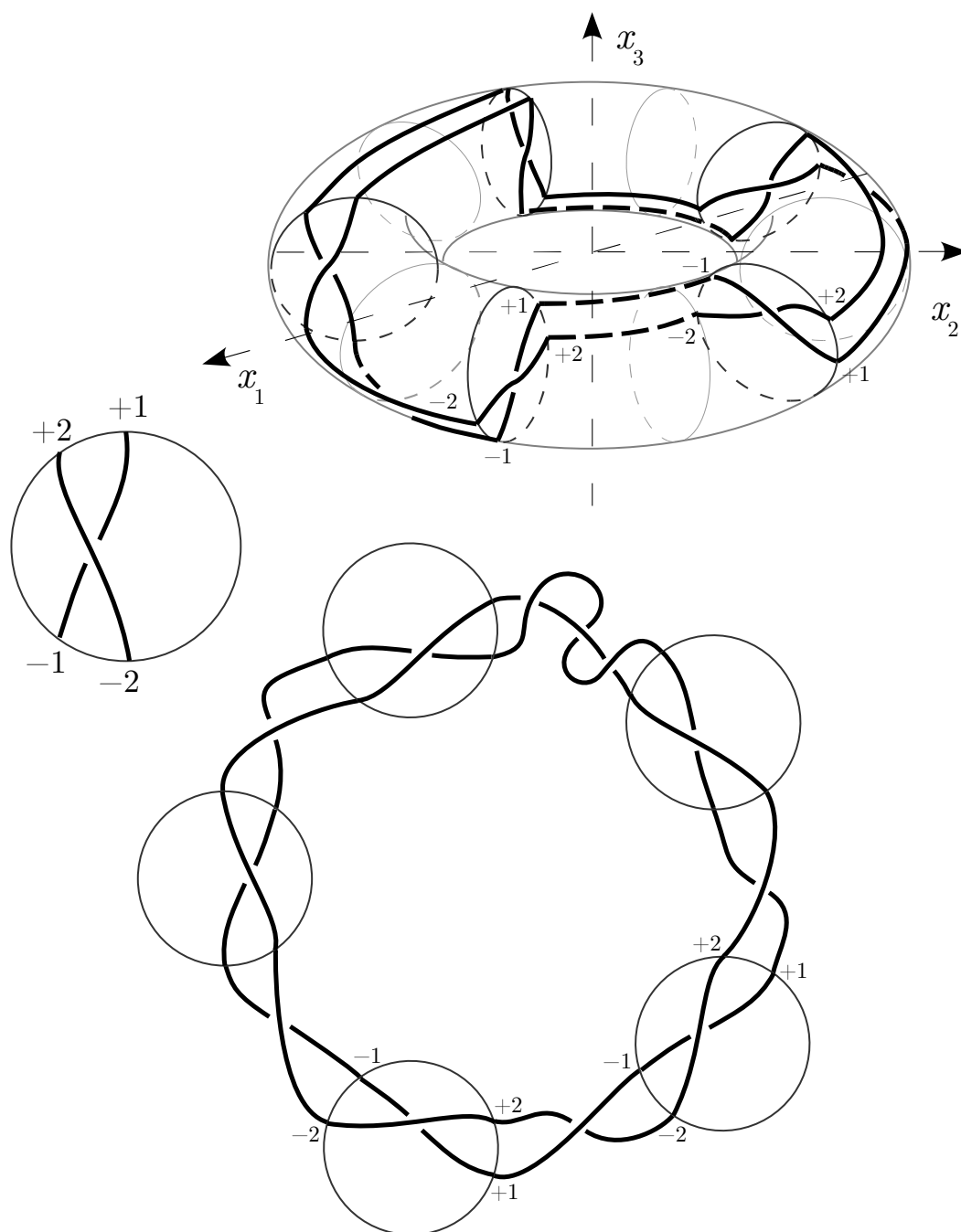
Figure 6.2: Lift in $\mathbf{S}^3$ of a link in $L(5,2)$.

the plane $\{x_3 = 0\}$ and rotate D_i around this diameter by $\pi/2$ radians, so that D_i is turned upward. As a result, the connection lines between the two disks D_i and D_{i+1} are braided by Δ_t^{-1} in order to avoid the projection of the two disks. Furthermore, when a toric braid, twisting around the core of $2\pi q$, becomes planar, we have to add another piece of braid, namely Δ_t^{2q}. In this way we will have exactly the planar diagram of Figure 6.1. $\qquad\square$

The previous planar diagram of the lift has not the least possible number of crossings. Indeed if, in the last step of the previous proof, we rotate D_1 of $\pi/2$ radians and D_2 of $-\pi/2$ radians around the diameter of the diagram, we avoid the braid Δ_t^{-1} between the two disks. We now explain how to get a diagram with fewer crossings. First of all, let us define the reverse disk diagram $\overline{D}$ of D: it is the diagram that can be obtained rotating the link inside the lens model by π radians around the x_1 axis. The diagram $\overline{D}$ can be obtained directly by the diagram D: consider the image of D under a simmetry with respect to an external line and then exchange all overpasses/underpasses.

Theorem 6.3. *Let L be a link in the lens space $L(p,q)$ and let D be a standard disk diagram for L; then a diagram for the lift $\widetilde{L} \subset \mathbf{S}^3$ can be found as follows (refer to Figure 6.3):*

- *consider p copies $D_1, \ldots D_p$ of the standard disk diagram D, then denote $F_i = D_i$ if i is odd, and $F_i = \overline{D}_i$ if i is even;*
- *for each $i = 1, \ldots, p - 1$, using a trivial braid, connect the diagram F_{i+1} with the diagram F_i joining the boundary point $-j$ of D_{i+1} with the boundary point $+j$ of D_i;*
- *connect D_1 with D_p via the braid Δ_t^{2q-p}, where the boundary points are connected as in the previous case.*

Please refer to Figure 7.2 for an example of diagram of the lift.

Proof. Consider the planar diagram of the lift of Theorem 6.2 and comb it, reversing upside down D_2, reversing two times D_3, three times D_4 and so
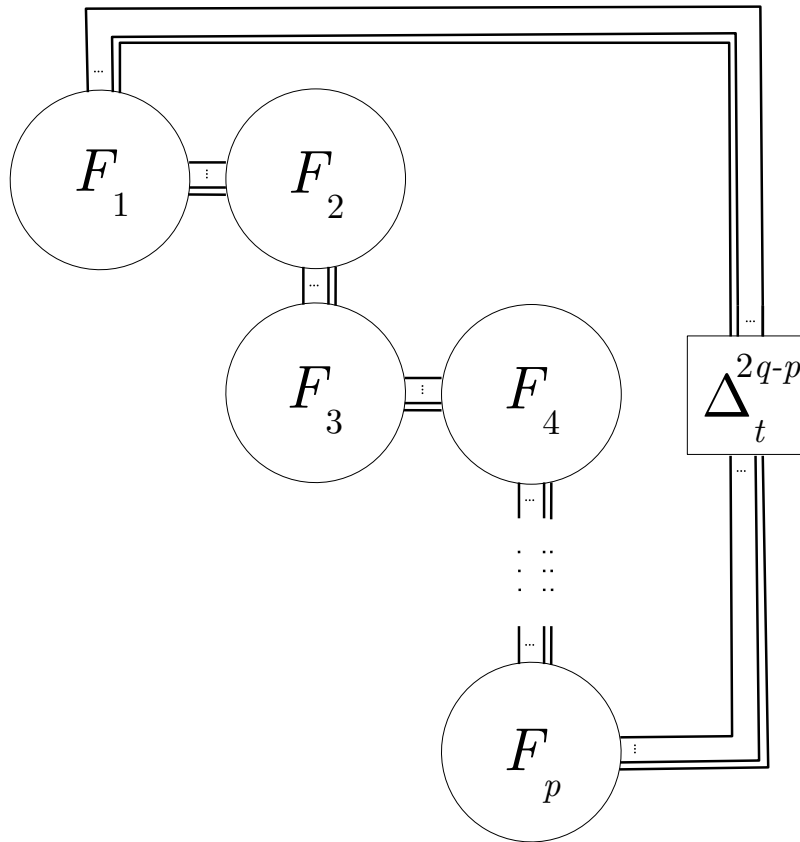
Figure 6.3: Another diagram of the lift in $\mathbf{S}^3$ of a link in $L(p,q)$.

on. The odd-index diagrams are unchanged and all the even-index diagrams become $\overline{D}_2, \overline{D}_4, \ldots$ in the new diagram of the lift. The $p-1$ braids Δ_t^{-1} between the disks are shifted near the braid Δ_t^{2q-1}, so that you get Δ_t^{2q-p} in this new form of the diagram and the number of crossings is reduced. $\square$

6.2 Diagram for the lift via band and grid diagrams

Other geometrical constructions are similar to the one of the lift for links in lens spaces.

Diagram for the lift via band diagrams   The following theorem, finding a diagram for the lift starting from a band diagram, is really useful to relate links in lens spaces to freely periodic links in the 3-sphere.

Proposition 6.4. *Let L be a link in the lens space $L(p,q)$ and let B be a band diagram for L with t boundary points; then a diagram for the lift $\widetilde{L} \subset \mathbf{S}^3$ can be found by juxtaposing p copies of B and closing them with the braid Δ_t^{2q} (refer to Figure 6.4).*
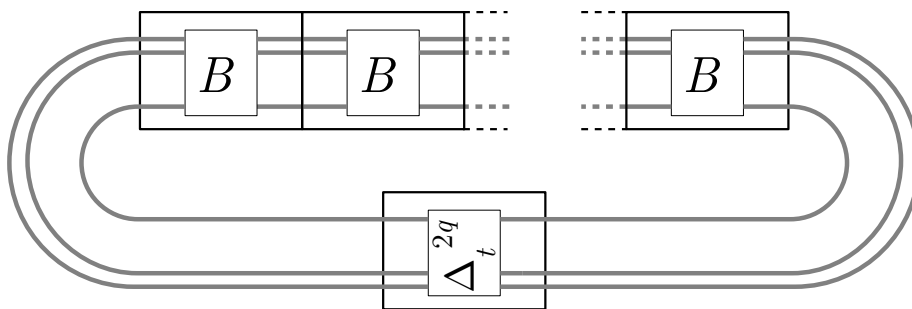

Figure 6.4: Diagram of the lift of a link in lens spaces from its band diagram.

Proof. Consider the planar diagram of the lift of Theorem 6.2 and convert the standard disk diagram D_L plus the braid Δ_t^{-1} to the equivalent band diagram B_L. This gives exactly the diagram for $\widetilde{L}$ illustrated in Figure 6.4. $\square$

Remark 6.5. The lift in $\mathbf{S}^3$ of a link $L \subset L(p,q)$ is exactly a (p,q)-*lens link* in $\mathbf{S}^3$, according to [28]. Precisely, the n-tangle T that Chbili uses in his construction is the band diagram B_L for L. In the same paper he makes explicit that the lift is a freely periodic link in $\mathbf{S}^3$.

Diagram for the lift via grid diagrams   Baker, Grigsby and Hedden in [6], exploiting grid diagrams for links in lens spaces, are able to construct the lifts of these links.

Proposition 6.6. [6] *A grid diagram in $\mathbf{S}^3$ for the lift of links in lens spaces can be obtained by piling up p copies of a grid diagram of the link in $L(p,q)$. An example is described in Figure 6.5.*
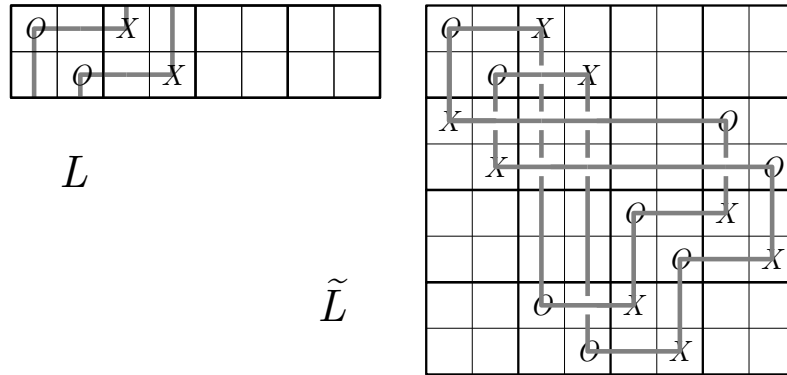
Figure 6.5: Example of the lift of a link represented by a grid diagram.

6.3   Lift of split and composite links

In this section we show the behavior of the lift on split links and composite knots, in order to better understand the lift diagram construction. Remember that a knot is *trivial* if it bounds a 2-disk in $L(p,q)$ and that a link $L \subset L(p,q)$ is *local* if it is contained inside a 3-ball. The disk diagram of a local link, up to generalized Reidemeister moves, can avoid ∂B_0^2. As a consequence of Theorem 6.2, a local link is lifted to p disjoint copies of itself.

Split links   Remember that a link $L \subset L(p,q)$ is *split* if there exists a 2-sphere in the complement $L(p,q) \smallsetminus L$ that separates one or more components of L from the others. The 2-sphere splits $L(p,q)$ into a ball $\hat{B}^3$ and $\overline{L(p,q) \smallsetminus \hat{B}^3}$; as a consequence, a split link is the disjoint union of a local link and of another link in a lens space. If we consider the lift of a split link $L = L_1 \sqcup L_2$, where $L_1 \subset \hat{B}^3$ and $L_2 \subset L(p,q) \smallsetminus \hat{B}^3$, then L_1 is lifted to p split copies of L_1 and L_2 is lifted to some link $\widetilde{L}_2$. In formulae:

$$\widetilde{L} = \underbrace{L_1 \sqcup \ldots \sqcup L_1}_{p} \sqcup \widetilde{L}_2.$$

Connected sum   Let $K_1 \subset L(p,q)$ be a *primitive*-homologous knot, that is to say, a knot whose homology class in $H_1(L(p,q))$ is coprime with p (we

require this because, according to Proposition 6.1, its lift is a knot). Let $K_2 \subset \mathbf{S}^3$ be a knot. Then the lift $\widetilde{K}$ of the connected sum $K = K_1 \sharp K_2$ is

$$\widetilde{K} = \widetilde{K}_1 \sharp \underbrace{K_2 \sharp \ldots \sharp K_2}_{p}.$$

This formula can be proved in the following way: up to generalized Reidemeister moves, we can suppose that the disk diagram of $K_1 \sharp K_2$ has the projection of K_2 all contained in a disk inside B_0^2, therefore from the diagram of Theorem 6.2 we can easily see the result.

In order to define the connected sum for links we have to specify the component of each link to which we add the pattern. If we consider a knot $K_1 \subset L(p,q)$ such that $\gcd([K_1], p) \neq 1$ or a link L_1 with more than one component, then, because of Proposition 6.1, its lift has more than one component. In this case the lift can be found selecting the components of $\widetilde{K}_1$ or $\widetilde{L}_1$ where the copies of K_2 have to be connected.

Proposition 6.7. *Given a link $L \subset L(p,q)$, if $\widetilde{L}$ is prime, then L is prime.*

Proof. From the previous considerations, if a link $L \subset L(p,q)$ is composite, then also its lift $\widetilde{L} \subset \mathbf{S}^3$ is composite. $\square$

6.4   Lift of links in lens spaces from braids

We can construct a link $L \subset L(p,q)$ starting from a braid B on t strands by considering the standard disk diagram where the braid B has the two ends of its strands on the boundary, indexed respectively by the points $(+1, \ldots, +t)$ and $(-1, \ldots, -t)$. See an example in Figure 6.6. In this case, we say that B represents L.

Proposition 6.8. *If $L \subset L(p,q)$ is a link represented by the braid B on t strands, then $\widetilde{L}$ is the link obtained by the closure in $\mathbf{S}^3$ of the braid $(B\Delta_t^{-1})^p \Delta_t^{2q}$.*
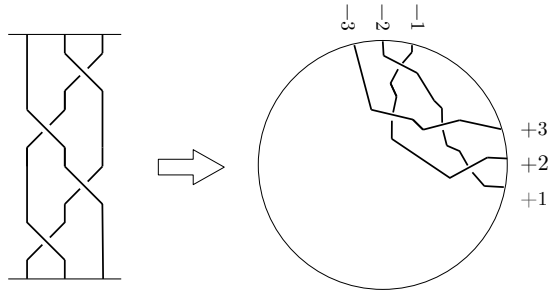
Figure 6.6: The braid $B = \sigma_2\sigma_1\sigma_2\sigma_1$ becomes a standard disk diagram.

Proof. Using Theorem 6.2, we replace the p copies of the disk diagram D with the braid B representing the link. The result is the closure of the braid $(B\Delta_t^{-1})^p\Delta_t^{2q}$ in $\mathbf{S}^3$. $\qquad\square$

Remark 6.9. The braid $(B\Delta_t^{-1})^p\Delta_t^{2q}$ is exactly the (p,q)-*lens braid* of [27]. It is also possible to simplify this braid. Consider the automorphism of the braid group B_t that sends the generators $\sigma_1, \sigma_2, \ldots, \sigma_{t-1}$ respectively to $\sigma_{t-1}, \sigma_{t-2}, \ldots, \sigma_1$. We denote by $\overline{B}$ the image of the braid B, and this is exactly the construction requested for getting the diagram $\overline{D}$ from D. Then, the braid $(B\Delta_t^{-1})^p\Delta_t^{2q}$ representing the lift can be rewritten as $F_1 F_2 \cdots F_p \Delta_t^{2q-p}$, where $F_i = B$ if i is odd and $F_i = \overline{B}$ if i is even. This is a direct consequence of Theorem 6.3.

Which links in lens spaces are lifted to torus links? We have the following result, stated in [28], that generalizes a result of [61] for torus knots. Remember that the torus link $T_{n,m} \subset \mathbf{S}^3$ is the closure of the braid $(\sigma_1\sigma_2 \cdots \sigma_{n-1})^m$.

Proposition 6.10. [28] *The torus link $T_{n,m}$ is a (p,q)-lens link (that is to say, it is the lift of some link in $L(p,q)$) if and only if p divides $m - nq$.*

Proof. The torus link is the closure of the braid $(\sigma_1\sigma_2 \cdots \sigma_{n-1})^m$ and the lift of our braid link is the closure of the braid $(B\Delta_t^{-1})^p\Delta_t^{2q}$. We know that in the braid group the element Δ_n^2 can be represented by the word $(\sigma_1 \cdots \sigma_{n-1})^n$. Therefore the equality becomes $(\sigma_1\sigma_2 \cdots \sigma_{n-1})^m = (B\Delta_n^{-1})^p(\sigma_1\sigma_2 \cdots \sigma_{n-1})^{nq}$ and the result is straightforward. $\qquad\square$

Chapter 7

Different links with equivalent lifts

An invariant I of links is *complete* if for every pair of links L_1 and L_2, then $I(L_1) = I(L_2)$ implies that L_1 and L_2 are equivalent.

In this chapter we investigate if the lift is a complete invariant of unoriented links. Several counterexamples are shown, namely a pair of knots in $L(p, \frac{p \pm 1}{2})$ that lift to the trivial knot, a pair of links in $L(4, 1)$ that lift to the Hopf link and an infinite family of cables of the second pair in $L(4, 1)$. These results are reported in [82]

In the last section we describe what happens for oriented links and what happens for links considered up to diffeo-equivalence (see Section 2.1 for the definition). When both these assumptions hold, a result of Sakuma, Boileau and Flapan about freely periodic knots, if translated into the language of knots in lens spaces, states the completeness of the lift for primitive-homologous knots in $L(p, q)$ that does not lift to the trivial knot.

It is still unknown if this result holds for knots up to ambient isotopy (but we expect to find counterexamples also for this case). Moreover we have not been able to find counter-examples for all lens spaces, so we ask: is the lift a complete invariant for links in some fixed lens space?

7.1   Counterexamples from braid tabulation

In this section we use the braid construction of the lift described in Section 6.4 to find different links in lens spaces with equivalent lifts, that is, to prove that the lift is not a complete invariant.

Given a braid B, denote by $\widehat{B}$ the link in $\mathbf{S}^3$ obtained by the standard closure of B, that is to say, where corresponding ends are connected in pairs. We would like to perform a small tabulation using braids. The first step is to understand whether the Garside braid produces equivalent links $\widehat{\Delta_t^k} \subset \mathbf{S}^3$ for different t and k. The computations are summed up in Table 7.1; the labels of the links are the one of the Knot Atlas [8]. In this table the links are considered up to mirror image, only when it will be necessary the specification will be done.

t	B	$\widehat{B}$
1	Δ_1^0	0_1
2	Δ_2^0	$0_1 \sqcup 0_1$
2	Δ_2^1	0_1
2	Δ_2^2	$L2a1$
2	Δ_2^3	3_1
2	Δ_2^4	$L4a1$
2	Δ_2^5	5_1
2	Δ_2^6	$L6a3$

t	B	$\widehat{B}$
3	Δ_3^0	$0_1 \sqcup 0_1 \sqcup 0_1$
3	Δ_3^1	$L2a1$
3	Δ_3^2	$L6n1$
3	Δ_3^3	$L9n15$
4	Δ_4^0	$0_1 \sqcup 0_1 \sqcup 0_1 \sqcup 0_1$
4	Δ_4^1	$L4a1$
5	Δ_5^0	$0_1 \sqcup 0_1 \sqcup 0_1 \sqcup 0_1 \sqcup 0_1$
5	Δ_5^1	$L8n3$

Table 7.1: Links arising from the closure of Garside braids.

Greater string numbers or greater powers give links outside standard tabulations. Moreover, for negative powers, we obtain the link that is the mirror image of the link with the corresponding positive power. If the link is amphicheiral, like the trivial knot or the Hopf link (also denoted by $L2a1$), then the closures are equivalent.

At this stage we are looking for a braid Δ_t^k representing a link in $L(p,q)$ such that its lift is one of the possibilities in Table 7.1. As a consequence of

Proposition 6.8, the lift is the link represented by the braid $(\Delta_t^k \Delta_t^{-1})^p \Delta_t^{2q}$. Hence we look for solutions of the equation: $\Delta_t^{(k-1)\cdot p} \Delta_t^{2q} = \Delta_t^h$, where h is the suitable power of Δ_t that gives us the desired lift.

Now we list all the possible cases where the braid closures of Table 7.1 are equivalent, the desired examples will rise from the following computations.

Example 7.1. Different knots in $L\left(p, \frac{p\pm 1}{2}\right)$ with trivial knot lift. The trivial knot can be obtained either as the closure of any power of Δ_1 or as the closure of $\Delta_2^{\pm 1}$. In the first case, the link in any lens space $L(p, q)$ represented by the braid on one single string is lifted to the trivial knot. In the second case, namely $\Delta_2^{\pm 1}$, we have to study the equation $\Delta_2^{(k-1)\cdot p} \Delta_2^{2q} = \Delta_2^{\pm 1}$, that is to say, $kp - p + 2q = \pm 1$. For the positive case $kp + 2q - p = 1$, integer solutions with $0 < q < p$ can be obtained only for $k = 0$, p odd and $q = \frac{p+1}{2}$. For the negative case, the solution is $k = 0$, p odd and $q = \frac{p-1}{2}$.

If we look for a pair of different knots in the same $L(p, q)$, we have to restrict to $L\left(p, \frac{p\pm 1}{2}\right)$ with p odd. Consider K_1 as the knot represented by the braid $\Delta_1 = 1_1$ and K_2 as the knot represented by the braid $\Delta_2^0 = 1_2$, they are illustrated in Figure 7.1.
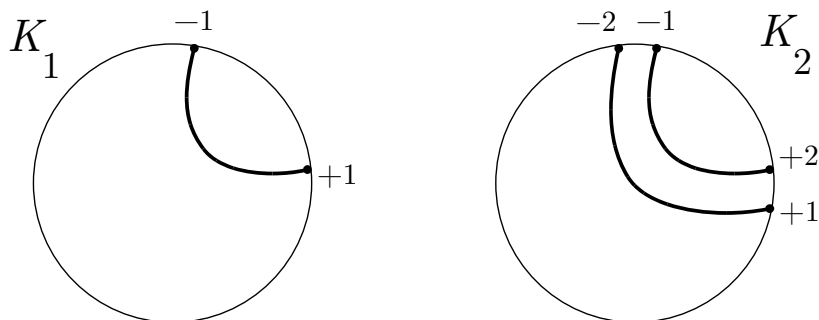

Figure 7.1: Two different knots with equivalent lift in $L\left(p, \frac{p\pm 1}{2}\right)$.

Since the homology classes are $[K_1] = 1$ and $[K_2] = 2$ as in Example 4.5, the two knots considered above in $L\left(p, \frac{p\pm 1}{2}\right)$ are different if $p > 3$ and odd; if $p = 3$ they are equivalent.

Example 7.2. Different links in $L(4,1)$ **with Hopf link lift.** As in the previous case, all the possible solutions of the corresponding equations are considered for the Hopf link $L2a1$. Table 7.2 sums up the results.

lift braid	equation	solutions
Δ_2^2	$kp + 2q - p = 2$	for all p, $L(p,1)$, $k = 1$ for all p even, $L\left(p, \frac{p+2}{2}\right)$, $k = 0$
Δ_2^{-2}	$kp + 2q - p = -2$	for all p, $L(p, p-1)$, $k = -1$ for all p even, $L\left(p, \frac{p-2}{2}\right)$, $k = 0$
Δ_3^1	$kp + 2q - p = 1$	for all p odd, $L\left(p, \frac{p+1}{2}\right)$, $k = 0$
Δ_3^{-1}	$kp + 2q - p = -1$	for all p odd, $L\left(p, \frac{p-1}{2}\right)$, $k = 0$

Table 7.2: Links in lens spaces lifting to Hopf link.

We look for solutions in the same lens space, and after excluding equivalent links, we get only the following pair of links in $L(4,1)$: consider the knot L_A represented by the braid $B_1 = 1_2$ and the link L_B represented by $B_2 = \Delta_2$. They are different because they have a different number of components, but they have the same lift, the Hopf link. In order to better understand the topological construction of the lift, we illustrate it in Figure 7.2.

The last case of Table 7.1 is the link $L4a1$, that is not amphicheiral, as a consequence Table 7.3 is divided into two cases. Let $m(L4a1)$ denote the mirror image of $L4a1$. No example rises from this case.

7.2   Counterexamples from satellite construction

The examples found in Section 7.1 consist of links that are easy to distinguish, because they have different numbers of components or different homology classes. Therefore we now construct some satellite link of the previous examples, in order to get an infinite family of different links with the same number of components and the same homology class.
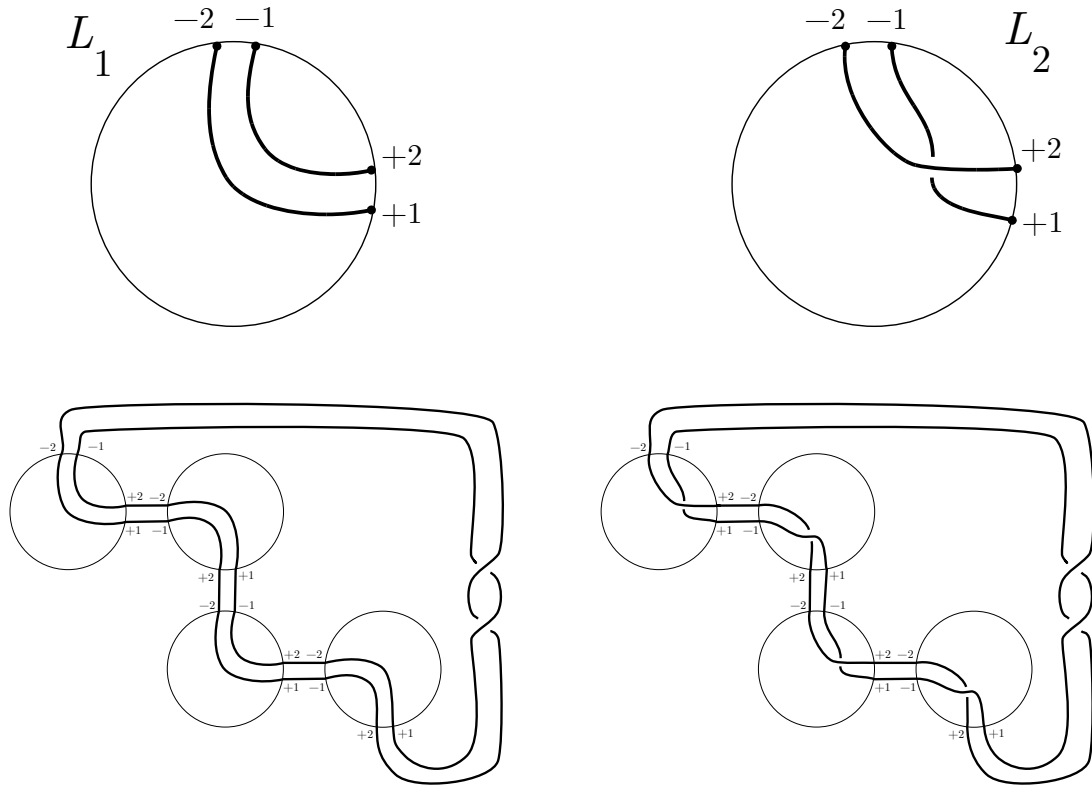
Figure 7.2: Two different links with equivalent lift in $L(4,1)$.

link	lift braid	equation	solutions
m(L4a1)	Δ_4^1	$kp + 2q - p = 1$	for all p odd, $L\left(p, \frac{p+1}{2}\right)$, $k = 0$
m(L4a1)	Δ_2^4	$kp + 2q - p = 4$	for all p, $L(p, 2)$, $k = 1$ for all p even, $L\left(p, \frac{p+4}{2}\right)$, $k = 0$
L4a1	Δ_4^{-1}	$kp + 2q - p = -1$	for all p odd, $L\left(p, \frac{p-1}{2}\right)$, $k = 0$
L4a1	Δ_2^{-4}	$kp + 2q - p = -4$	for all p, $L(p, p-2)$, $k = -1$ for all p even, $L\left(p, \frac{p-4}{2}\right)$, $k = 0$

Table 7.3: Links in lens spaces lifting to $L4a1$ or $m(L4a1)$.

Example 7.3. Different links in $L(4,1)$ with cables of Hopf link as lift. Consider the knot L_A and the link L_B of Example 7.2. A satellite of L_B can be the link where the two patterns are described by two braids τ_n

and ψ_m on n and m strands respectively, as in part B1) of Figure 7.3. Label B such link.
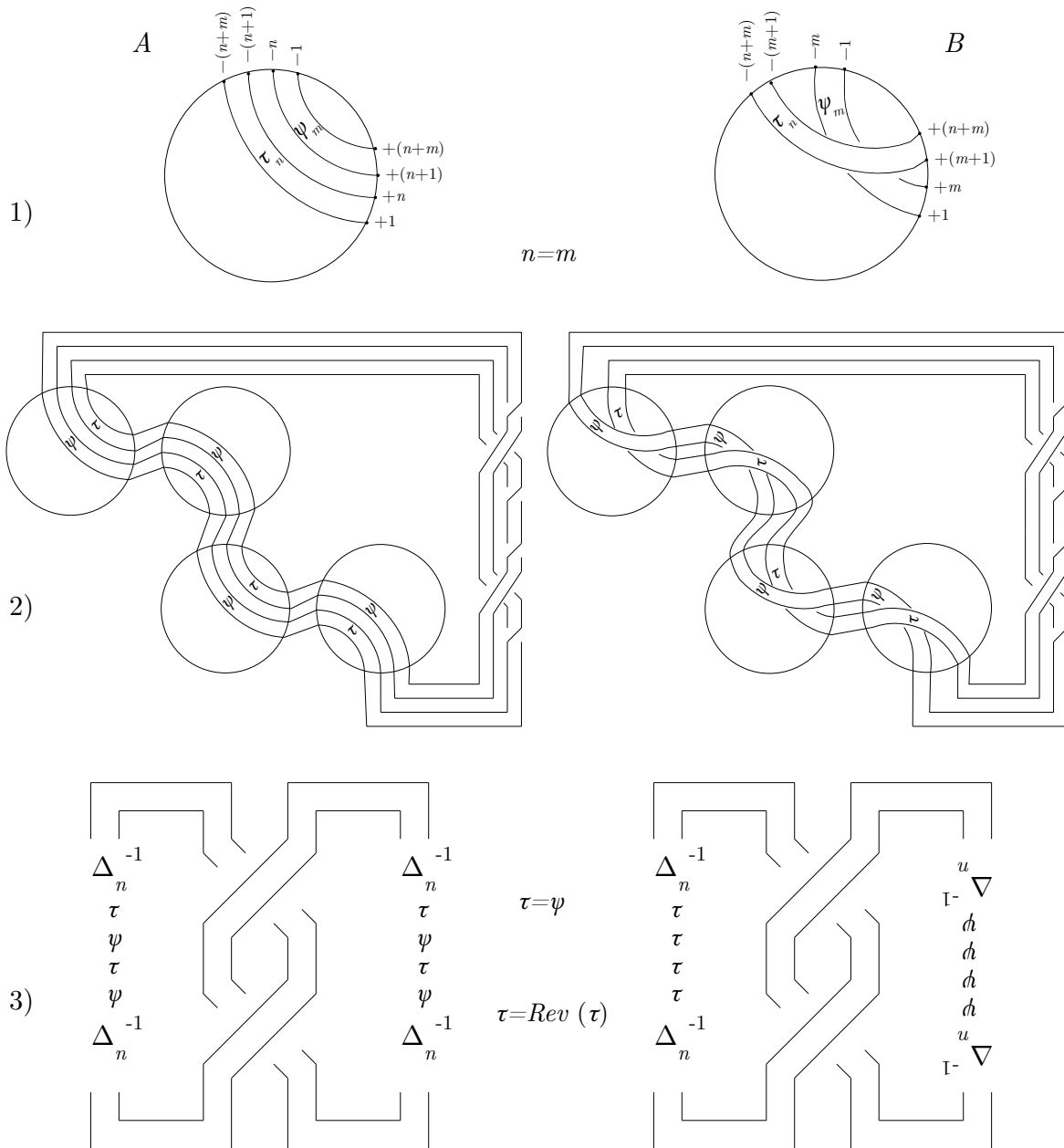

Figure 7.3: Satellite construction of different links with equivalent lift.

We need to make a satellite of the knot L_A making the lift equivalent

to the previous one, therefore we have to put the braids τ_n and ψ_m on each overpass of the diagram of L_A, as in part A1) of Figure 7.3. Label A such link. Note that the boundary points of the two braids mix up, unless we assume $n = m$.

The lift diagrams of the two considered links are illustrated in part 2) of Figure 7.3 and in part 3) it is clear that the companion link is the Hopf link. The pattern braids are $\Delta_n^{-1}\tau\psi\tau\psi\Delta_n^{-1}$ on both sides of A, while for B we have the braid $\Delta_n^{-1}\tau^4\Delta_n^{-1}$ and the braid $\Delta_n^{-1}\psi^4\Delta_n^{-1}$ that is reversed upside down. With the assumption $\tau = \psi$ we get $\Delta_n^{-1}\tau^4\Delta_n^{-1}$ on both sides of A, whereas for B we have the same braid on one side and the reversed braid on the other side.

A paper of Garside [53] tells us that the operation of reversing a braid is the antihomomorphism of the braid group $Rev\colon B_n \to B_n$ which sends $\sigma_{i_1}\sigma_{i_2}\cdots\sigma_{i_r}$ into the braid $\sigma_{i_r}\sigma_{i_{r-1}}\cdots\sigma_{i_1}$. He proves that $Rev(\Delta)$ is equivalent to Δ into the braid group; for this reason, it is enough to assume $\tau = Rev(\tau)$ in order to have an equivalent lift for A and B. An easy example of reversible braids are palindromic ones (see [34] for details).

We can make some more assumptions on τ in order to handle a smaller family of links with known number of components. Let $i > 0$ and $j \geq 0$ be two integer numbers and let $\tau = \Delta_i^j$, denote with $A_{i,j}$ and $B_{i,j}$ the correspondent links. The considered braid produces a pattern of the satellite that is a torus link, that is to say, $A_{i,j}$ and $B_{i,j}$ are cables of L_A and L_B. The links of this family have different behaviors for different values of i and j:

for $i = 1$, for all j: we have $A_{1,j} = L_A$ and $B_{1,j} = L_B$;

for all even i, for $j = 0$: the link $A_{i,0}$ and $B_{i,0}$ are equivalent (it is an easy exercise using generalized Reidemeister moves);

for all odd i, for $j = 0$: the links $A_{i,0}$ and $B_{i,0}$ have respectively $n = i$ and $n = i + 1$ components, hence they are an infinite family of different links with equivalent lift;

for all odd $i > 1$ or for all odd $j > 0$: the links $A_{i,j}$ and $B_{i,j}$ have a different number of components, hence they are an infinite family of different

links with equivalent lift;

for all even $i > 1$ and for all even $j > 0$: the links $A_{i,j}$ and $B_{i,j}$ have the
same number of components $n = i$, moreover each of these components
has the same homology class $\delta = 2$; the smaller case, $A_{2,2}$ and $B_{2,2}$
is illustrated in Figure 7.4; we cannot prove that all the pairs of links
in this family are different, anyway the computation of the Alexander
polynomials of $A_{2,2}$ and $B_{2,2}$ (see Table 8.3) says that the first case
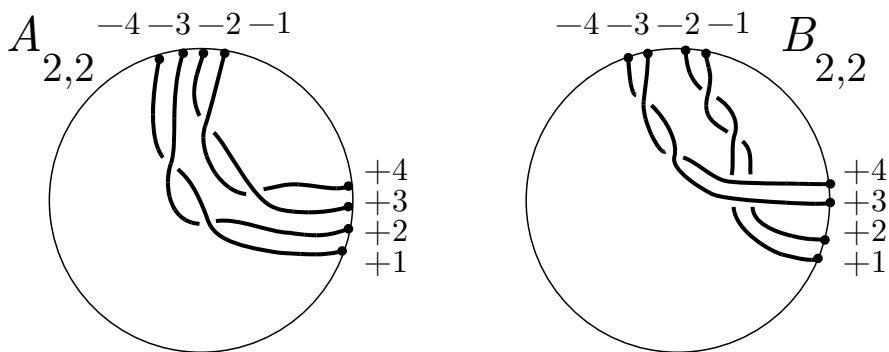consists of different links.

Figure 7.4: Two different links with equivalent lift in $L(4, 1)$.

7.3 The case of oriented and diffeomorphic links

Up to this stage we have considered unoriented links up to ambient iso-
topy. The problem of understanding whether the lift is a complete invariant
can be referred also to oriented links and to links up to diffeo-equivalence.
The answer is slightly different.

First of all, an orientation on the previous counter-examples allows us to
find new examples with different oriented link in lens spaces having equivalent
oriented lift. Moreover another family of counter-examples arises.

Remark 7.4. If we take an oriented knot $K \subset L(p, q)$ such that $\widetilde{K}$ is invertible
(i.e., it is equivalent to the knot with reversed orientations), then also the

knot $-K \subset L(p,q)$ with reversed orientation has the same lift. Usually $-K$ is not equivalent to K because the homology class changes. A really simple example consists of the two knots in $L(3,1)$ illustrated in Figure 7.5: they both lift to the trivial knot, nevertheless they have different homology classes ($[K] = 1$ and $[-K] = 2$). For links something similar happens, but you have to be careful to the orientation of each component.
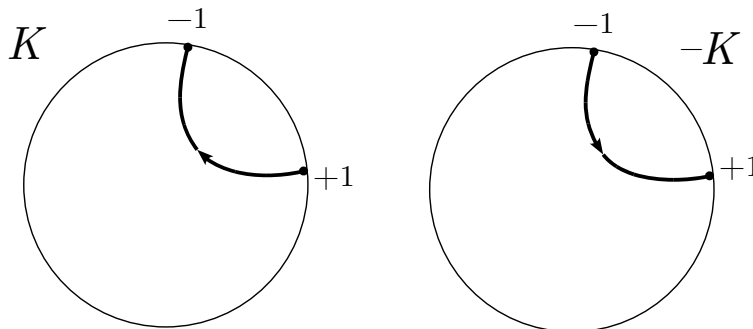

Figure 7.5: Two different oriented knots with equivalent trivial lift in $L(3,1)$.

Furthermore we can consider oriented links up to diffeo-equivalence (see Section 2.1 for definitions). In this case we analyze the following theorem of Sakuma, also proved by Boileau and Flapan, about freely periodic knots. Let K be a knot in the 3-sphere; if $\mathrm{Diff}^*(\mathbf{S}^3, K)$ is the group of diffeomorphisms of the pair $(\mathbf{S}^3, K)$, which preserves the orientation of both $\mathbf{S}^3$ and K, then a symmetry G of a knot K in $\mathbf{S}^3$ is a finite subgroup of $\mathrm{Diff}^*(\mathbf{S}^3, K)$, up to conjugation.

Theorem 7.5. [101, 12] *Suppose that a knot $K \subset \mathbf{S}^3$ has free period p. Then there is a unique symmetry G of K realizing it, provided that (i) K is prime, or (ii) K is composite and the slope is specified.*

If we translate it into the language of knots in lens spaces, we have that the specification of the slope is equivalent to fixing the q of the lens space. As a consequence, two primitive-homologous knots K_1 and K_2 in $L(p,q)$ with equivalent non-trivial lift are necessarily diffeo-equivalent in $L(p,q)$.

From the group of diffeotopies of $L(p,q)$ displayed in [13] and [66], we know that a diffeomorphism in $L(p,q)$ does not always induce an ambient isotopy of knots, thus this does not provide a complete answer about the equivalence of K_1 and K_2 up to ambient isotopy.

Remark 7.6. The Examples 7.1, 7.2 and 7.3 show non isotopic links that have equivalent lift. Are they still different up to diffeo-equivalence? None of the examples is included in Theorem 7.5, since the lift is the unknot or a link with more than one component. In order to investigate this question we use the group of diffeotopies of $L(p,q)$. For Example 7.1 in the case $L(5,2)$, we know that the diffeomorphism $\sigma_-\colon L(5,2) \to L(5,2)$, described in [13], brings K_1 to K_2, that is to say, these knots are equivalent up to diffeo-equivalence. On the contrary, the other two examples provide links that are not diffeo-equivalent: if they were diffeo-equivalent, their complement would be diffeomorphic and their fundamental group isomorphic. The links L_1 and L_2 of Example 7.2 have a different number of component, hence a different homology group and a different group of the link. The links $A_{2,2}$ and $B_{2,2}$ of Example 7.3 have different Alexander polynomials, hence different groups of the links.

Chapter 8

Essential geometric invariants

It is clear that every invariant of links in $\mathbf{S}^3$ becomes an invariant of links in lens spaces if the first invariant is computed on their lift in $\mathbf{S}^3$. This allow us to compute a lot of invariants. On the contrary, to create a new invariant for links in lens space, we have to pay attention that this invariant is not only an invariant of the lift; we will call *essential* this kind of invariant.

The different links with equivalent lift of Chapter 7 are the perfect tool to check whether an invariant I of links in lens spaces is essential: just find two different knots K_1 and K_2 with equivalent lift such that $I(K_1) \neq I(K_2)$. From now on, the thesis will focus on checking the essentiality of several invariants of links in lens spaces.

In this chapter we investigate the most geometric invariants: the fundamental quandle, the group of the link and the twisted Alexander polynomials. Then, in the last section we review the relation between some invariants of links in lens spaces and the corresponding invariant on their lifts.

8.1   The fundamental quandle is inessential

The fundamental quandle is a very strong invariant of links in the 3-sphere: in fact it is a complete invariant. It can be defined also for links in lens spaces [86, 44]: is it still a complete invariant? This question is strictly

related also with the essentiality of the invariant.

Given an oriented link $L \subset L(p, q)$, let $N(L)$ denote an open tubular neighborhood of L, consider the manifold $Q = \overline{L(p, q) \smallsetminus N(L)}$ and fix a base point x_L in it. Let Γ_L be the set of homotopy classes of paths from x_L to $\partial N(L)$. We can define an operation $\circ$ on this set: for every a and b in Γ_L, consider the toric component of $\partial N(L)$ containing the starting point of b and let m be a meridian of this torus, the operation $a \circ b$ gives the class of the path $bmb^{-1}a$. The set Γ_L with the operation $\circ$ is a distributive groupoid or equivalently, a quandle. The proof of this fact can be found in [86]. The algebraic structure $(\Gamma_L, \circ)$ is the *fundamental quandle* of an oriented link L in $L(p, q)$.

Proposition 8.1. [44, Lemma 5.4] *The fundamental quandle of a link in a lens space is isomorphic to the fundamental quandle of its lift in $\mathbf{S}^3$.*

Proof. The fundamental quandle is invariant under cyclic coverings, and if we consider the cyclic covering $P \colon (\mathbf{S}^3 \smallsetminus \widetilde{L}) \to (L(p, q) \smallsetminus L)$, the fundamental quandle of links in lens space is isomorphic to the fundamental quandle of its lift.   □

From this result, follows at once the succeeding corollary.

Corollary 8.2. *The fundamental quandle of links in lens spaces is an inessential invariant.*

The fundamental quandle of a link in a 3-manifold is a geometric invariant that can be explicitly computed on a diagram only for links in $\mathbf{S}^3$ [71, 86] and in $\mathbb{RP}^3$ [59]. Proposition 8.1 allows us to compute the fundamental quandle of a link L in lens spaces by computing the fundamental quandle of the lift $\widetilde{L}$.

Theorem 7.5 can be combined to Proposition 8.1 to get the following statement.

Corollary 8.3. *The fundamental quandle of oriented primitive-homologous knots in lens spaces can classify them up to diffeo-equivalence, unless the fundamental quandle is trivial.*

This result, for the case $\mathbb{RP}^3 = L(2,1)$, was directly stated in [58], where it is extended also to non primitive-homologous knots.

Proposition 8.4. [58, Theorem 1] *Two knots in $\mathbb{RP}^3$ are diffeo-equivalent if and only if the corresponding fundamental quandles are isomorphic.*

We cannot generalize Corollary 8.3 to knots in all lens spaces up to ambient isotopy because of Example 7.1. Moreover also for links up to diffeo-equivalence this is impossible, as a consequence of the non diffeomorphic pairs of Examples 7.2 and 7.3 (see Remark 7.6).

Corollary 8.5. *The fundamental quandle of links in lens spaces is not a complete invariant for $L(4,1)$ and $L(p, \frac{p\pm1}{2})$ with $p > 3$, odd.*

Following [17], we can compute other invariants of links in lens space derived from the quandle theory, such as quandle co-cycles invariants. If they are an invariant of the quandle, then they are inessential. If we consider bi-quandles instead, there is an example [59] for links in the projective space where the co-cycle invariant seems more significant.

If we want a quandle-like structure that results essential we should turn to the oriented augmented fundamental rack [44], that is a complete invariant of framed links in 3-manifolds, and for framed links in lens spaces can be computed using mixed link diagrams.

8.2 The group and the twisted Alexander polynomials are essential

In Chapters 4 and 5 several geometric invariants for links in lens spaces are considered. In order to understand if they are essential or not, we compute them on Examples 7.1, 7.2 and 7.3, and we list them respectively in Tables 8.1, 8.2 and 8.3.

Remember that ν is the number of components of the link. The integer d is the homology torsion index. Thanks to a presentation of the fundamental

group, we are able to compute the d one-variable twisted Alexander polynomials: $\bar{\Delta}^1$, $\bar{\Delta}^\zeta$, …, $\bar{\Delta}^{\zeta^{d-1}}$, where ζ is a d-th primitive root of unity. It is necessary to consider oriented links for the computation of these polynomials: we choose the orientations (shown by the figures in each table) that make the corresponding oriented lifts equivalent.
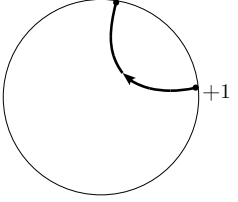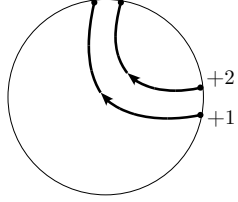
	K_1	K_2
ν	1	1
$[K] \subset H_1(L(p,q))$	1	2
$\pi_1(L(p,q) \smallsetminus K)$	$\mathbb{Z}$	$\mathbb{Z}$
$H_1(L(p,q) \smallsetminus K)$	$\mathbb{Z}$	$\mathbb{Z}$
$\bar{\Delta}^1(t)$	1	1

Table 8.1: Geometric invariants of K_1 and K_2 in $L\left(p, \frac{p-1}{2}\right)$.

Moreover, we have examples of links with isomorphic link group but inequivalent lift: the links arise from Table 7.3 and the invariants are on Table 8.4.

The following two remarks sum up the comments arising from these computations.

Remark 8.6 (Properties of the group of the link). The results of Table 8.2 show that the fundamental group of the complement of the link is an essential invariant. As noted in Example 4.5, from Table 8.1 we have another interesting information: the knot group is not a complete invariant of prime knots in lens spaces because the knots K_1 and K_2 of Example 7.1 are inequivalent prime knots with isomorphic knot group. Finally Table 8.4 says that sometimes the lift can distinguish links with equivalent link group.
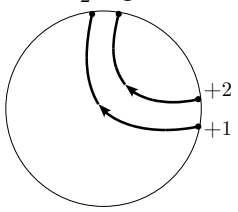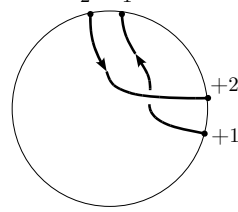
	L_A	L_B
ν	1	2
$[K] \subset H_1(L(p,q))$	2	$1, 1$
$\pi_1(L(p,q) \smallsetminus L)$	$\langle a, f \mid af^{-1}af^{-3} = 1 \rangle$	$\langle a, f \mid af = fa \rangle$
$H_1(L(p,q) \smallsetminus L)$	$\mathbb{Z} \oplus \mathbb{Z}_2$	$\mathbb{Z} \oplus \mathbb{Z}$
$\bar{\Delta}^1(t)$	$t + 1$	$t - 1$
$\bar{\Delta}^{-1}(t)$	1	

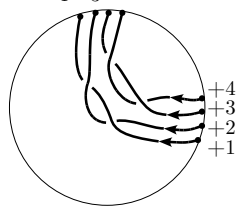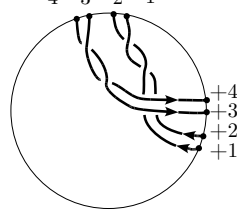Table 8.2: Geometric invariants of L_A and L_B in $L(4,1)$.

	$A_{2,2}$	$B_{2,2}$
ν	2	2
$[K] \subset H_1(L(p,q))$	$2, 2$	$2, 2$
$H_1(L(p,q) \smallsetminus L)$	$\mathbb{Z} \oplus \mathbb{Z} \oplus \mathbb{Z}_2$	$\mathbb{Z} \oplus \mathbb{Z} \oplus \mathbb{Z}_2$
$\bar{\Delta}^1(t)$	$t^7 + t^6 - t - 1$	$t^7 - t^6 + t^5 - t^4 + t^3 - t^2 + t - 1$
$\bar{\Delta}^{-1}(t)$	$t^6 + 1$	$t^6 + t^4 + t^2 + 1$

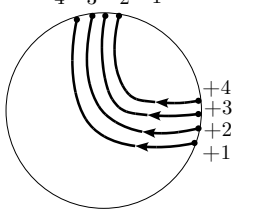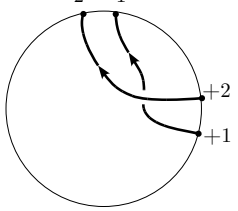Table 8.3: Geometric invariants of $A_{2,2}$ and $B_{2,2}$ in $L(4,1)$.

	M_1	M_2
	$-4\ -3\ -2\ -1$ ... $+4\ +3\ +2\ +1$	$-2\ \ -1$ ... $+2\ \ +1$
ν	2	2
$[K] \subset H_1(L(p,q))$	$2,2$	$1,1$
$\pi_1(L(p,q) \smallsetminus L)$	$\langle a, f \mid af^2 = f^2a \rangle$	$\langle a, f \mid af^2 = f^2a \rangle$
$H_1(L(p,q) \smallsetminus L)$	$\mathbb{Z} \oplus \mathbb{Z}$	$\mathbb{Z} \oplus \mathbb{Z}$
$\bar{\Delta}^1(t)$	$t^2 - 1$	$t^2 - 1$

Table 8.4: Geometric invariants of M_1 and M_2 in $L(5,2)$.

Remark 8.7 (Properties of the Twisted Alexander polynomials). The computations of Tables 8.2 and 8.3 shows that twisted Alexander polynomials are essential invariants. Table 8.1 says that this invariant is not complete, while Table 8.4 shows that the lift is sometimes stronger than the Alexander polynomial.

8.3   Characterization of invariants of the lift

Links in the lens space $L(p,q)$ can be seen also as (p,q)-lens links in $\mathbf{S}^3$ [28] and their lift as a freely p-periodic link. This gives us the opportunity to relate the invariants of the link to the corresponding invariant of its lift. Moreover when $q = 0$, interesting results for p-periodic links arise.

The first question that deserves our interest is the following: do the Alexander polynomial of the lift depends on the twisted Alexander polynomials of the link in lens spaces? Hartley gave the answer for the Alexander polynomial of freely periodic knots: in [65] there is a formula connecting the twisted Alexander polynomials in the case that both $K \subset L(p,q)$ and

$\widetilde{K} \subset \mathbf{S}^3$ are knots (see also Example 8.10).

Proposition 8.8. [65] *Let ζ be a primitive p-root of unity. If the map $\sigma\colon \pi_1(L(p,q) \smallsetminus K) \to \mathbb{Z}[\zeta][t^{\pm 1}]$ is the representation we use for the knot in the lens space and the map $\widetilde{\sigma}\colon \pi_1(\mathbf{S}^3 \smallsetminus \widetilde{K}) \to \mathbb{Z}[t^{\pm 1}]$ is the lift of this representation to the knot lift, then:*

$$\bar{\Delta}_{\widetilde{K}}^{\widetilde{\sigma}}(t) = \prod_{i=0}^{p-1} \bar{\Delta}_K^{\sigma}(\zeta^i t) \tag{8.1}$$

Furthermore, Chbili has shown in [27, 26, 25] some interesting characterizations for multi-variable Alexander, Jones and HOMFLY-PT polynomials of the lift of links in lens spaces. Then, in [28], the author exploited these results to find some criterions to establish whether a certain link in $\mathbf{S}^3$ can be a freely periodic link (or the lift of a link in a lens space, in our perspective).

We report here his result about multivariable Alexander polynomials since we treat them extensively. Suppose that the link L in the lens space $L(p,q)$ is represented by a braid B. Specifically, we express the result in terms of the Alexander invariant D_L instead of Δ_L. Recall that $D_L = \Delta_L/(1-t)$ if L is a knot, and D_L is exactly the Alexander polynomial for links with more than one component.

Proposition 8.9. [27] *Let p be a prime, $q \in \mathbb{N}$ and B an n-braid. Then we have the following congruence modulo p:*

$$(1 - t_1^{n_1} \cdots t_k^{n_k}) D_{\widehat{(B\Delta_n^{-1})^p \Delta_n^{2q}}}(t_1,...,t_k) \equiv 1 + (t_1^{n_1} \cdots t_k^{n_k})^q A_1^p(t_1,\ldots,t_k) +$$

$$+ \ldots + (t_1^{n_1} \cdots t_k^{n_k})^{(n-1)q} A_{n-1}^p(t_1,\ldots,t_k) \tag{8.2}$$

where k is the number of components of $\widehat{(B\Delta_n^{-1})^p \Delta_n^{2q}}$, $n_1 + \ldots + n_k = n$, and $A_1,\ldots,A_{n-1}$ are elements of $\mathbb{Z}[t_1^{\pm 1},\ldots,t_k^{\pm 1}]$.

Moreover Jeong and Park in [70] give some conditions on the Vassiliev invariants for links in $\mathbf{S}^3$ in order to be the lift of some lens link: they get pieces of information about Vassiliev invariants by exploiting the previous results about Jones and HOMFLY-PT polynomials.

Finally, Futer, Kalfagianni and Purcell [48] observe that $vol(\mathbf{S}^3 \smallsetminus \widetilde{K}) = p \cdot vol(L(p,q) \smallsetminus K)$ and give a bound for the hyperbolic volume of freely periodic knots.

We can illustrate Propositions 8.8 and 8.9 with an example.

Example 8.10. Consider the knot $H \subset L(4,1)$ of Figure 8.1, that is described by the braid σ_2^{-1}. Its lift is represented by the braid $(\sigma_2^{-1}\Delta_3^{-1})^4\Delta_3^2$.
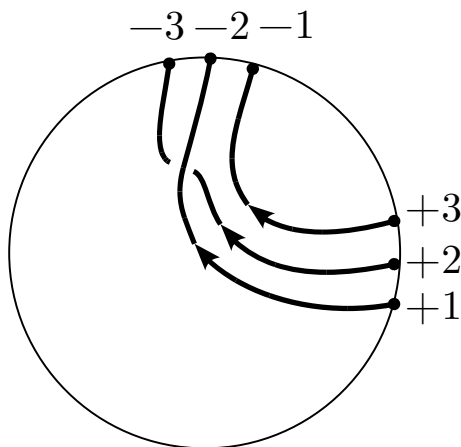

Figure 8.1: Knot in $L(4,1)$ described by the braid σ_2^{-1}.

The Alexander polynomial of the lift is $1-t+t^3-t^4+t^5-t^7+t^8$. The Alexander polynomial of H in $L(4,1)$ is $p(t) = 1-t+t^3-t^4+t^5-t^7+t^8$, but the map σ sends the non-torsion generator of the homology presentation we are considering to t^4. As a consequence, the map $\widetilde{\sigma}$ for the Alexander polynomial of the lift sends the generator of the homology to t^4 too and the corresponding Alexander polynomial of the lift becomes $1-t^4+t^{12}-t^{16}+t^{20}-t^{28}+t^{32}$. Hence, if we substitute t with respectively t, $-t$, it and $-it$ in $p(t)$, Formula 8.1 is verified:

$$(1 - t^4 + t^{12} - t^{16} + t^{20} - t^{28} + t^{32}) = p(t)p(-t)p(it)p(-it).$$

Moreover, Formula 8.2 can be written as:

$$(1 - t^3)D\widehat{_{(B\Delta_n^{-1})^p\Delta_n^{2q}}}(t_1, ..., t_k) = (1 - t^3)\frac{\Delta\widehat{_{(B\Delta_n^{-1})^p\Delta_n^{2q}}}(t)}{1 - t} = 1 + t^5 + t^{10} \equiv$$

$$\equiv 1 + (t^3)^1 A_1^4(t) + (t^3)^{2\cdot1} A_2^4(t) \equiv 1 + (t^3)t^2 + (t^6)t^4 \text{ mod } 4,$$

where the number of strings of the braid is $n = 3$.

Remark 8.11. On the contrary of these results, can we find pieces of information about the twisted Alexander polynomial of a link $L \subset L(p, q)$ from the Alexander polynomial of its lift? From Tables 8.2 and 8.3 we see that this is not possible, neither for knots nor for links. Another interesting counterexample for this question is the next one: considering the unknot and the local trefoil in $L(2, 1)$, their lifts are the unlink with two components and two split trefoils respectively. The twisted Alexander polynomials of these links in $L(2, 1)$ are different, their lifts in $\mathbf{S}^3$ are different, but their lifts have the same Alexander polynomial (equal to zero).

Chapter 9

# Essential KBSM and HOMFLY-PT invariants

In this chapter we investigate whether the Kauffman Bracket Skein Module for unoriented links in lens spaces and the HOMFLY-PT polynomial for oriented links in lens spaces, developed in [31], are essential invariants.

9.1 The KBSM of $L(p,q)$ via band diagrams

In this section we describe the rules of the Kauffman Bracket Skein Module (also called $(2,\infty)$-skein module) of $L(p,q)$ introduced in [67].

A framed link in a 3-manifold M is a submanifold of M diffeomorphic to the disjoint union of ν copies of an annulus $\mathbf{S}^1 \times B^1$. Let $\mathcal{L}_{fr}$ be the set of ambient isotopy classes of unoriented framed links in the 3-manifold M – we also add the empty knot $\emptyset$ to this set. Let $L^{(n)}$ denote the framed link obtained by $L \subset \mathcal{L}_{fr}$ by adding n full right-handed twists to the frame. Let $R = \mathbb{Z}[A^{\pm 1}]$ be the ring of Laurent polynomials in the variable A. Define $\mathcal{S}_{fr}$ to be the submodule of $R\mathcal{L}_{fr}$ generated by the skein relations $L - AL_0 - A^{-1}L_\infty$ and $L^{(1)} + A^3 L$, where L_0 and L_∞ denote the links obtained by the resolutions of one crossing of L as Figure 9.1 shows.

The *Kauffman bracket skein module* (*KBSM* for sake of conciseness) is
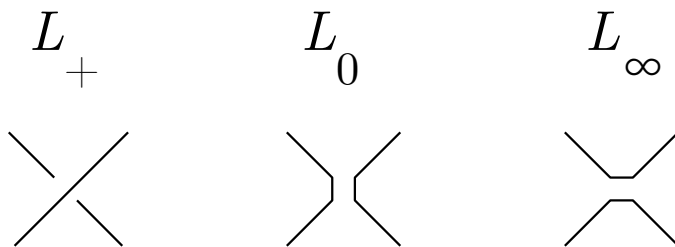
Figure 9.1: Resolution of a crossing of L.

the quotient module $S_{2,\infty}(M) = R\mathcal{L}_{fr}/\mathcal{S}_{fr}$.

If we want to understand this skein module $S_{2,\infty}(L(p,q))$, we have to find a free basis of it. The KBSM of the solid torus is necessary to find this free basis. We use the representation of links in lens space given by punctured disk/band diagrams. These diagrams are useful also to represent links in the solid torus (see Section 2.3). Let x_0 denote the local unknot in the solid torus and x_i denote the link with i components described in Figure 9.2.
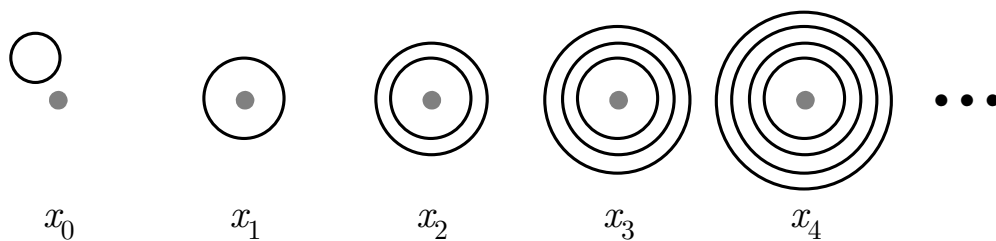

Figure 9.2: KBSM basis for the punctured disk diagram.

Proposition 9.1. [67, Corollary 2] *The KBSM of the solid torus is freely generated by the set $\{x_i\}_{i\in\mathbb{N}}$.*

From this proposition Hoste and Przytycki obtain the following one.

Proposition 9.2. [67, Theorem 4] *For $p \geq 1$ the KBSM of $L(p,q)$ is freely generated by $x_0, x_1, \ldots, x_{\lfloor p/2 \rfloor}$, where $\lfloor r \rfloor$ denotes the integer part of r.*

Remark 9.3. The computation of the Kauffman bracket of a link L in $L(p, q)$ described by a punctured disk diagram is performed using the following algorithm: simplify all the crossings with the skein relation, obtaining a linear combination with coefficients in $\mathbb{Z}[A^{\pm 1}]$ of the diagrams of Figure 9.2, then substitute each x_i for all $i \neq \lfloor p/2 \rfloor$ with a suitable linear combination of the basis $x_0, x_1, \ldots, x_{\lfloor p/2 \rfloor}$. The formula for x_i, $i > \lfloor p/2 \rfloor$, can be found by considering x_{i-p} (or x_{p-i} if $i - p < 0$), applying an SL move and resolving the crossings with the skein relation. We denote the final result by $\mathrm{KBSM}(L)$.

As a consequence, the KBSM of a knot in $L(p, q)$ can be recovered from the KBSM of the corresponding knot in the solid torus. Through this method, in [50] the author provided the KBSM of all knots in $L(p, q)$ represented by punctured disk diagrams, up to 5 crossings.

9.2   KBSM is an essential invariant

Similarly to the other invariants of Chapter 8, we would like to know whether the KBSM is an essential invariant. For this reason, we compute the KBSM on the Examples 7.1, 7.2 and 7.3 which consist of different links with equivalent lift. In order to perform the calculations, we should transform the disk diagrams into punctured disk diagrams, by using the geometric algorithm of Proposition 3.5. The result of the computations is that the KBSM is an essential invariant.

Example 9.4. In Figure 9.3 are represented the punctured disk diagrams of the knots K_1 and K_2 in $L\left(p, \frac{p \pm 1}{2}\right)$ of Example 7.1, that is to say, when $p > 3$ and odd.

After an easy calculation, it holds $\mathrm{KBSM}(K_1) = x_1$ and $\mathrm{KBSM}(K_2) = Ax_2 + A^{-1}x_0$.

Example 9.5. The two links L_A and L_B in $L(4, 1)$ of Example 7.2 are represented by the punctured disk diagrams of Figure 9.4. After an easy computation, we find that $\mathrm{KBSM}(L_A) = Ax_2 + A^{-1}x_0$ and $\mathrm{KBSM}(L_B) = x_2$.
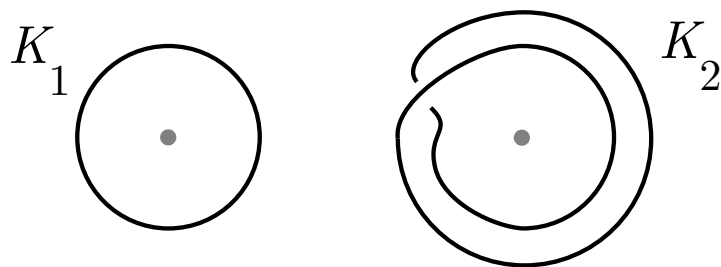
Figure 9.3: Punctured disk diagrams K_1 and K_2 in $L\left(p, \frac{p\pm 1}{2}\right)$.
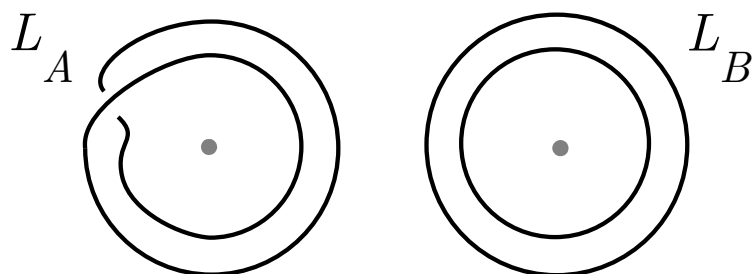

Figure 9.4: Punctured disk diagrams for L_A and L_B in $L(4, 1)$.

Example 9.6. The two links $A_{2,2}$ and $B_{2,2}$ in $L(4, 1)$ of Example 7.3 are represented by the punctured disk diagrams illustrated in Figure 9.5, according to Proposition 3.5. The skein reduction tree is quite big, therefore we report
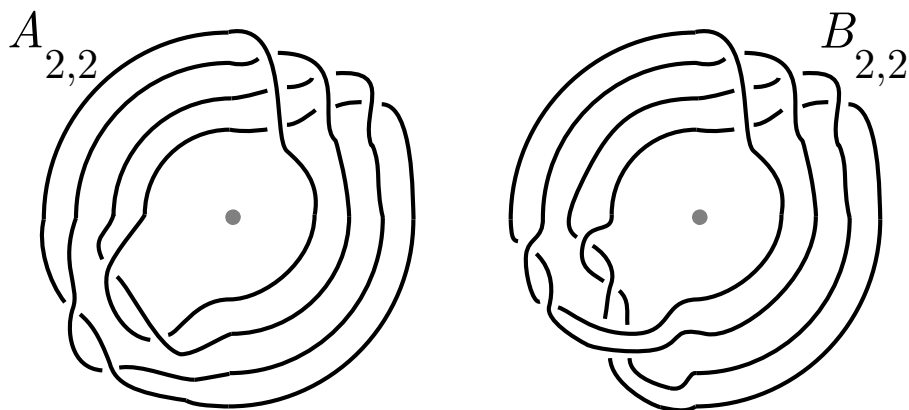

Figure 9.5: Punctured disk diagrams for $A_{2,2}$ and $B_{2,2}$ in $L(4, 1)$.

here only the final result:

$$\mathrm{KBSM}(A_{2,2}) = (3A^{14} + A^{10} - 2A^8 - A^6 - 1)x_2 +$$
$$+ (-A^{20} + A^{12} - A^6 - A^{-2} + A^{-4} - A^{-8} + A^{-12} - A^{-16})x_0$$

$$\mathrm{KBSM}(B_{2,2}) = (3A^{12} + A^8 - 2A^6 + 2A^2 + 2 + 4A^{-2} + 2A^{-4})x_2 +$$
$$+(-A^{18}+A^{10}-A^4+1+3A^{-4}-A^{-6}+5A^{-8}-3A^{-10}+4A^{-12}-3A^{-14}-A^{-18})x_0.$$

9.3 The HOMFLY-PT invariant via grid diagrams

In this section we introduce the HOMFLY-PT invariant for oriented links in lens spaces, developed in [31] (see this reference for the details). This definition is given on the grid diagrams described in Section 2.4. The aim is to understand whether the HOMFLY-PT invariant is essential, according to Chapter 8.

The trivial knot in $\mathbf{S}^3$, that is to say, the knot that bounds a disk, is the ending point of the skein reduction of the HOMFLY-PT polynomial in $\mathbf{S}^3$. In the lens spaces this is not enough. For this reason the definition of trivial links of Section 2.1 is generalized by [31] to a wider family. We say that a link in $L(p, q)$ is *trivial* if it can be represented by a grid diagram satisfying the following conditions:

- the markings in each box lie only on the principal diagonal (the one going from NE-corner to the SW-corner);
- all the O-markings are contained in the the first box (from the left);
- the X-markings in the same box are contiguous, and if the first box contains X-markings, one of them lies in the SW corner;
- for each X-marking, all the other X-markings lying in a row below, must lie in a column on the left.

A trivial link will be denoted as $U_{i_0, i_1, \dots, i_{p-1}}$ where $i_j \in \mathbb{N}$ is the number of components of the link belonging to the j-th homology class. In Figure 9.6 is illustrated the trivial link $U_{1,0,1,2} \subset L(4,1)$ having one 0-homologous component, zero 1-homologous component, one 2-homologous component and two 3-homologous components.

O								X							
	O				X										
		O				X									
			$Ø$												

Figure 9.6: Grid diagram for the trivial link $U_{1,0,1,2}$ in $L(4,1)$.

Theorem 9.7. [31] *Let $\mathcal{L}$ be the set of isotopy classes of links in $L(p,q)$ and let $\mathcal{TL} \subset \mathcal{L}$ denote the set of isotopy classes of trivial links. Define $\mathcal{TL}^* \subset \mathcal{TL}$ to be those trivial links with no nullhomologous components. Let U be the isotopy class of the standard unknot, a local knot in $L(p,q)$ that bounds an embedded disk. Given a value $J_{p,q}(T) \in \mathbb{Z}[a^{\pm 1}, z^{\pm 1}]$ for every $T \in \mathcal{TL}^*$, there is a unique map $J_{p,q} \colon \mathcal{L} \to \mathbb{Z}[a^{\pm 1}, z^{\pm 1}]$ such that:*

- *$J_{p,q}$ satisfies the skein relation $a^{-p} J_{p,q}(L_+) - a^p J_{p,q}(L_-) = z J_{p,q}(L_0)$;*
- *$J_{p,q}(U) = \left(\frac{a^{-1} - a}{z} \right)^{p-1}$;*
- *$J_{p,q}(U \sqcup L) = \left(\frac{a^{-p} - a^p}{z} \right) J_{p,q}(L)$.*

As usual, the links L_+, L_-, and L_0 differ only in a small neighborhood of a double point: Figure 9.7 shows how this difference appears on grid diagrams.

The HOMLFY-PT invariant produced by Theorem 9.7 is not yet a polynomial, Cornwell suggests to produce a polynomial in the usual HOMFLY two variables by defining $J_{p,q}$ on the trivial links as the classic HOMFLY-PT
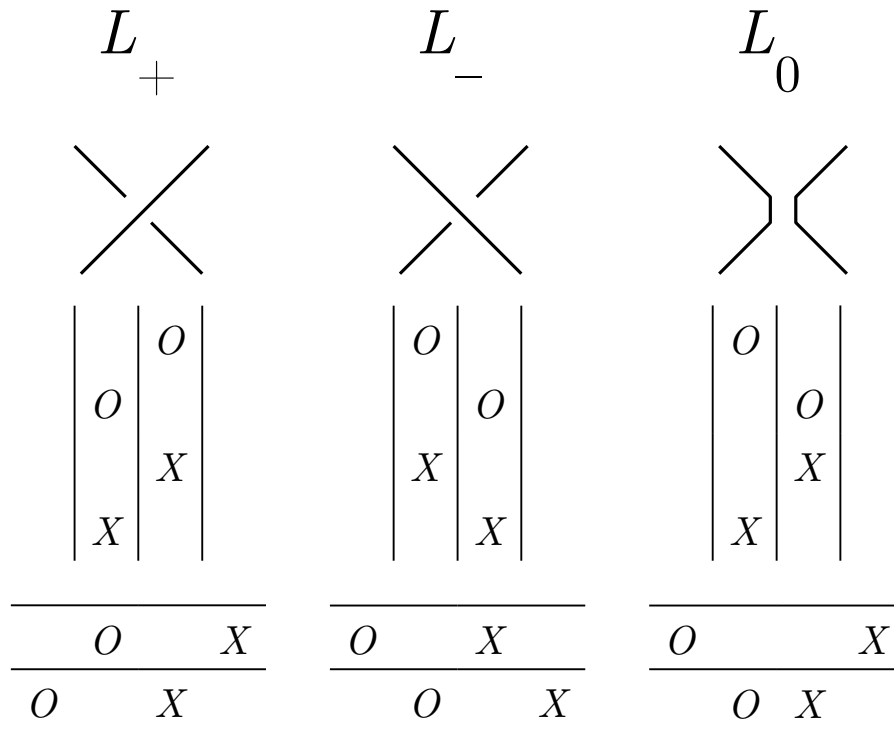
Figure 9.7: Grid skein relation.

polynomial of their lift in the 3-sphere. Proposition 6.6 describes the construction of the lift starting from a grid diagram. Clearly, the essentiality of the HOMFLY-PT invariant depends on the assignment of a value to $J_{p,q}$ on the class $\mathcal{TL}^*$: an assignment based on the lift makes the invariant much less sensitive in this direction.

9.4   Behavior under change of orientation

The HOMFLY-PT invariant refers to oriented links, therefore, to understand if it is an essential invariant, we have to consider different oriented link with equivalent oriented lift. Remark 7.4 provide a wide class of examples. For this reason we investigate what happens to this invariant when we change the orientation of every component of the link. In the case of $\mathbf{S}^3$, the

classic HOMFLY-PT polynomial does not change, but, in $L(p,q)$ things are different since $L(p,q)$ is homologically non-trivial. The result is reported in [20]

Proposition 9.8. *Let L be a link in $L(p,q)$ and denote with $-L$ the link obtained by reversing the orientation of each component. If the HOMFLY-PT invariant of L can be written as $J_{p,q}(L) = \sum a^k z^h J_{p,q}(U_{i_0,i_1,i_2,\ldots,i_{p-1}})$, then $J_{p,q}(-L) = \sum a^k z^h J_{p,q}(U_{i_0,i_{p-1},\ldots,i_2,i_1})$.*

Proof. As for the HOMFLY-PT polynomial for links in the 3-sphere, the skein reduction of both L and $-L$ is the same, because if we change the orientation in L_+, L_- and L_0, we still get respectively L_+, L_- and L_0. However when the orientation of a trivial link is changed, then a different trivial link is obtained; to be more precise, looking at Figure 9.8, if we change the orientation on the trivial link $U_{i_0,i_1,\ldots,i_{p-2},i_{p-1}}$, and perform at first a sequence of non-interleaving row commutations, a sequence of non-interleaving column commutations and finally some cyclic permutation of columns, then we obtain the trivial link $U_{i_0,i_{p-1},i_{p-2},\ldots,i_1}$. $\qquad\square$

Usually, in $L(p,q)$, the links L and $-L$ are non-equivalent (since they are generally homologically different). Therefore, the last proposition suggests a way to construct examples of non-equivalent oriented links with the same lift in $\mathbf{S}^3$, distinguished by the HOMFLY-PT invariant. Indeed it is enough to find a link L lifting to an invertible link and such that L is non isotopic to $-L$.

Example 9.9. The oriented knots K and $-K$ in $L(3,1)$ in Figure 9.9 are different since the first one is 1-homologous whereas the second one is 2-homologous, but they both lift to the trivial knot in $\mathbf{S}^3$. In formulae: $J_{3,1}(K) = J_{3,1}(U_{0,1,0})$, while $J_{3,1}(-K) = J_{3,1}(U_{0,0,1})$.
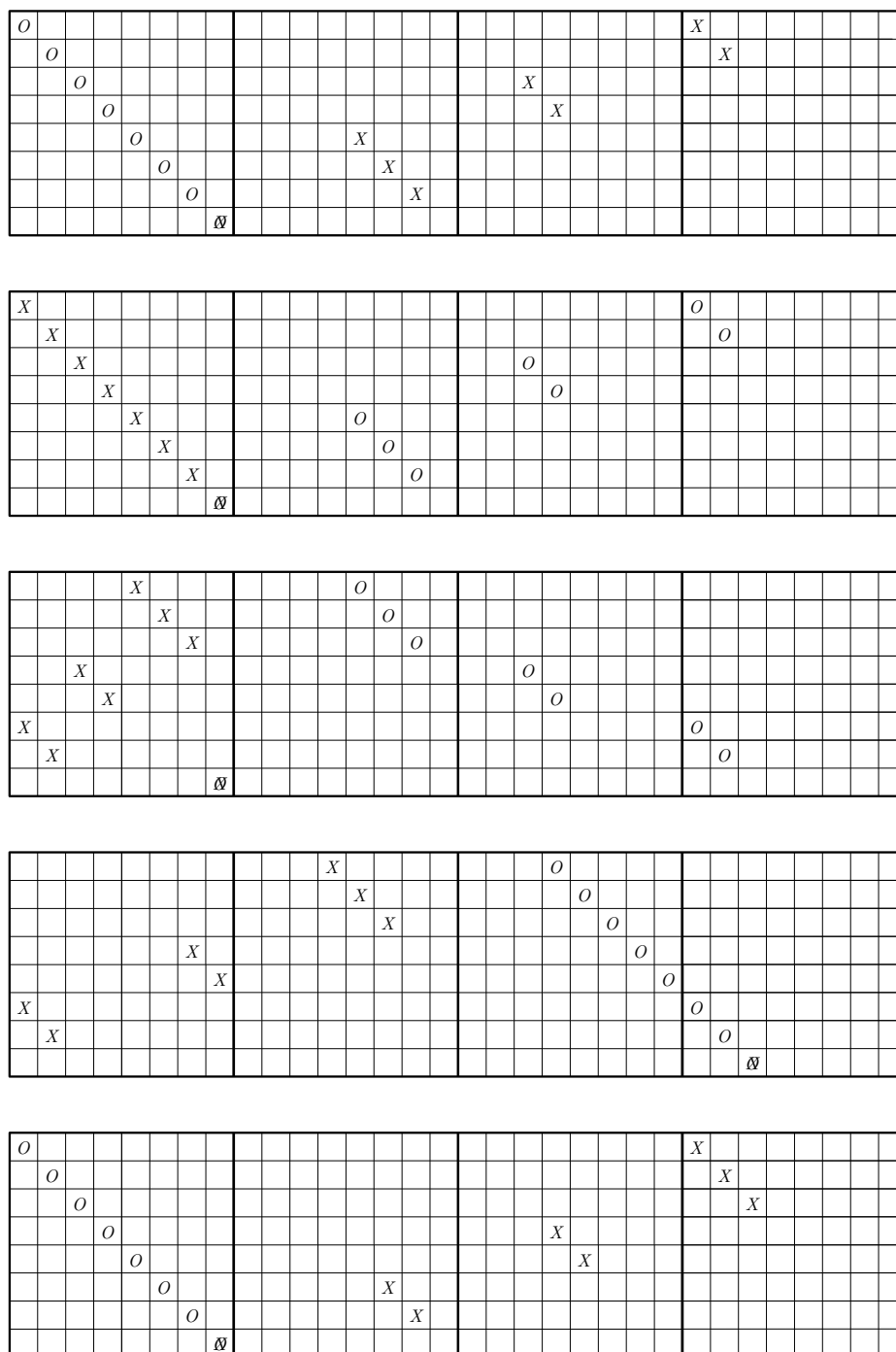
Figure 9.8: Reduction to trivial link of $-U_{1,2,2,3}$ in $L(4,1)$ to $U_{1,3,2,2}$.

Figure 9.9: Knots K and $-K$ in $L(3, 1)$ both lifting to the trivial knot in $\mathbf{S}^3$.

9.5 The HOMFLY-PT invariant is essential

What does it happen if the links with the same lift do not differ only from an orientation change? The many examples of Chapter 7 consisting of different links in $L(p, q)$ with the same covering in $\mathbf{S}^3$ help us. We compute the HOMFLY-PT invariant of some of them. The first two examples are quite simple, since they are pairs of different trivial links: having the same HOMFLY-PT invariant or not depends on how we define $J_{p,q}$ on $\mathcal{TL}^*$. On the contrary, in the third example, that is much more complicated, the two links are distinguished by the HOMFLY-PT polynomial. These results are reported in [20].

Example 9.10. In Figure 9.10 are represented the grid diagrams of the knots K_1 and K_2 in $L(5, 2)$ of Example 7.1; the grid diagrams are found from disk diagrams thanks to Proposition 3.8. The knots are different since K_1 is 1-

Figure 9.10: Grid diagrams for different knots in $L(5, 2)$ with trivial lift.

homologous, while K_2 is 2-homologous, but they both lift to the trivial knot in $\mathbf{S}^3$. Moreover they are trivial: $K_1 = U_{0,0,0,0,1}$ and $K_2 = U_{0,0,0,1,0}$. As a

consequence, if we assume $J_{p,q}(L) := J_{1,0}(\widetilde{L})$ on trivial links, we clearly have $J_{p,q}(K_1) = 1 = J_{p,q}(K_2)$. It is possible to generalize this example to $L\left(p, \frac{p\pm 1}{2}\right)$ (see Example 7.1).

Example 9.11. The two links L_A and L_B in $L(4,1)$ of Example 7.2 are represented by the grid diagrams in Figure 9.11, according to Proposition 3.8. The
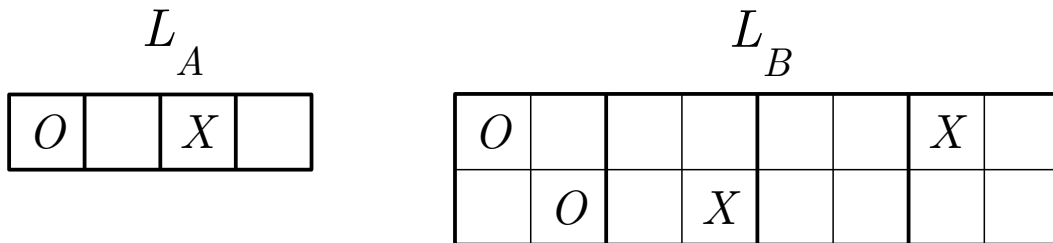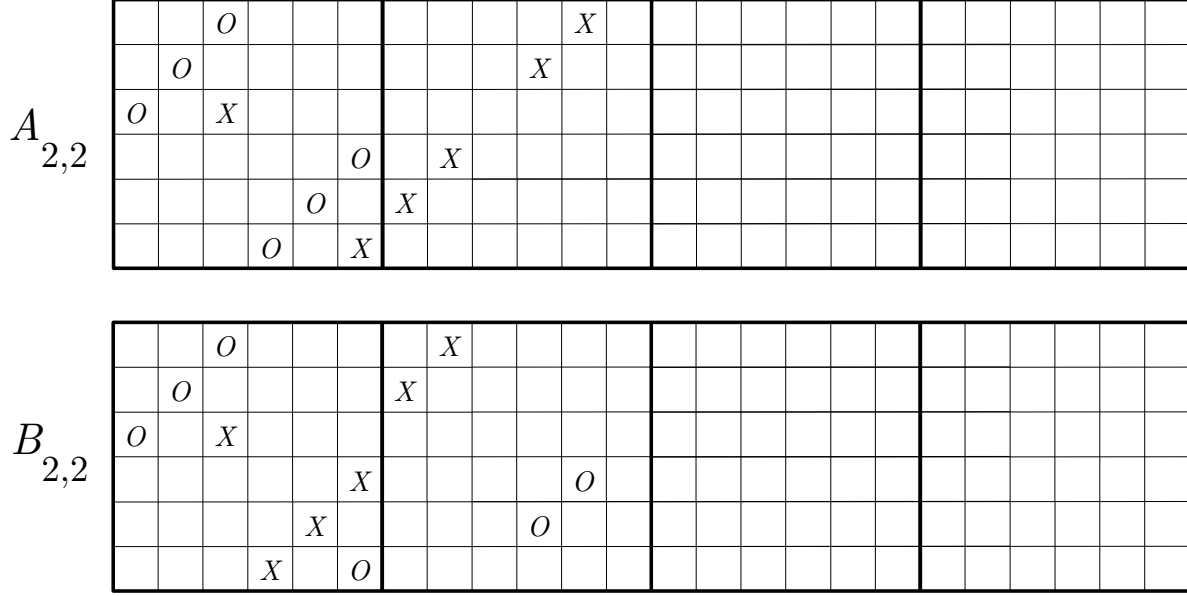

Figure 9.11: Grid diagrams for different links in $L(4,1)$ with Hopf link lift.

knots are non-equivalent since the first one is a knot, whereas the second one is a two component link. Nevertheless, they both lift to the Hopf link in $\mathbf{S}^3$. After performing some destabilizations and non-interleaving commutations on L_A, we see that they are nothing else than the trivial links $L_A = U_{0,0,1,0}$ and $L_B = U_{0,1,0,1}$. As a consequence, if we assume $J_{p,q}(L) := J_{1,0}(\widetilde{L})$ on trivial links, we clearly have $J_{4,1}(L_A) = az + az^{-1} - a^3 z^{-1} = J_{4,1}(L_B)$.

Example 9.12. The two links $A_{2,2}$ and $B_{2,2}$ in $L(4,1)$ of Example 7.3 are represented by the grid diagrams illustrated in Figure 9.12, according to Proposition 3.8. The two links are non equivalent, since they have different Alexander polynomials, but they both lift to the same cable of the Hopf link in $\mathbf{S}^3$. The computation of their HOMFLY-PT invariant is very long. The

$A_{2,2}$

		O							X		
	O							X			
O		X									
				O		X					
			O		X						
		O		X							

$B_{2,2}$

		O				X					
	O				X						
O		X									
				X				O			
			X				O				
		X		O							

Figure 9.12: Grid diagrams for different links in $L(4,1)$ with equivalent lift.

skein reduction tree is quite big, therefore we report here only the final result:

$$
\begin{aligned}
J_{4,1}(A_{2,2}) &= (a^{24} + 3a^{24}z^2 + a^{24}z^4)J_{4,1}(U_{0,0,2,0}) + \\
&\quad + (3a^{28}z + 4a^{28}z^3 + a^{28}z^5)J_{4,1}(U_{1,0,0,0}) + \\
&\quad + (3a^{24}z^2 + 4a^{24}z^4 + a^{24}z^6)J_{4,1}(U_{0,1,0,1}), \\
J_{4,1}(B_{2,2}) &= (a^{24} + 2a^{24}z^2 + a^{24}z^4)J_{4,1}(U_{0,0,2,0}) + \\
&\quad + (a^{28}z + 2a^{28}z^3 + a^{28}z^5)J_{4,1}(U_{1,0,0,0}) + \\
&\quad + (a^{24}z^2 + 2a^{24}z^4 + a^{24}z^6)J_{4,1}(U_{0,1,0,1}) + \\
&\quad + (a^{20}z + a^{20}z^3)J_{4,1}(U_{0,2,1,0}) + \\
&\quad + (a^{20}z + a^{20}z^3)J_{4,1}(U_{0,0,1,2}) + a^{24}z^2 J_{4,1}(U_{0,2,0,2}).
\end{aligned}
$$

The lift of $U_{0,1,0,1}$ is the Hopf link, the lift of $U_{1,0,0,0}$ is the trivial link with four components and $U_{0,2,1,0}$, $U_{0,2,0,2}$, $U_{0,0,1,2}$, $U_{0,0,2,0}$ lift to the closure of the braid Δ_4^2, where Δ_4 denotes the Garside braid on 4-strands (see Figure 3.8). Hence, if we assume $J_{4,1}(L) := J_{1,0}(\widetilde{L})$ on trivial links, we get the following

different HOMFLY-PT polynomials:

$$
\begin{aligned}
J_{4,1}(A_{2,2}) = \ & a^9 z^{-3} - 3a^{11} z^{-3} + 3a^{13} z^{-3} - a^{15} z^{-3} + 3a^{25} z^{-2} - 9a^{27} z^{-2} + \\
& + 9a^{29} z^{-2} - 3a^{31} z^{-2} + 3a^9 z^{-1} - 15a^{11} z^{-1} + 21a^{13} z^{-1} + \\
& - 9a^{15} z^{-1} + 4a^{25} - 12a^{27} + 12a^{29} - 4a^{31} + a^9 z - 25a^{11} z + \\
& + 62a^{13} z - 38a^{15} z + 3a^{25} z - 3a^{27} z + a^{25} z^2 - 3a^{27} z^2 + \\
& + 3a^{29} z^2 - a^{31} z^2 - 19a^{11} z^3 + 102a^{13} z^3 - 99a^{15} z^3 + 7a^{25} z^3 + \\
& - 4a^{27} z^3 - 7a^{11} z^5 + 94a^{13} z^5 - 155a^{15} z^5 + 5a^{25} z^5 - a^{27} z^5 + \\
& - a^{11} z^7 + 46a^{13} z^7 - 129a^{15} z^7 + a^{25} z^7 + 11a^{13} z^9 - 56a^{15} z^9 + \\
& + a^{13} z^{11} - 12a^{15} z^{11} - a^{15} z^{13},
\end{aligned}
$$

$$
\begin{aligned}
J_{4,1}(B_{2,2}) = \ & a^9 z^{-3} - 3a^{11} z^{-3} + 3a^{13} z^{-3} - a^{15} z^{-3} + 2a^5 z^{-2} - 6a^7 z^{-2} + \\
& + 6a^9 z^{-2} - 2a^{11} z^{-2} + a^{25} z^{-2} - 3a^{27} z^{-2} + 3a^{29} z^{-2} - a^{31} z^{-2} + \\
& + 3a^9 z^{-1} - 15a^{11} z^{-1} + 21a^{13} z^{-1} - 9a^{15} z^{-1} + 2a^5 - 18a^7 + 30a^9 + \\
& - 14a^{11} + 2a^{25} - 6a^{27} + 6a^{29} - 2a^{31} + a^9 z - 25a^{11} z + \\
& + 62a^{13} z - 38a^{15} z + a^{25} z - a^{27} z - 20a^7 z^2 + 70a^9 z^2 + \\
& - 50a^{11} z^2 + a^{25} z^2 - 3a^{27} z^2 + 3a^{29} z^2 - a^{31} z^2 - 19a^{11} z^3 + \\
& + 102a^{13} z^3 - 99a^{15} z^3 + 3a^{25} z^3 - 2a^{27} z^3 - 10a^7 z^4 + 88a^9 z^4 + \\
& - 110a^{11} z^4 - 7a^{11} z^5 + 94a^{13} z^5 - 155a^{15} z^5 + 3a^{25} z^5 - a^{27} z^5 + \\
& - 2a^7 z^6 + 58a^9 z^6 - 128a^{11} z^6 - a^{11} z^7 + 46a^{13} z^7 - 129a^{15} z^7 + \\
& + a^{25} z^7 + 18a^9 z^8 - 74a^{11} z^8 + 11a^{13} z^9 - 56a^{15} z^9 + 2a^9 z^{10} + \\
& - 20a^{11} z^{10} + a^{13} z^{11} - 12a^{15} z^{11} - 2a^{11} z^{12} - a^{15} z^{13}.
\end{aligned}
$$

Bibliography

[1] J. W. Alexander, G. B. Briggs, *On types of knotted curves*, Ann. of Math. **28** (1926/27), 562–586.

[2] K. Baker, *Small genus knots in lens spaces have small bridge number*, Algebr. Geom. Topol. **6** (2006), 1519–1621.

[3] K. Baker, *Once-punctured tori and knots in lens spaces*, Comm. Anal. Geom. **19** (2011), 347–399.

[4] K. Baker, *A cabling conjecture for knots in lens spaces*, preprint, 2013, arXiv:1306.0596.

[5] K. Baker, J. E. Grigsby, *Grid diagrams and Legendrian lens space links*, J. Symplectic Geom. **7** (2009), 415–448.

[6] K. Baker, J. E. Grigsby, M. Hedden, *Grid diagrams for lens spaces and combinatorial knot Floer homology*, Int. Math. Res. Not. IMRN **10** (2008), Art. ID rnm024, 39 pp.

[7] K. Baker, J. E. Johnson, E. A. Klodginski, *Tunnel number one, genus-one fibered knots*, Comm. Anal. Geom. **17** (2009), 1–16.

[8] D. Bar-Natan, S. Morrison et al., *The Knot Atlas*, http://katlas.org.

[9] J. Berge, *Some knots with surgeries yielding lens spaces*, unpublished manuscript.

[10] C. Blanchet, N. Habegger, G. Masbaum, P. Vogel, *Three-manifold invariants derived from the Kauffman bracket*, Topology **31** (1992), 685–699.

[11] M. Boileau, S. Boyer, R. Cebanu, G. S. Walsh, *Knot commensurability and the Berge conjecture*, Geom. Topol. **16** (2012), 625–664.

[12] M. Boileau, E. Flapan, *Uniqueness of free actions on $\mathbf{S}^3$ respecting a knot*, Canad. J. Math. **39** (1987), 969–982.

[13] F. Bonahon, *Difféotopies des espaces lenticulaires*, Topology **22** (1983), 305–314.

[14] E. J. Brody, *The topological classification of the lens spaces*, Ann. of Math. **71** (1960), 163–184.

[15] D. Buck, M. Mauricio, *Connect sum of lens spaces surgeries: application to Hin recombination*, Math. Proc. Cambridge Philos. Soc. **150** (2011), 505–525.

[16] G. Burde, H. Zieschang, *Knots*, Second edition, de Gruyter Studies in Mathematics, 5, Walter de Gruyter & Co., Berlin, 2003.

[17] J. Scott Carter, *A survey of quandle ideas*, Introductory lectures on knot theory, 22–53, Ser. Knots Everything, 46, World Sci. Publ., Hackensack, NJ, 2012.

[18] A. Cattabriga, *The Alexander polynomial of (1,1)-knots*, J. Knot Theory Ramifications **15** (2006), 1119–1129.

[19] A. Cattabriga, E. Manfredi, M. Mulazzani, *On knots and links in lens spaces*, Topology Appl. **160** (2013), 430–442.

[20] A. Cattabriga, E. Manfredi, L. Rigolli, *Equivalence of two diagram representations of links in lens spaces and essential invariants*, preprint, 2013, arXiv:1312.2230.

[21] A. Cattabriga, M. Mulazzani, *Strongly-cyclic branched coverings of $(1,1)$-knots and cyclic presentations of group*, Math. Proc. Cambridge Philos. Soc. **135** (2003), 137–146.

[22] A. Cattabriga, M. Mulazzani, $(1, 1)$-*knots via the mapping class group of the twice punctured torus*, Adv. Geom. **4** (2004), 263–277.

[23] A. Cattabriga, M. Mulazzani, *All strongly-cyclic branched coverings of* $(1, 1)$-*knots are Dunwoody manifolds*, J. London Math. Soc. **70** (2004), 512–528.

[24] A. Cattabriga, M. Mulazzani, *Representations of (1,1)-knots*, Fund. Math. **188** (2005), 45–57.

[25] N. Chbili, *Le polynôme de Homfly des nœuds librement périodiques*, C. R. Acad. Sci. Paris Sér. I Math. **325** (1997), 411–414.

[26] N. Chbili, *The Jones polynomials of freely periodic knots*, J. Knot Theory Ramifications **9** (2000), 885–891.

[27] N. Chbili, *The multi-variable Alexander polynomial of lens braids*, J. Knot Theory Ramifications **11** (2002), 1323–1330.

[28] N. Chbili, *A new criterion for knots with free periods*, Ann. Fac. Sci. Toulouse Math. **12** (2003), 465–477.

[29] D. H. Choi, K. H. Ko, *Parametrizations of 1-bridge torus knots*, J. Knot Theory Ramifications **12** (2003), 463–491.

[30] C. Cornwell, *Invariants of topological and Legendrian links in lens spaces with a universally tight contact structure*, Ph. D. Dissertation, Michigan State University, 2011.

[31] C. Cornwell, *A polynomial invariant for links in lens spaces*, J. Knot Theory Ramifications **21** (2012), 1250060, 31 pp.

[32] C. Cornwell, *Bennequin type inequalities in lens spaces*, Int. Math. Res. Not. IMRN 2012, 1890–1916.

[33] R. H. Crowell, R. H. Fox, *Introduction to knot theory*, Ginn and Co., Boston, Mass., 1963.

[34] F. Deloup, D. Garber, S. Kaplan, M. Teicher, *Palindromic braids*, Asian J. Math. **12** (2008), 65–71.

[35] A. Deruelle, *Thin presentation of knots in lens spaces and RP3-conjecture*, C. R. Math. Acad. Sci. Paris **336** (2003), 937–940.

[36] A. Deruelle, D. Matignon, *Thin presentation of knots and lens spaces*, Algebr. Geom. Topol. **3** (2003), 677–707.

[37] A. Deruelle, D. Matignon, *Spinal knots in lens spaces*, J. Knot Theory Ramifications **15** (2006), 1371–1389.

[38] I. Diamantis, S. Lambropoulou, *Braid equivalence in 3-manifolds with rational surgery description*, preprint, 2013, arXiv:1311.2465.

[39] H. Doll, *A generalized bridge number for links in 3-manifold*, Math. Ann. **294** (1992), 701–717.

[40] H. Doll, J. Hoste, *A tabulation of oriented link*, Math. Comp. **57** (1991), 747–761.

[41] C. H. Dowker, M. B. Thistlethwaite, *Classifications of knot projections*, Topology Appl. **16** (1983), 19–31.

[42] Y. V. Drobotukhina, *An analogue of the Jones polynomial for links in $\mathbb{R}P^3$ and a generalization of the Kauffman-Murasugi theorem*, Leningrad Math. J. **2** (1991), 613–630.

[43] J. Drobotukhina, *Classification of links in $\mathbb{R}\mathbb{P}^3$ with at most six crossings*, Topology of manifolds and varieties, 87–121, Adv. Soviet Math., 18, Amer. Math. Soc., Providence, RI, 1994.

[44] R. Fenn, C. Rourke, *Racks and links in codimension two*, J. Knot Theory Ramifications **1** (1992), 343–406.

[45] R. H. Fox, *Knots and periodic transformations*, 1962, in *Topology of 3-manifolds and related topics* (Proc. The Univ. of Georgia Institute, 1961) pp. 177–182 Prentice-Hall, Englewood Cliffs, N.J..

[46] S. Friedl, S. Vidussi, *A survey of twisted Alexander polynomials*, The mathematics of knots, 45–94, Contrib. Math. Comput. Sci., 1, Springer, Heidelberg, 2011.

[47] H. Fujii, *Geometric indices and the Alexander polynomial of a knot*, Proc. Am. Math. Soc. **128** (1996), 2923–2933.

[48] D. Futer, E. Kalfagianni , J. Purcell, *Symmetric links and Conway sums: volume and Jones polynomial*, Math. Res. Lett. **16** (2009), 233–253.

[49] D. Gabai, *Foliations and the topology of 3-manifolds. III*, J. Differential Geom. **26** (1987), 479–536.

[50] B. Gabrovšek, *Classification of knots in lens spaces*, Ph.D. thesis, University of Ljubljana, Slovenia, 2013.

[51] B. Gabrovšek, M. Mroczkowski, *Knots in the solid torus up to 6 crossings*, J. Knot Theory Ramifications **21** (2012), 1250106, 43 pp.

[52] B. Gabrovšek, M. Mroczkowski, *The HOMFLY-PT skein module of the lens space $L(p,1)$*, submitted to Algebr. Geom. Topol.

[53] F. A. Garside, *The braid group and other groups*, Quart. J. Math. Oxford, **20** (1969), 235–254.

[54] H. Geiges, S. Onaran *Legendrian rational unknots in lens spaces*, preprint, 2013, arXiv:1302.3792.

[55] E. Giroux, N. Goodman, *On the stable equivalence of open books in three-manifolds*, Geom. Topol. **10** (2006), 97–114.

[56] M. Gonzato, *Invarianti polinomiali per link in spazi lenticolari*, M. Sc. Thesis, University of Bologna, 2007.

[57] C. McA. Gordon, J. Luecke, *Knots are determined by their complements*, Bull. Amer. Math. Soc. **20** (1989), 83–87.

[58] D. V. Gorkovets, *Distributive groupoids for knots in projective space*, Vestn. Chelyab. Gos. Univ. Mat. Mekh. Inform. **6**/10 (2008), 89–93.

[59] D. V. Gorkovets, *Cocycle invariants for links in projective space*, Vestn. Chelyab. Gos. Univ. Mat. Mekh. Inform. **23**/12 (2010), 88–97.

[60] J. E. Greene, *The lens space realization problem*, Ann. of Math. **177** (2013), 449–511.

[61] R. Hartley, *Knots with free period*, Can. J. Math. **33** (1981), 91–102.

[62] A. Hatcher, *Algebraic Topology*, Cambridge University Press, 2002.

[63] C. Hayashi, *Genus one* 1-*bridge positions for the trivial knot and cabled knots*, Math. Proc. Camb. Philos. Soc. **125** (1999), 53–65.

[64] M. Hedden, *On Floer homology and the Berge conjecture on knots admitting lens space surgeries*, Trans. Amer. Math. Soc. **363** (2011), 949–968.

[65] J. A. Hillman, C. Livingston, S. Naik, *Twisted Alexander polynomials of periodic knots*, Algebr. Geom. Topol. **6** (2006), 145–169.

[66] C. Hodgson, J. H. Rubinstein, *Involutions and isotopies of lens spaces*, in *Knot theory and manifolds (Vancouver, B.C., 1983)*, 60–96, Lecture Notes in Math., 1144, Springer, Berlin, 1985.

[67] J. Hoste, J. H. Przytycki, *The* $(2, \infty)$-*skein module of lens spaces; a generalization of the Jones polynomial*, J. Knot Theory Ramifications **2** (1993), 321–333.

[68] V. Q. Huynh, *Reidemeister torsion, twisted Alexander polynomial, the A-polynomial and the colored Jones polynomial of some classes of knots*, Ph.D Thesis, State University of New York, 2005.

[69] V. Q. Huynh, T. T. Q. Le, *Twisted Alexander polinomial of links in the projective space*, J. Knot Theory Ramifications **17** (2008), 411–438.

[70] M. Jeong, C. Park, *Lens knots, periodic links and Vassiliev invariants*, J. Knot Theory Ramifications **13** (2004), 1041–1056.

[71] D. Joyce, *A classifying invariant of knots, the knot quandle*, J. Pure Appl. Algebra **23** (1982), 37–65.

[72] A. Kawauchi, *A survey of knot theory*, Birkhäuser Verlag, Basel, 1996.

[73] R. C. Kirby, L. C. Siebenmann, *Foundational essays on topological manifolds, smoothings, and triangulations*, Ann. of Math. Stud. **88** Princeton Univ. Press., 1977.

[74] P. Kirk, C. Livingston, *Twisted Alexander invariants, Reidemeister torsion, and Casson-Gordon invariants*, Topology **38** (1999), 635–661.

[75] T. Kitano, *Twisted Alexander polynomial and Reidemeister torsion*, Pacific J. Math. **174** (1996), 431–442.

[76] S. Lambropoulou, *Solid torus links and Hecke algebras of $\mathcal{B}$-type*, Proc. Conf. Quant. Topology (1994), 225–245.

[77] S. Lambropoulou, C. P. Rourke, *Markov's theorem in 3–manifolds*, Topology Appl. **78** (1997), 95–122.

[78] S. Lambropoulou, C. P. Rourke, *Algebraic Markov equivalence for links in three-manifolds*, Compos. Math. **142** (2006), 1039–1062.

[79] J. E. Licata, *Invariants for Legendrian knots in lens spaces*, Commun. Contemp. Math. **13** (2011), 91–121.

[80] J. E. Licata, *Legendrian grid number one knots and augmentations of their differential algebras*, The mathematics of knots, 143–168, Contrib. Math. Comput. Sci., 1, Springer, Heidelberg, 2011.

[81] E. Manfredi, *Fundamental group of knots and links in lens spaces*, M. Sc. Thesis, University of Trieste, 2010.

[82] E. Manfredi, *Lift in the 3-sphere of knots and links in lens spaces*, preprint, 2013, arXiv:1312.1256.

[83] C. Manolescu, P. Ozsváth, S. Sarkar, *A combinatorial description of knot Floer homology*, Ann. of Math. **169** (2009), 633–660.

[84] J. Marché, *L'intégrale de Kontsevich des nœuds dans les variétés de dimension 3*, Ph. D. Thesis, Université Denis Diderot, Paris, 2004.

[85] J. M. Masley, H. L. Montgomery, *Cyclotomic fields with unique factorization*, J. Reine Angew. Math. **286/287** (1976), 248–256.

[86] S. V. Matveev, *Distributive groupoids in knot theory*, Math. USSR Sb. **47** (1984), 73–83.

[87] M. Mauricio, *Distance bounding and Heegaard Floer homology methods in reducible Dehn surgery*, PhD thesis, Imperial College London, 2012.

[88] K. Morimoto, M. Sakuma, *On unknotting tunnels for knots*, Math. Ann. **289** (1991), 143–167.

[89] D. Moussard, *On Alexander modules and Blanchfield forms of null-homologous knots in rational homology spheres*, J. Knot Theory Ramifications **21** (2012), 1250042, 21 pp.

[90] D. Moussard, *Finite type invariants of rational homology 3-spheres*, Algebr. Geom. Topol. **12** (2012), 2389–2428.

[91] M. Mroczkowski, *Diagrammatic unknotting of knots and links in the projective space*, J. Knot Theory Ramifications **12** (2003), 637–651.

[92] M. Mroczkowski, *Polynomial invariants of links in the projective space*, Fund. Math. **184** (2004), 223–267.

[93] F. H. Norwood, *Every two-generator knot is prime*, Proc. Amer. Math. Soc. **86** (1982), 143–147.

[94] P. Ozsváth, Z. Szabó, *Holomorphic disks and knot invariants*, Adv. Math. **186** (2004), 58–116.

[95] V. V. Prasolov, A. B. Sossinsky, *Knots, links, braids and 3-manifolds. An introduction to the new invariants in low-dimensional topology*, Transl. of Math. Monographs **154**, Amer. Math. Soc., Providence, RI, 1997.

[96] J. Rasmussen, *Lens space surgeries and L-space homology spheres*, preprint, 2007, arXiv:0710.2531.

[97] K. Reidemeister, *Elementare Begründung der Knotentheorie*, Abh. Math. Sem. Univ. Hamburg **5** (1927), 24–32.

[98] N. Reshetikhin, V. G. Turaev, *Invariants of 3-manifolds via link polynomials and quantum groups*, Invent. Math. **103** (1991), 547–597.

[99] D. Rolfsen, *Knots and links*, Amer. Math. Soc., Providence, RI, 2003.

[100] D. Roseman, *Elementary moves for higher dimensional knots*, Fund. Math. **184** (2004), 291–310.

[101] M. Sakuma, *Uniqueness of symmetries of knots*, Math. Z. **192** (1986), 225–242.

[102] S. Stevan, *Torus Knots in Lens Spaces & Topological Strings*, preprint, 2013, arXiv:1308.5509.

[103] J. Stillwell, *Classical topology and combinatorial group theory*, Second edition, Grad. Texts in Math. **72**, Springer-Verlag, New York, 1993.

[104] C. J. Stitz, *Linking numbers and Jones polynomials for lens spaces and other 3-manifolds*, Ph. D. Thesis, Kent State University, 2000.

[105] C. J. Stitz, *A combinatorial approach to linking numbers in rational homology spheres*, J. Knot Theory Ramifications **9** (2000), 703–711.

[106] P. G. Tait, *On Knots I,II,III*, in: *Scientific Papers*, Vol. I, Cambridge University Press, London, 273–347, 1898.

[107] V. G. Turaev, *The Conway and Kauffman modules of a solid torus*, J. Soviet Math. **52** (1990), 2799–2805.

[108] V. Turaev, *Torsion of 3-dimensional manifolds*, Birkhäuser Verlag, Basel-Boston-Berlin, 2002.

[109] K. Volkert, *Lens spaces in dimension 3: a history*, The manifold atlas (2013), http://www.map.mpim-bonn.mpg.de/Lens_spaces_in_dimension_three:_a_3history.

[110] M. Wada, *Twisted Alexander polynomial for finitely presentable groups*, Topology **33** (1994), 241–256.

[111] M. R. Watkins, *A Short Survey of Lens Spaces*, (unpublished, 1990). Available online at http://empslocal.ex.ac.uk/people/staff/mrwatkin/lensspaces.pdf.

[112] J. H. C. Whitehead, *On incidence matrices, nuclei and homotopy types*, Ann. of Math. **42** (1941), 1197–1239.

[113] W. Whitten, *Knot complements and groups*, Topology **26** (1987), 41–44.

[114] E. Witten, *Quantum field theory and the Jones polynomial*, Comm. Math. Phys. **121** (1989), 351–399.

[115] Y.-Q. Wu, *∂-reducing Dehn surgeries and 1-bridge knots*, Math. Ann. **295** (1993), 319–331.

Acknowledgements

These three years of Ph.D. course have been incredibly fruitful for me. Besides the collaborations for the mathematical work I have already highlighted during the dissertation, I want to thank every person who has supported me.

First of all, I thank my advisor Michele Mulazzani and his collaborator Alessia Cattabriga, no need to say why.

Special thanks go to Sergey Matveev and to the whole department of "Topology and computer algebra" of Chelyabinsk State University where I spent three valuable months, in particular Evgeny Fominykh has been really keen on the organization. Dmitry Gorkovets, Filip Korablev and Valentin Potapov, I really appreciated how you involved me in mathematical discussions.

I thank Matija Cencelj for inviting me to give a talk in Ljubljana and his student Bostjan Gabrovšek, for sharing with me his precious knowledge of knots in lens spaces.

I enjoyed the time I spent in Pisa and Cortona for several workshops and conferences, hence I owe some thanks to the organizers Bruno Martelli and Renzo Ricca, and the University of Pisa and Centro de Giorgi. During these events, Mattia Mecchia gave me useful insights to my work. I would also like to thank Lorenzo Losa for a lot of worthy conversations about hyperbolic geometry.

I am pleased I went to Montreal for the "Summer School: Physics and Mathematics of Link Homology" and for the "Conference Low-dimensional Topology after Floer", I thank the CRM of Montreal and INDAM of Italy